MN(II) OXIDATION IN THE PRESENCE OF METAL OXIDES

Thesis by

Simon Henry Richard Davies

In Partial Fulfillment of the Requirements

for the Degree of

Doctor of Philosophy

California Institute of Technology

Pasadena, California

1985

(Submitted 16th October, 1984)

ACKNOWLEDGEMENTS

I would like to thank my advisor James Morgan for his interest, advice, and support throughout my graduate career. Michael Hoffmann's advice and interest is also greatly appreciated. I would also like to thank Richard Flagan, John Bercaw, Yuk Yung, John List, George Rossman, and Fred Anson for serving on my examining committees.

Many students in the Keck Laboratory contributed to this work through their advice, support and friendship. Particular thanks go to Alan Stone and Roger Bales for their assistance. I would like to thank the staff of Keck Laboratory for their assistance, especially Elaine Granger, Sandy Brooks, Rayma Harrison, and Gunilla Hastrup.

I thank my family and friends for their support and friendship.

Financial support from the Haagen-Smit/Tyler Fellowship Fund, Jessie Smith Noyes Foundation, President's Fund and NOAA is gratefully acknowledged.

ABSTRACT

The oxidation of Mn(II) by oxygen in the presence of goethite (α-FeOOH), lepidocrocite (γ-FeOOH), silica and alumina was studied. All the solids, except perhaps alumina, enhanced the rate of Mn(II) oxidation. The degree of enhancement was as follows:

lepidocrocite > goethite > silica > alumina.

At constant pO_2 Mn(II) oxidation on goethite, lepidocrocite and silica can be described by the following equation

$$-\frac{d[Mn(II)]}{dt} = k^* \frac{<\equiv SOH> [Mn^{2+}]}{[H^+]^2} \cdot a \cdot pO_2$$

where $<\equiv SOH>$ is the concentration of the surface hydroxyl group and a is the solids concentration.

Mn(II) oxidation in the presence of goethite or lepidocrocite is first order in pO_2. Both these reactions are strongly temperature dependent (apparent activation energy ~ 100 kJ/mol). Normal laboratory lighting has no effect on the rate of these reactions.

The rate of Mn(II) oxidation in the presence of lepidocrocite is about 4 times slower in 0.7M $NaClO_4$, than in 0.1M $NaClO_4$. This reaction is inhibited by the following ions; Mg^{2+}, Ca^{2+}, silicate, salicylate, phosphate, chloride, and sulfate. Phthlate has little or no effect on the rate of this reaction.

The adsorptive behaviour of Mn(II) on the metal oxides

studied could be described using a surface complexation model. Using this model it was shown that the rate of Mn(II) oxidation on the metal oxides studied is described by the equation

$$-\frac{d[Mn(II)]}{dt} = k''<(\equiv SO)_2Mn> \cdot a \cdot pO_2$$

where $(\equiv SO)_2Mn$ is a bidentate surface complex. It is possible that a hydrolyzed surface complex ($\equiv SOMnOH$) rather than the bidentate complex is involved in the reaction.

The results of the laboratory studies indicate that in natural waters the important factors which influence Mn(II) on metal oxides are pH, iron oxide concentration, temperature, $[Mg^{2+}]$, $[Cl^-]$, and ionic strength. These studies predict that at pH < 7.5 the rate of Mn(II) oxidation in natural waters is slow ($t_{\frac{1}{2}}$ < 100 days). Mn(II) may be completely oxidized within a few days in iron-rich, high pH waters.

TABLE OF CONTENTS

	Page
ACKNOWLEDGEMENTS	iii
ABSTRACT	iv
TABLE OF CONTENTS	vi
LIST OF TABLES	ix
LIST OF FIGURES	xii
NOTATION	xiv
1 INTRODUCTION	
1.1 The importance of manganese in the aquatic environment	1
1.2 Aqueous chemistry of manganese	1
1.3 The geochemistry of manganese in the aquatic environment	3
1.4 The persistence of Mn(II) in oxic waters	6
1.5 Scope and purpose of this work	7
2 ANALYTICAL TECHNIQUES, PREPARATION, CLEANING AND CHARACTERIZATION OF METAL OXIDES	
2.1 Analytical techniques	
2.1.1 General remarks	9
2.1.2 pH measurements	10
2.1.3 Solids concentration	12
2.1.4 Manganese	14
2.1.5 Calcium and magnesium	17
2.1.6 Anions	17
2.2 Preparation and cleaning of metal oxides	
2.2.1 Geothite (α-FeOOH)	17
2.2.2 Lepidocrocite (γ-FeOOH)	19
2.2.3 Silica SiO_2	20
2.2.4 Alumina	20

TABLE OF CONTENTS (continued)

2.3 Identification of solid phase
2.3.1 X-Ray diffraction 20
2.3.2 Electron microscopy 23
2.3.3 Additional information and summary 26

2.4 Surface properties of the metal oxides
2.4.1 Surface area by B.E.T. analysis 26
2.4.2 Exchange capacity 28
2.4.3 Site density 28
2.4.4 Acid-base titration 28
2.4.5 Mn(II) adsorption experiments 29
2.4.6 Other adsorption studies 30

2.5 Oxidation studies 30

2.6 Methods for the calculation of the equilibrium distribution of chemical species 32

3 SURFACE CHEMICAL PROPERTIES OF METAL OXIDES

3.1 Theory 33

3.2. Results and discussion 38
3.2.1 Titration 38
3.2.2 Mn(II) adsorption 45
3.2.2.1 Kinetics of adsorption 45
3.2.2.2 Effect of pH on Mn(II) adsorption 45

3.3 Speciation on the metal oxide surface 55

4 OXIDATION OF MN(II) IN THE PRESENCE OF METAL OXIDE SURFACES.

4.1 Introduction 60

4.2 Previous oxidation studies 60

4.3 Interpretation of kinetic data 62

4.4 Results and discussion 65
4.4.1 Validity of the interpretation of kinetic data 65
4.4.2 'Homogeneous' oxidation of Mn(II) 75
4.4.3 Oxidation of Mn(II) in the presence of metal oxide surfaces 81
4.4.3.1 Reproducibility 84
4.4.3.2 The influence of pH 84
4.4.3.3 Influence of oxygen 94
4.4.3.4 Influence of solids concentration 94
4.4.3.5 Effect of ionic strength 97

TABLE OF CONTENTS (continued)

4.4.3.6 Effect of light 100
4.4.3.7 Effect of buffer composition 100
4.4.3.8 Oxidation of Mn(II) on the alumina surface 103
4.4.3.9 Temperature dependence 104

4.5 Rate law formulation and mechanism 107

5 THE EFFECT OF OTHER IONS ON MN(II) OXIDATION IN THE PRESENCE OF LEPIDOCROCITE.

5.1 Introduction 117

5.2 Results and Discussion 119
5.2.1 Adsorption studies 119
5.2.2 Oxidation studies 123

6 MN(II) OXIDATION IN NATURAL WATERS: IMPLICATIONS OF EXPERIMENTAL STUDIES

6.1 Introduction 133

6.2 Comparison of the rate of Mn(II) oxidation on different metal oxides 133

6.3 Factors influencing Mn(II) oxidation kinetics in natural waters 137

6.4 Mn(II) oxidation in natural waters : A comparison with predictions based on laboratory data 146

6.5 Summary 150

7 CONCLUSIONS AND RECOMMENDATIONS

7.1 Conclusions 152
7.1.1 Mn(II) adsorption 152
7.1.2 Mn(II) oxidation on metal oxide surfaces 152
7.1.3 The influence of other ions on the rate of Mn(II) oxidation on lepidocrocite 154
7.1.4 Mn(II) oxidation in natural waters: implications of experimental studies 155

7.2 Recommendations for further study 156

REFERENCES 159

APPENDICES 167

LIST OF TABLES

Table		Page
2.1	A comparison of direct pH measurements taken in silica suspensions with those taken after filtering the suspension.	13
2.2	Experimental conditions used for atomic absorption spectrophotometric analyses for iron and manganese.	13
2.3	A comparison of the results for filterable Mn using formaldioxime and atomic absorption spectrophotometric.	16
2.4	Experimental conditions used for atomic absorption spectrophotometric analyses for calcium and magnesium.	18
2.5	X-ray diffraction data for G1, G2, and goethite.	21
2.6	X-ray diffraction data for L2, L3 and lepidocrocite.	22
2.7	Specific surface area, exchange capacity, and site density for goethite, lepidocrocite, silica and alumina.	27
3.1	The acidity constants, pH_{zpc} and capacitances of α-FeOOH, γ-FeOOH, and δ-Al_2O_3 surfaces.	42
3.2	Physical and chemical properties of the Aerosil 200 surface (after Young, 1981).	44
3.3	Kinetics of adsorption of Mn(II) on goethite at pH 9.00.	46
3.4	Kinetics of adsorption of Mn(II) on goethite at pH 8.05.	46
3.5	Kinetics of adsorption of Mn(II) on lepidocrocite.	47
3.6	Kinetics of adsorption of Mn(II) on Aerosil 200.	47
3.7	Kinetics of adsorption of Mn(II) on alumina.	48

LIST OF TABLES (continued)

Table		Page
3.8	Adsorption of Mn(II) on goethite as a function of pH.	50
3.9	Adsorption of Mn(II) on lepidocrocite as a function of pH.	51
3.10	Adsorption of Mn(II) on silica as a function of pH.	52
3.11	Adsorption of Mn(II) on alumina as a function of pH.	53
3.12	Stability constants for interaction of Mn(II) with metal oxide surfaces.	56
4.1	Oxidation of Mn(II) in the absence of metal oxides.	79
4.2	Results and experimental conditions for Mn(II) oxidation studies in the presence of goethite.	85
4.3	Results and experimental conditions for Mn(II) oxidation studies in the presence of lepidocrocite.	86
4.4	Results and experimental conditions for Mn(II) oxidation studies in the presence of silica.	87
4.5	Results and experimental conditions for Mn(II) oxidation studies in the presence of alumina.	87
4.6	Reproducibility of measurements of the rate of oxidation of Mn(II) in the presence of goethite at pH $\sim$ 8.64.	88
4.7	Reproducibility of measurements of the rate of oxidation of Mn(II) in the presence of lepidocrocite at pH $\sim$ 8.04.	89
4.8	Reproducibility of measurements of the rate of oxidation of Mn(II) in the presence of lepidocrocite at pH $\sim$ 8.51.	89
4.9	Mn(II) oxidation in the presence of geothite or lepidocrocite as a function of oxygen concentration.	95

LIST OF TABLES (continued)

Table		Page
4.10	Mn(II) oxidation in the presence of lepidocrocite as a function of ionic strength.	99
4.11	Mn(II) oxidation in the presence of goethite or lepidocrocite as a function of temperature.	105
4.12	k" for the oxidation of Mn(II) on goethite, lepidocrocite, silica and alumina.	112
5.1	Interactions of anions, Ca^{2+} and Mg^{2+} with the lepidocrocite surface.	121
5.2	Adsorption of anions, Ca^{2+}, and Mg^{2+} on the lepidocrocite surface.	122
5.3	Oxidation of Mn(II) in the presence of other ions.	124
5.4	Oxidation of Mn(II) in the presence of lepidocrocite and other ions.	125
5.5	Comparison of experimental and calculated values for the ratio $k_1/k_{1,\ control}$.	128
6.1	Input data for surface equilibria calculations 1. Comparison of metal oxides.	134
6.2	Input data for surface equilibria calculations 2. Influence of other ions.	140
6.3	Predicted half-lives for Mn(II) oxidation in fresh-water, estuarine-water, and 0.1 M $NaClO_4$.	141
6.4	Calculated speciation in fresh-water, estuarine-water, and 0.1M $NaClO_4$.	143
6.5	Removal times for manganese in natural waters.	147

LIST OF FIGURES

Figure		Page
2.1	Potential drift of a pH electrode immersed in a silica suspension.	11
2.2	a. Transmission electromicrograph of L3.	24
	b. Transmission electromicrograph of G2.	25
3.1	Schematic representation of the potential distribution of the metal oxide-water interface.	37
3.2	A plot pK_{a1}^{s} as a function of surface charge σ_o.	40
3.3	Titration data for δ-Al_2O_3.	43
3.4	Kinetics of adsorption of Mn(II) on goethite, lepidocrocite, silica and alumina.	49
3.5	Mn(II) adsorption as a function of pH.	54
3.6	Calculated speciation on the metal oxide surface.	57
4.1	Oxygen concentration as a function of time.	67
4.2	Filterable Mn as a function time in a system supersaturated with respect to $MnCO_3(s)$.	69
4.3	Filterable Mn in α-FeOOH suspension with carbonate present.	71
4.4	Filterable Mn in a silica suspension with carbonate present.	73
4.5	Removal of Mn from a silica suspension under N_2.	74
4.6	Loss of filterable Mn under N_2 and under O_2 with no solid present initially.	77
4.7	First order plot for removal of filterable Mn under O_2.	78
4.8	Typical oxidation experiment in presence of metal oxide.	82

LIST OF FIGURES (continued)

Figure		Page
4.9	Log Mn_f as a function of time for system where metal oxide is present.	83
4.10	Log k_1 vs. pH and log A vs. pH for the goethite data.	90
4.11	Log k_1 vs. pH and log A vs. pH for the lepidocrocite data.	91
4.12	Log k_1 vs. pH and log A vs. pH. for the silica data.	92
4.13	Log k_1 as a function of solids concentration for the oxidation of Mn(II) in the presence of geothite or lepidocrocite.	96
4.14	Log $(k_1/[Mn^{2+}]$ as a function of log [≡SOH] for the oxidation of Mn(II) in the presence of goethite or lepidocrocite.	98
4.15	The effect of light upon the oxidation of Mn(II) oxidation in the presence of goethite or lepidocrocite.	101
4.16	Ln k_1 as a function of 1/T for the oxidation of Mn(II) in the presence of goethite or lepidocrocite.	106
4.17	Initial oxidation rate as a function of initial $(\equiv SO)_2$ Mn concentration.	110
4.18	Possible mechanism for the oxidation of Mn(II) on a metal oxide surface.	113
6.1	Half-life for Mn(II) oxidation on lepidocrocite.	138

NOTATION

[i]	concentration of species i, mole/L (M)
{i}	thermodynamic activity of species i, M
<i>	concentration of species i, moles/g of solid
≡SOH	surface hydroxyl group
a	solids concentration, g/L
A	specific surface area, m^2/g
A	$k_1/([\equiv SOH][Mn^{2+}])$, see equation 4.22
C	capacitance, $farad/m^2$
C_A	concentration of strong acid added, M
C_B	concentration of strong base added, M
C_+	capacitance of positively charged surface
C_-	capacitance of negatively charged surface
E_a	activation energy, kJ/mol
E.C.	exchange capacity, moles of sites/g of solid
F	faraday 96490 coul/mol
$Fe(III)_{total}$	total Fe(III) concentration, M
IAP	ion activity product
k_1	pseudo-first order rate constant, min^{-1}
k^*	rate constant (see equation 4.27)
k''	rate constant (see equation 4.1)
k_1^*	rate constant (see equation 4.1)
k_2^*	rate constant (see equation 4.1)
k_{Fe}	rate constant (see equation 4.2)
k_{hom}	rate constant (see equation 4.18)
k_{Mn}	rate constant (see equation 6.4)

NOTATION (continued)

k_{obs}	rate constant (see equation 4.18)
K^s	surface equilibrium constant
$K^s(intr)$	intrinsic surface equilibrium constant
K_{s0}	solubility product
Mn(II)	manganese in the +2 oxidation state
Mn(III)	manganese in the +3 oxidation state
Mn(IV)	manganese in the +4 oxidation state
Mn_T	total manganese concentration, M
Mn_f	filterable manganese (i.e. that which passes through the filter), M
Mn_{ads}	adsorbed manganese, M
Mn_{sol}	soluble manganese, M
MnO_x	oxidized manganese, M
$phth^{2-}$	phthlate ion
$p\epsilon$	$-\log\{e^-(aq)\}$
p_aH	$-\log\ \{H^+\}$
p_cH	$-\log\ [H^+]$
pH_{zpc}	pH at zero point of charge
pCO_2	partial pressure of CO_2, ppm
pN_2	partial pressure of nitrogen, atmospheres
pO_2	partial pressure of oxygen, atmospheres
R	oxygen consumption rate mg/L-min (see equation 4.13),
R	gas constant 8.314 J/mol-K
sal^{2-}	salicylate ion

NOTATION (continued)

S_T	total surface sites concentration, M
$t_{1/2}$	half-life
T	absolute temperature, K
$\alpha_{Mn^{2+}}$	fraction of soluble manganese present as Mn^{2+}
γ	activity coefficient
Γ	site density, moles/m^2
ΔH_{ads}	heat of adsorption, kJ/mol
σ_0	surface charge equiv./L
ψ_0	surface potential, V
ψ_1	potential at the mean plane of the counter ions, V

CHAPTER 1

INTRODUCTION

1.1 The importance of manganese in the aquatic environment

Manganese is an important element in the aquatic environment. It is the subject of much interest, because its oxides and hydroxides are highly adsorptive and are thought to scavenge other heavy metals (Jenne, 1968; Murray and Brewer, 1977; Singh and Subramanian, 1984). Of particular interest are ferromanganese nodules which are abundant in the aquatic environment. These deposits contain, in addition to iron and manganese, high concentrations of cobalt, nickel, copper, and other metals. The occurrence, origin, and importance of manganese deposits in the aquatic environment has been reviewed in three recent books (Glasby, 1977; Varentsov and Grasselly, 1980; Roy, 1981). Manganese is also of importance because it is an essential micronutrient for all organisms (Bowen, 1966; Wetzel, 1975; Sunda et al., 1983). It is a particularly important nutrient in plants because of its role in photosynthesis.

1.2 Aqueous chemistry of manganese

This section briefly reviews the aqueous chemistry of manganese of relevance to natural waters.

Manganese can exist in a number of oxidation states. The aqueous chemistry of manganese involves primarily the II, III, IV, VI, and VII oxidation states (Cotton and Wilkinson, 1980). The II and IV oxidation states are of

greatest importance in natural waters (Morgan, 1967). The III oxidation state is found in manganese minerals (Giovanoli, 1980), but probably is not found in solution in natural waters (Morgan, 1967). The relative stability of each oxidation state depends upon the pH and oxidation potential of the system. At the pH's found in natural waters, Mn(IV) is the thermodynamically stable form of manganese in the presence of oxygen. In reducing environments, Mn(II) is the thermodynamically stable form of manganese.

Mn(IV) is essentially insoluble in water. The crystal chemistry of Mn(IV) oxides is complex; more than 20 manganese oxides and hydroxides are found in nature. The occurrence, structure, and properties of these minerals has been extensively reviewed (see for example Bricker, 1965; Glasby, 1977; Burns and Burns, 1979; Giovanoli, 1980; Roy, 1981).

Mn(II) is relatively soluble and forms many complexes in aqueous solution. The sulfato and chloro complexes of Mn(II) are important in sea-water (Carpenter, 1983). Less than 5% of the dissolved manganese in sea-water is associated with carbonate, bicarbonate, or organic ligands (Carpenter, 1983). Wilson (1978) calculated that in low alkalinity fresh-waters (10^{-4} equiv./L), dissolved Mn(II) exists predominantly as the free aquo ion. In high alkalinity waters (10^{-2} equiv./L), $MnHCO_3^+(aq)$ and

$MnCO_3^o(aq)$ are important dissolved manganese species (Wilson, 1978).

In natural waters the solubility of Mn(II) is controlled by rhodocrocite, $MnCO_3(s)$ or by a mixed carbonate phase, $(Mg, Ca, Mn)CO_3(s)$ (Holdren et al., 1975; Suess, 1979; Klinkhammer, 1980; Pedersen and Price, 1982).

The aqueous chemistry of Mn(III) is not extensive. It is thermodynamically unstable and disproportionates in aqueous solution. The reaction is described by the equation

$$2Mn^{3+} + 2H_2O \rightleftharpoons Mn^{2+} + MnO_2 + 4H^+ : K = 10^9 \quad (1.1)$$

Strong Mn(III) complexes such as Mn(III) pyrophosphate can exist in aqueous solution, but probably are not found in natural waters (Morgan, 1967).

1.3 The geochemistry of manganese in the aquatic environment

This section presents an overview of manganese geochemistry in the aquatic environment. The review is selective, rather than comprehensive and serves to illustrate the importance of redox processes in manganese geochemistry. Since Mn(II) is relatively soluble and Mn(III) and Mn(IV) insoluble, the cycling of manganese in the aquatic environment is strongly influenced by redox conditions. The behaviour of manganese in environments where redox conditions change rapidly is of particular interest. Such environments include marine anoxic basins, stratified lakes, estuaries and some coastal waters.

Marine anoxic basins and stratified lakes

The behaviour of manganese in reducing fjords and other anoxic marine basins (see for example Spencer and Brewer, 1971; Emerson et al., 1979) and stratified lakes (see for example Delfino and Lee, 1971; Davison, 1982; Tipping et al., 1984) has been extensively studied. In these environments the manganese concentrations in the reducing bottom waters are very high and may exceed 5 μM (Emerson et al., 1979). Mn(II) diffusing from the bottom waters is oxidized above the oxycline. The oxidation of Mn(II) may be rapid. In the fjord, Saanich Inlet, the manganese residence time at the O_2-H_2S interface is of the order of a few days (Emerson et al, 1982).

Estuaries

The cycling of manganese in estuaries has been extensively studied (see for example Graham et al., 1976; Sholkovitz, 1976; Bewers and Yeats, 1978; Duinker et al., 1979; Eaton, 1979; Moore et al., 1979; Morris et al., 1979, 1982; Wollast et al., 1979). In estuaries both the pH and redox conditions may change rapidly. The pH changes may influence the kinetics of Mn(II) oxidation (as is discussed in Chapter 4, the kinetics of Mn(II) oxidation are strongly pH dependent). Manganese behaviour in estuaries is often non-conservative. Many processes are thought to influence manganese cycling in estuaries including adsorption and desorption from sediments (Graham et al., 1976; Duinker et

al., 1979), diffusion from and mixing of reduced manganese in sediment pore waters with the overlying waters (Graham et al, 1976; Duinker et al. 1979; Eaton, 1979; Morris et al., 1979, 1982), flocculation of manganese associated with colloids (Sholkovitz, 1976) and oxidative removal (Graham et al, 1976; Duinker et al. 1979; Eaton, 1979; Morris et al., 1979, 1982).

Coastal waters

Yeats et al. (1979) found that in the Gulf of St. Lawrence suspended particles in the bottom waters were rich in manganese. They suggested that Mn(II) diffusing from the bottom sediments was being oxidized on these suspended particles, then eventually these manganese-rich particles are transported off-shore and deposited in the deep-sea. Trefry and Presley (1982) suggest a similar process is occurring in the Mississippi Delta.

Open ocean

The manganese concentrations in open ocean are so low that reliable measurements have only recently been made of the concentration of manganese in this environment. The depth profile of manganese shows that it is enriched in the top few hundred metres of the ocean (Klinkhammer and Bender, 1980; Landing and Bruland, 1980; Martin and Knauer, 1980, 1982). In the surface waters most of the manganese is 'dissolved' (i.e. in a form that passes through a membrane filter). Sunda et al. (1983) suggest that the enrichment of

manganese in the surface waters is due to (i) high input rates from riverine and aeolian sources and (ii) photoactivated reduction of manganese oxides to Mn(II). These authors suggest that below the photic zone manganese is removed from solution as the result of oxidation. In this region manganese is associated with particles, which through settling are removed from the water column. An alternative explanation is that manganese is removed by adsorption on calcite (Martin and Knauer, 1982). Dissolved manganese may be regenerated at depth. It is suggested that the regeneration of manganese at depth is due to some or all of the following processes (i) hydrothermal injection, (ii) sediment resuspension, (iii) in-situ breakdown of particulate manganese, and (iv) advective- diffusive transport of dissolved manganese from the sediments (Landing and Bruland, 1980).

1.4 The persistence of Mn(II) in oxic waters

Geochemical and other evidence suggest that Mn(II) persists in oxygenated waters (Brewer, 1975; Carpenter, 1983), though Mn(IV) is the most stable oxidation state in these waters. The persistence of Mn(II) in oxic waters can be explained by the reduction of higher oxidation states by naturally occurring organics (Sunda et al., 1983; Stone and Morgan, 1984) and by the slow oxidation kinetics of Mn(II) (Morgan, 1967; Diem and Stumm, 1984). The rates of Mn(II) oxidation in natural waters, though slow, are typically

orders of magnitude faster than the rate of oxidation of Mn(II) in homogeneous solution (Diem and Stumm, 1984). It has been suggested that the enhanced oxidation of Mn(II) in natural waters is due to bacterial oxidation (Emerson et al., 1979, 1982; Chapnick et al., 1982; Diem and Stumm, 1984; Tipping et al., 1984) or to the "catalytic" effects of abiotic surfaces such as metal oxides (Morgan, 1967; Wilson; 1980; Morris et al., 1982; Sung and Morgan, 1981). The existing evidence suggests that in certain environments such as Saanich Inlet, bacterial mediation of the reaction is important (Emerson et al., 1979, 1982). But in general the relative importance of bacterial and abiotic "catalysis" in natural waters is unknown.

1.5 Scope and purpose of work

This work addresses the question of the importance of Mn(II) oxidation on metal oxide surfaces in natural waters. In this work the rate of Mn(II) oxidation on four metal oxides: goethite (α-FeOOH), lepidocrocite (γ-FeOOH), silica and alumina (δ-Al_2O_3) has been studied (see Chapter 4). The oxides of iron, silicon, and aluminium were chosen, because the oxides of these elements are the most abundant in the Earth's crust.

In addition to studying the effect of these metal oxides on the rate of Mn(II) oxidation, the adsorptive behaviour of manganese on these oxides was studied (see Chapter 3). The purpose of these studies was to develop a

model describing the adsorptive behaviour of Mn(II). This model was used in subsequent work to interprete the results from the oxidation experiments and to make predictions from these experiments about the behaviour of Mn(II) in natural waters.

The influence of solution chemistry on the rate of Mn(II) oxidation in the prescence of lepidocrocite is considered in Chapter 5. Lepidocrocite was used in these experiments, because it enhanced the rate of Mn(II) oxidation more than the other metal oxides studied.

The implications of the laboratory studies with regard to the rates of Mn(II) oxidation in natural waters are discussed in Chapter 6. In this chapter the important factors which influence Mn(II) oxidation in natural waters and the time scales for Mn(II) oxidation on metal oxide surfaces under the conditions found in natural waters are discussed.

CHAPTER 2

ANALYTICAL TECHNIQUES; PREPARATION, CLEANING AND CHARACTERIZATION OF METAL OXIDES; AND EXPERIMENTAL METHODS.

2.1 Analytical techniques

2.1.1 General remarks

Deionized distilled water was used to prepare all solutions. All reagents were analytical grade unless otherwise noted. The gases used were filtered and scrubbed in a Dreschel bottle.

The glassware and plasticware were cleaned in a strong detergent (Alconox), soaked in 4 M nitric acid for at least 12 hours, and rinsed five times with deionized distilled water. The solutions used in the adsorption and oxidation experiments, other than those prepared from strong acids, were filtered. 1M and 5M NaOH were filtered through Whatman GF-C filters; otherwise, 0.22 micron membrane filters (Millipore Type GSWP) were used.

The use of metals or materials containing metals was avoided whenever possible. The seals used in the Swinnex filters (Millipore) are made of silicone rubber, which contains a few percent by weight zinc oxide. However, as the Swinnex filters are used to filter the solutions immediately before they are analyzed or fixed to prevent any further oxidation of Mn(II), contamination at this stage of the experiment should not affect the results. The other equipment that contacted the solutions used in the adsorption and

oxidation experiments were constructed of pyrex glass, polyethylene, polypropylene or teflon; these materials contain few trace metal impurities (Robertson, 1968). PVC tubing (Nalge) was used for the gas lines.

2.1.2 pH measurements

pH measurements were made using a glass electrode and a double junction reference electrode; the outer compartment of the reference electrode was filled with 0.1 M $NaClO_4$. The electrode was calibrated using three or four NBS buffers (pHydrion or Radiometer). The buffers were adjusted to a temperature within 1°C of that used in the experiment.

Accurate pH measurements in suspensions containing a high solids concentration were difficult to make, because the electrode potential drifted slowly with time. In Figure 2.1 the potential drift in a silica suspension is shown. The suspension had been equilibrated for 2 weeks, so it is unlikely that the potential drift was due to a change in pH. Potential readings also drifted in suspensions containing alumina, goethite and lepidocrocite. In a suspension of high solids content an electrode may behave abnormally due to the "suspension effect", i.e., a junction potential induced by the motion of charged particles near the electrode surface (Warner, 1975), but this does not explain the potential drift. The drift may be due to the coating of the electrode with an oxide film. If the electrodes are stored for extended periods in an iron oxide suspension they become

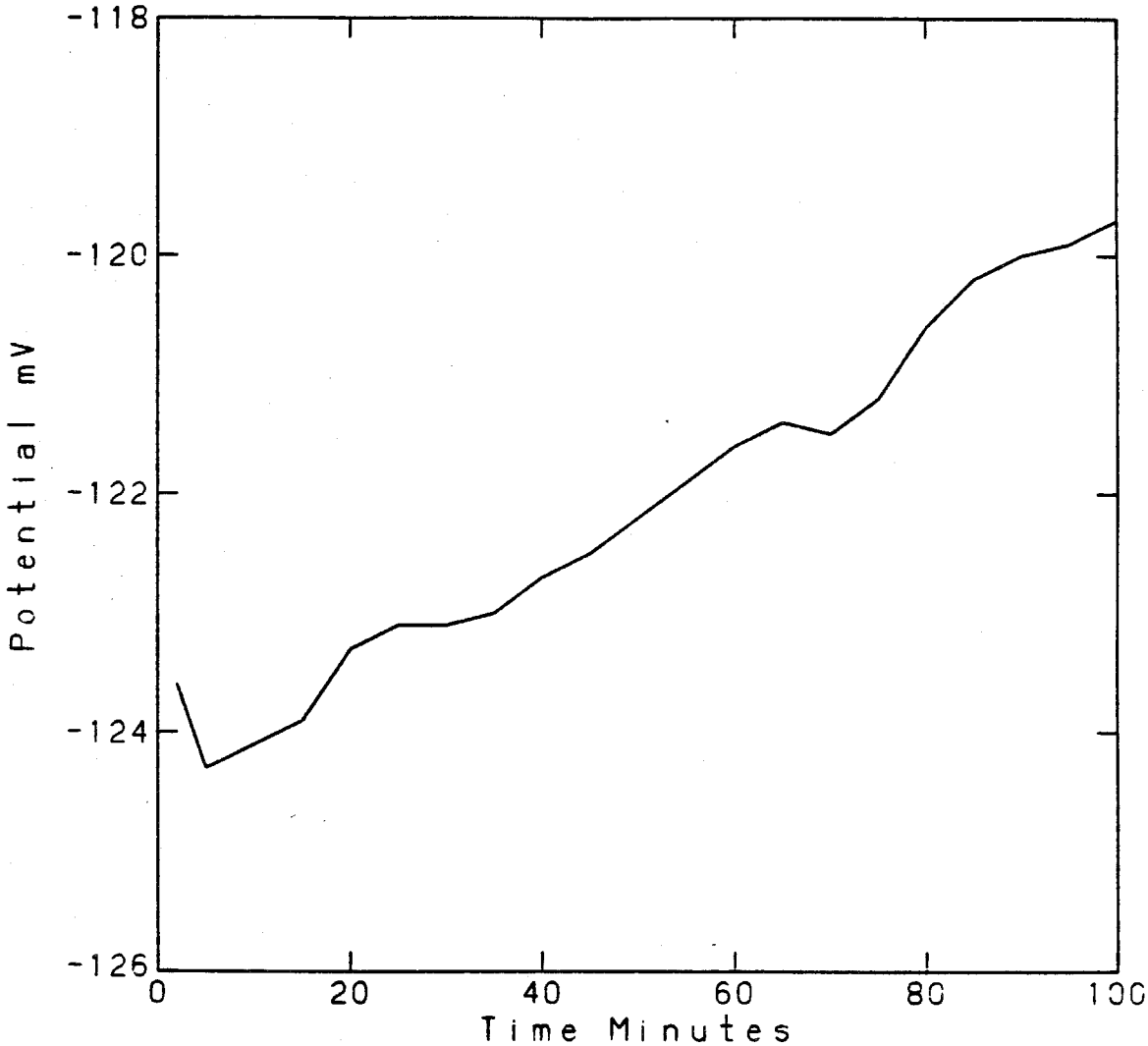

Figure 2.1 Potential drift of a pH electrode immersed in a silica suspension.

coated with film of the oxide. This film appears to affect the potential reading, since, if the electrodes were stored in a suspension for 1 hour, removed, washed with water and replaced in the suspension, the potential reading before and after washing differed by as much as 4mV.

The method adopted to measure pH in suspensions was as follows: the electrodes were placed in a gently stirred suspension and potential reading taken after 5 minutes. The electrodes were then removed, washed and stored in 0.1 M $NaClO_4$. During lengthy experiments, the pH meter was recalibrated every 2-3 hours. The results obtained by this method were compared with those obtained on filtered samples. As shown in Table 2.1, the results obtained by the two methods are in excellent agreement. The former method was adopted for routine measurements, because it is more convenient, and because pH changes may occur on filtration if the suspension is not equilibrated with the atmosphere.

2.1.3 Solids concentration

The concentration of the solid in the goethite and lepidocrocite suspensions was determined by dissolving a 10 mL aliquot of the suspension in 10 mL of concentrated HCl, diluting the sample 10 fold and analyzing for total iron by atomic absorption spectrophotometry (AAS) using a Varian AA-6. The experimental conditions employed are indicated in Table 2.2. The standards used to calibrate the instrument were prepared by dilution of stock solutions

Table 2.1 A comparison of direct pH measurements taken in silica suspensions with those taken after filtering the suspension.

Sample*	Direct	After filtration
A	7.152	7.159
B	8.214	8.238
C	8.517	8.506
D	9.154	9.187

* Samples are 0.5 g/L silica suspensions in 0.1 M $NaClO_4$, that have been adjusted to the desired pH, then equilibrated with the atmosphere for 1 week.

Table 2.2 Experimental conditions used for the atomic absorption spectrophotometric analyses for iron and manganese.

	Fe	Mn
Wavelength, nm	248.3	279.5
Spectral band pass, nm	0.2	0.5
Oxidant	Air	Air
Fuel	Acetylene	Acetylene
Flame condition	Oxidizing	Oxidizing
Lamp current, mA	5	3

(Baker, Dilut-it Standards) in the same matrix as the samples (0.6 M HCl). Repeated analysis of a 0.18 mM Fe sample indicates that the relative standard deviation for the analytical technique is ± 1.3%. The relative standard deviation for the overall procedure as determined by replicate analysis of a 5 mM geothite suspension is about ±4%.

The solids concentration of the alumina and silica suspensions were determined by gravimetry.

2.1.4. Manganese

Filterable manganese was determined by two methods; spectrophotometry using the formaldioxime method (Morgan and Stumm,1965) and atomic absorption spectrophotometry (AAS).

Formaldioxime The formaldioxime reagent was prepared by dissolving 20 g of hydroxylamine hydrochloride in 200mL water, adding 10mL of 37% formaldehyde to the solution and diluting to 500mL. 2mL of the formaldioxime reagent, 10mL of a 0.22 micron filtered sample, and 5mL of 5 M NaOH were pipetted into a 25 mL volumetric flask and made up to volume with deionized distilled water. Deoxygenated samples were oxygenated by bubbling pure oxygen through the sample. Full colour development was complete within 10 minutes, and the colour decreased slowly over a period of hours. Measurements of absorbance were taken 10-15 minutes after mixing the reagents. The absorbance was measured at a wavelength of 450 nm. The molar absorptivity was 1.3×10^4 M^{-1} cm^{-1} and

was not affected by the electrolytes used in this study (0.1 M $NaClO_4$, 0.0333 M Na_2SO_4, 0.7 NaCl and 0.7 M $NaClO_4$). Manganese standards were prepared by dissolving manganous perchlorate in deionized distilled water. The manganese content of the standard was determined by AAS. The relative standard deviation for the technique is ±0.7% at 20 μM Mn. Using a 5cm cell the detection limit was approximately 0.1 μM.

Atomic Absorption Spectrophotometry (AAS) Manganese was also determined by AAS using a Varian AA-6 spectrophotometer. The experimental conditions used are as indicated in Table 2.2. The standards used to calibrate the instrument were prepared by dilution of stock solutions (Baker, Dilut-it Standard) in 0.1 M $NaClO_4$. The relative standard deviation for the analytical technique is ±0.8% at 20 μM Mn. The detection limit for the technique was approximately 0.05 μM.

The two analytical techniques were compared by analyzing samples taken during an oxidation experiment by both methods. The results found by the two methods are the same within the precision of the analytical techniques (see Table 2.3).

The amount of adsorbed Mn was determined by difference, i.e.,

adsorbed Mn = total Mn - filterable Mn

Samples of the filtrate were analyzed for oxidizing

Table 2.3 A comparison of the results for filterable Mn using the formaldioxime and atomic absorption spectrophotometric methods.

	Filterable Mn, μM	
Sample	Formaldioxime	AAS
1	39.3	39.5
2	39.0	38.6
3	37.5	37.0
4	36.1	35.9
5	33.6	33.2
6	30.4	29.8
7	29.2	29.2
8	26.5	26.7
9	22.9	23.4
10	20.5	20.8

titre ([Mn(III)] + 2[Mn(IV)]) using the method of Kessick et al. (1972). The results indicated that the amount of Mn(III) and Mn(IV) solids that passed through the filter was less than 0.2 µM.

2.1.5 Calcium and magnesium

Calcium and magnesium were determined by atomic absorption spectrophotomentry using a Varian AA6 spectrophotometer. The experimental conditions used in these analyses are given in Table 2.4. The standards used to calibrate the instrument were prepared by dilution of stock solutions (Baker , Analysed Reagent) in 0.1 M $NaClO_4$. The samples were diluted to bring their concentration into the optimum working range.

2.1.6 Anions

Silicate, phosphate, sulfate, and chloride were determined using techniques described in Standard Methods (1980). The molybdisilicate method was used for silicate. Phosphate was determined by the vanadomolybdophosphoric acid method. Sulphate was determined by gravimetry. Chloride was determined by the mercuric chloride method. Salicylate and phthlate were determined by UV absorbance at 254 nm in a phosphate buffer (pH 7).

2.2 Preparation and cleaning of metal oxides

2.2.1 Geothite (α-FeOOH)

Geothite was prepared using the method of Atkinson et al. (1967). 200mL of 2.5 M KOH was added to 50g of

Table 2.4 Experimental conditions used for the atomic absorption spectrophotometric analyses for calcium and magnesium.

	Ca	Mg
Wavelength, nm	422.7	285.2
Spectral band pass, nm	0.2	0.1
Oxidant	N_2O	Air
Fuel	Acetylene	Acetylene
Flame condition	Reducing	Oxidizing
Lamp current, mA	6	3

$Fe(NO_3)_3.9H_2O$ (Mallinckrodt, AR grade) in 800mL of distilled deionized water. The precipitate was aged for 24hrs in 60°C oven. Polyethylene vessels were used to prevent silicate contamination.

The precipitate was washed by repeated centrifugation and decantation, then stored at pH 7.3 in a polyethylene bottle.

Two batches of geothite were prepared; they are designated G1 and G2.

2.2.2 Lepidocrocite (γ-FeOOH)

The method used to prepare lepidocrocite was similar to that described by Sung and Morgan (1981). A solution was prepared by the addition of 40mL of 1.0 M $NaHCO_3$ and 600mL of distilled deionized water to 160mL of 1 M $NaClO_4$, then the pH of the solution was adjusted to 7.3 using a 1.1% CO_2 / air mixture. 500mL of 10^{-2} M $Fe(ClO_4)_2$ solution was added to this solution in 100mL aliquots at intervals of approximately 15 minutes.

The precipitate was washed by repeated centrifugation and decantation and stored in a polyethylene bottle at pH 7. The solid was aged for two weeks before using it in any experiments.

Two batches of lepidocrocite were used in this work; they are designated L2 and L3.

2.2.3 Silica SiO_2

Aerosil 200, a amorphous pyrogenic silica, manufactured by Degussa Corporation was used in this work. The silica was dried in a 105°C oven before use.

2.2.4 Alumina

Aluminium Oxide C (Alox) manufactured by the Degussa Corporation was used in this work. The solid was cleaned by soaking in 0.1 M NaOH, followed by repeated washing using centrifugation and decantation.

The solid was stored in 0.1 M $NaClO_4$ at pH 8 in a polyethylene bottle.

2.3 Identification of solid phase

2.3.1 X-Ray diffraction

X-ray diffractograms were run on G1, G2, L2 and L3. A Cu Kα source was used in the diffractometer. The sample container was a 0.15mm thick aluminium plate, with a 20mm x 10mm hole cut in it, which when covered on one side with a piece of adhesive tape forms a well into which the sample is placed. The samples were dried at 40-45° C, ground in a mortar and pestle, placed in the sample container, and compacted with a spatula so they did not fall out of the sample container when it was tilted.

The peaks in the diffractogram are listed in Tables 2.5 and 2.6. The peaks for G1 and G2 correspond closely with those expected for goethite. The major peaks in the

Table 2.5 X-ray diffraction data for G1, G2 and goethite.

G1		G2		Geothite(1)	
d (Å)	$\frac{I}{I_o}$	d (Å)	$\frac{I}{I_o}$	d (Å)	$\frac{I}{I_o}$
4.98	10	4.96	15	4.98	15
4.17	100	4.17	100	4.18	100
-	-	-	-	3.38	10
2.69	50	2.70	40	2.69	30
2.59	15	2.58	20	2.58	8
-	-	-	-	2.520	4
2.50	sh	-	-	2.490	16
2.455	55	2.455	85	2.452	25
2.254	20	2.260	20	2.252	10
2.196	30	2.191	25	2.192	20
-	-	-	-	2.009	2
-	-	-	-	1.920	6
1.804	20	1.804	15	1.799	8
-	-	-	-	1.770	2
1.722	15	1.725	35	1.721	20
-	-	-	-	1.694	10
-	-	-	-	1.661	4

sh shoulder
\- peak absent
I intensity of peak
I_o intensity of most intense peak

(1) From Joint Committee on Powder Diffraction Standards File 17-736.

Table 2.6 X-ray diffraction data for L2, L3 and lepidocrocite.

L2		L3		Lepidocrocite (1)	
d (Å)	$\frac{I}{I_o}$	d (Å)	$\frac{I}{I_o}$	d (Å)	$\frac{I}{I_o}$
6.26	100	6.28	100	6.26	100
3.30	30	3.27	50	3.29	90
2.58	20	2.57	10	-	-
2.43	60	2.45	60	2.47	80
-	-	-	-	2.36	20
-	-	2.25	10	-	-
-	-	2.19	10	-	-
-	-	-	-	2.09	20
1.93	20	1.93	40	1.937	70
-	-	-	-	1.848	20
1.79	10	-	-	-	-
-	-	-	-	1.732	40

- peak absent
I intensity of peak
I_o intensity of most intense peak

(1) From Joint Committee on Powder Diffraction Standards File 8-98.

diffractograms for L2 and L3 agree quite well with those expected for lepidocrocite. There are some additional weak peaks in these diffractograms. The peaks at a d-spacing of 2.25 Å and 2.19 Å, may be due to ferrihydrite, which is a common impurity in lepidocrocite preparations (Schwertmann and Taylor,1979; Waite,1983). The peaks in the diffractograms of L2 and L3 are weaker and relatively broader than those in in the diffractograms of G1 and G2. The broadening and low intensity of the peaks suggests that L2 and L3 are poorly crystalline, which is not surprising considering that in L3 the lath-like crystals are about 100-200 nm long and 10-50 nm wide (see section 2.3.2).

2.3.2 Electron microscopy

Transmission electron microscopy was used to identify the morphology of the crystals in G1, G2, L2 and L3. The samples were prepared by placing 20 µL of a suspension containing about 50 mg/L of the solid on a specimen grid coated with a thin film of carbon and evaporating off the water under an infra-red lamp.

Figure 2.2a shows that the crystals in the lepidocrocite preparation are laths, about 100-200 nm long and 10-50 nm wide. This is a morphology typical of lepidocrocite (Schwertmann and Taylor,1979).

Figure 2.2b shows that the crystals in the goethite preparation are acicular. This is a morphology typical of goethite (Cornell et al., 1974). The crystals are about

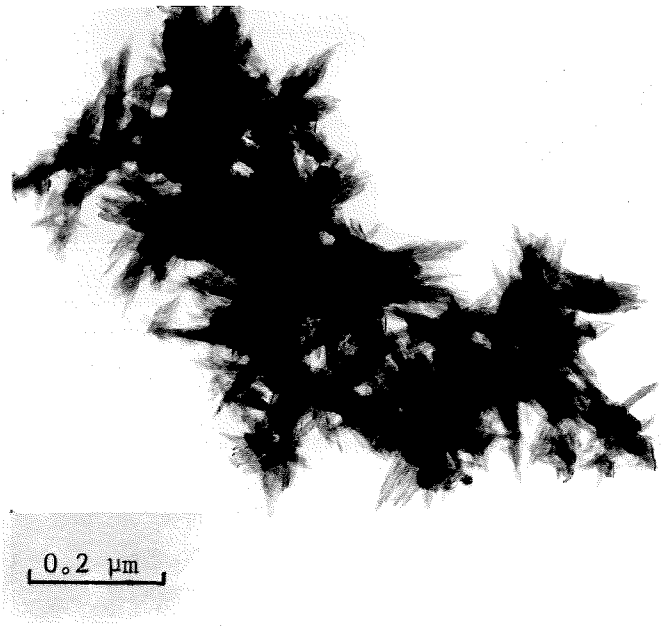

Figure 2.2a Transmission electron micrograph of L3 (lepidocrocite).

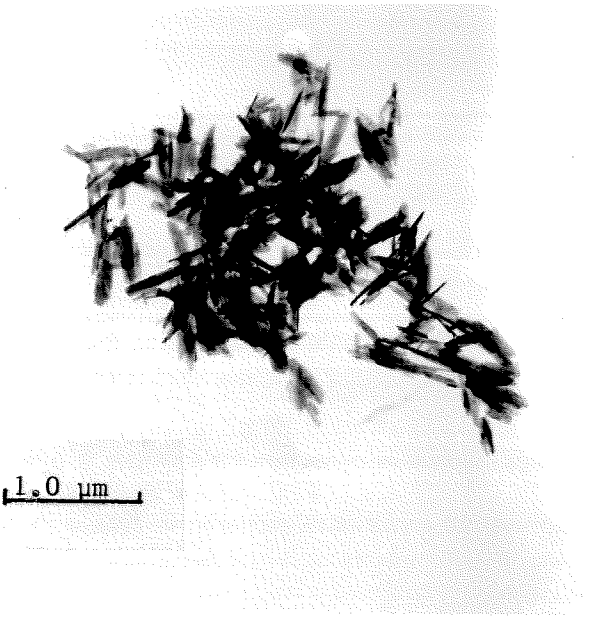

Figure 2.2b Transmission electron micrograph of G2 (goethite).

150-400 nm long and 10-50 nm wide.

2.3.3 Additional information and summary

The silica and alumina used in this study are commercial products that have been characterized by other workers. Aerosil 200 is an X-ray amorphous solid that consists of primary particles about 1nm in diameter which are condensed to form spherical secondary particles 12 to 14 nm in diameter (Kent, 1983).

Alox consists predominantly of δ-Al_2O_3 (Kummert and Stumm, 1980).

G1 and G2 are yellowish brown and L2 and L3 are orange, which are the the colours characteristic of goethite and lepidocrocite, respectively (Schwertmann and Taylor, 1977).

G1 and G2 appear to consist predominantly of goethite. Lepidocrocite is the major component in L2 and L3. Some ferrihydrite might be present as an impurity. These solids are poorly crystallized.

2.4 Surface properties of the metal oxides

2.4.1 Surface area by B.E.T. analysis

The surface area was determined by single point B.E.T. nitrogen adsorption. The solids were washed, dried and lightly ground in a mortar and pestle before analysis. R.J. Bales analysed the Alox sample.

The surface areas determined are reported in Table 2.7.

Table 2.7 Specific surface area, exchange capacity, and site density for goethite, lepidocrocite, silica and alumina.

	Specific Surface (m^2/g)	Exchange Capacity (moles/g)	Site Density (OH groups/nm^2)
Goethite			
G1	34	7.34×10^{-4}	13
G2	-	6.60×10^{-4}	-
Lepidocrocite			
L2	142	2.27×10^{-3}	9.6
L3	-	2.58×10^{-3}	-
Silica	182*	1.50×10^{-3}	5.0
Alumina	82+	7.28×10^{-4}	5.3

* after Young (1981)

\+ analysis by R.J. Bales.

2.4.2 Exchange capacity

The exchange capacity, i.e. the total number of exchangeable groups on the surface, was determined by fluoride adsorption. The method was as follows: an excess of F^- was added to the suspension and the pH adjusted to ~4, then the suspension was shaken for 1hour and filtered. The F^- in the filtrate was determined using an Orion 940900 fluoride electrode.

The exchange capacity of the solids is given in Table 2.7.

2.4.3 Site density

The site density, calculated from the exchange capacity and surface area measurements, is shown in Table 2.7. Using Parfitt et al.'s (1976) data, the calculated site density on the goethite surface is approximately 8 OH groups/nm^2. The site density on lepidocrocite is estimated to be 8.4 OH groups/nm^2 (Sung and Morgan, 1981). On the fully hydroxylated silica surface there are 4 to 5 OH groups/nm^2 (Iler, 1979). Kummert and Stumm (1980) found by tritium exchange, that the site density on the δ-Al_2O_3 surface was 8.5 OH groups/nm^2.

2.4.4 Acid-base titration

The surface acidity constants for the goethite, lepidocrocite and alumina surface were obtained by acid-base titration. The titrations were performed under high purity nitrogen at 25°C. The procedure was as follows: 100 mL of a

suspension containing a known amount of the oxide in 0.1 M $NaClO_4$ was adjusted to pH 10 - 11 using a known volume of 0.1 M NaOH (Baker, Dilut-it Standard, CO_2 free). Then additions of 0.01 M HNO_3 (Baker, Dilut-it Standard) were made using a buret. After each addition the suspension was allowed to equilibrate for 10 minutes before the pH reading was taken. Blank corrections were made by titrating 0.1 M $NaClO_4$.

2.4.5 Mn(II) adsorption experiments

The reaction vessel used in these experiments is shown in Appendix B. It consisted of a 1 liter Pyrex glass jacketed beaker sandwiched between two plates of Lucite. Holes were made in the top plate to accept a thermometer, electrodes and a gas dispersion tube and to allow sampling and the addition of reagents. The experiments were performed at 25 ± 0.2°C. The procedure was as follows: 600 mL of the suspension was placed in the reaction vessel and the pH adjusted to ~ 8 by the addition of 0.1 M NaOH (Baker, Dilut-it Standard). The solution was then deoxygenated by bubbling with nitrogen at a flow rate of 500 cc/minute. After bubbling N_2 for 1 hour, 3mL of 0.01 M $Mn(ClO_4)_2$ solution was added, then 10 minutes later the pH was recorded and a 20mL sample withdrawn. The sample was filtered using a 0.22 micron filter (Millipore, Type GSWP). The first 5mL of the filtrate was discarded and the remainder analyzed for Mn using the formaldioxime technique. After taking the first

measurements an aliquot of deoxygenated 0.1 M NaOH was added to the solution using a Radiometer ABU11 autoburet. After 10 minutes the pH was recorded and another sample taken for Mn analysis. This procedure was repeated until the experiment was completed. The amount of adsorbed Mn was calculated by difference.

The kinetics of adsorption were studied by adjusting the pH of 600 mL of the suspension to the desired value, deoxygenating the solution, adding 3 mL of 0.01 M $Mn(ClO_4)_2$ solution, and then following the removal of filterable Mn.

2.4.6 Other adsorption studies

The methods used in these experiments were similar to those used in Mn(II) adsorption studies, but in these studies the solution was not deoxgenated. Silicate was added as a monosilicic acid solution (Santschi and Schindler, 1974). Phosphate, chloride and sulfate were added as Na_2HPO_4, NaCl and $NaHSO_4$ solutions. Salicylate and phthlate were added as stock solutions. The stock solutions were prepared by adding the organic acid to distilled water and adjusting the pH to approximately 8.3 with 0.1 M NaOH. Ca^{2+} and Mg^{2+} were added as solutions of their perchlorate salts. As in the Mn(II) adsorption studies the amount adsorbed was determined by difference. The analytical methods used are described in section 2.1.6.

2.5 Oxidation studies

The reaction vessel used in these experiments was the

jacketed vessel described in Section 2.4.5. The initial volume of the suspension was 600 mL. Buffers were used to control the pH of the suspension. For all but one experiment, a carbonate buffer system was used. This buffer was prepared by equilibrating the suspension with a gas mixture containing CO_2. The CO_2 content of the gas was determined by the manufacturer (Matheson Gas). The pH of the solution was adjusted to the desired value by the addition of 0.1 M NaOH or 0.1 M $HClO_4$. In one experiment, a NH_4^+/NH_3 buffer was used. This buffer was prepared by adding 20 mL of 0.1 M NH_4OH to the suspension and adjusting the pH to the desired value using 0.1 M $HClO_4$. For the systems buffered with carbonate, after adjusting the pH, the solution was deoxygenated by bubbling with a N_2/CO_2 mixture (Matheson Gas, Certified standard) for at least 1 hour, then 3 mL of deoxygenated 0.01 M $Mn(ClO_4)_2$ was added to the suspension. Normally the Mn(II) was allowed to equilibrate with the suspension for 30 minutes before switching to O_2/CO_2 (Matheson Gas, Certified standard) or air bubbling, but in some of the earlier experiments longer equilibration times were used to investigate whether there was any slow adsorptive uptake of Mn. The adsorbed Mn prior to commencing the oxidation was measured. The rate of oxidation was monitored by following the rate of loss of filterable Mn. For the NH_4^+/NH_3 buffered system, essentially the same procedure was used, except that in this experiment CO_2 free

gases (Matheson Gas, high purity nitrogen or extra dry oxygen) were used.

Several experiments were performed with no solid present to measure the homogeneous oxidation rate. In these experiments the solution was not deoxgenated initially.

2.6 Methods for the calculation of the equilibrium distribution of chemical species

The simpler calculations of the equilibrium composition of the systems studied were made by hand or using a programmable calculator. The computer program SURFEQL (Faughnan, 1981) was used for the more complex calculations. SURFEQL is a modified version of the program MINEQL (Westall et al., 1976) that can consider surface equilibria.

The equilibrium constants used in these calculations are given in Appendix A and in Chapters 3 and 5.

CHAPTER 3

SURFACE CHEMICAL PROPERTIES OF METAL OXIDES

In this chapter the acid-base properties and Mn(II) adsorption characteristics of the metal oxides studied are discussed. The purpose of this work is to develop a model describing the adsorptive behaviour of Mn(II). This model is useful in subsequent work to interpret the results from the oxidation experiments and to make predictions from these experiments. The possible speciation of the oxide surface is considered.

3.1 Theory

The nature of the metal oxide surface in aqueous solution is discussed in detail by several authors (Bowden et al., 1977; Davis and Leckie, 1979; Stumm et al., 1980; Schindler, 1981). The surface reactions of a metal oxide surface can be formulated in a coordination chemical framework which is modified to take into account electrostatic forces.

The surface groups of a metal oxide are amphoteric and the surface hydrolysis reactions can be written

$$\equiv SOH_2^+ \overset{K^s_{a1}}{\rightleftharpoons} \equiv SOH + H^+ \qquad (3.1)$$

$$\equiv SOH \overset{K^s_{a2}}{\rightleftharpoons} \equiv SO^- + H^+ \qquad (3.2)$$

where $\equiv SOH$ represents a surface group,

$$K^s_{a1} = \frac{\langle \equiv SOH \rangle [H^+]}{\langle \equiv SOH_2^+ \rangle} \tag{3.3}$$

$$K^s_{a2} = \frac{\langle \equiv SO^- \rangle [H^+]}{\langle \equiv SOH \rangle} \tag{3.4}$$

$[H^+]$ is the concentration of the hydrogen ion in solution (in moles/L), and <i> is the concentration of species i at the surface. The surface concentration is expressed in units of moles of surface groups per gram of solid.

The acidity constants described by equations 3.1 and 3.2 are microscopic constants because each loss of a proton reduces the charge on the surface and thus affects the acidity of neighbouring groups. The acidity constants may be written

$$K^s_{ai} = K^s_{ai}(intr) \exp\left(\frac{F\psi_{H^+}}{RT}\right) \tag{3.5}$$

where the intrinsic acidity constant $K^s_{ai}(intr)$ is the acidity constant in a hypothetically chargeless surrounding, ψ_{H+} is the effective potential difference between the binding site for H^+ and the bulk solution, F, the Faraday, R the gas constant, and T the absolute temperature.

The adsorption of a manganese ion Mn^{2+} can be explained in terms of competition with protons for surface sites. Three possible surface species containing Mn^{2+} will be

considered, and defined as

monodentate,

$$\equiv SOH + Mn^{2+} \overset{{}^{*}K_1^s}{\rightleftharpoons} \equiv SOMn^{+} + H^{+} \qquad (3.6)$$

bidentate,

$$\begin{matrix} =S-OH \\ | \\ =S-OH \end{matrix} + Mn^{2+} \overset{{}^{*}\beta_2^s}{\rightleftharpoons} \begin{matrix} =SO \\ | \quad \diagdown \\ =SO \quad Mn \end{matrix} + 2H^{+} \qquad (3.7)$$

and hydrolyzed,

$$\equiv SOH + Mn^{2+} + H_2O \overset{{}^{*}K^s_{MnOH}}{\rightleftharpoons} \equiv SOMnOH + 2H^{+} \qquad (3.8)$$

The corresponding intrinsic constants are,

$${}^{*}K_1^s(intr) = {}^{*}K_1^s \exp\left(\frac{2F\psi_{Mn^{2+}}}{RT}\right) \exp\left(\frac{-F\psi_{H^+}}{RT}\right) \qquad (3.9)$$

$${}^{*}\beta_2^s(intr) = {}^{*}\beta_2^s \exp\left(\frac{2F\psi_{Mn^{2+}}}{RT}\right) \exp\left(\frac{-2F\psi_{H^+}}{RT}\right) \qquad (3.10)$$

$${}^{*}K^s_{MnOH}(intr) = {}^{*}K^s_{MnOH} \exp\left(\frac{2F\psi_{Mn^{2+}}}{RT}\right) \exp\left(\frac{-2F\psi_{H^+}}{RT}\right) \qquad (3.11)$$

where $\psi_{Mn^{2+}}$ is the effective potential difference between the binding site for Mn^{2+} and the bulk solution.

Though the existing models of the oxide surface agree that the properties of the oxide surface can be considered within a coordination chemical framework, there exists

considerable disagreement about how to take account of the electrostatic effects. These disagreements rest ultimately on the physical picture of the structure of the solid-solution interface that is assumed in the model. Westall and Hohl (1980) compared in detail five electrostatic models for the oxide surface-solution interface. They found that all the models could represent the experimental data equally well, but that the values of corresponding parameters in different models are not the same. Hence, while a model may describe the experimental data, this does not necessarily indicate that the description of the oxide surface-solution interface in the model is realistic. In this work the constant capacitance model (Stumm et al.,1980; Schindler, 1981) has been used. This model describes the properties of the interface in solutions of high ionic strength where the double layer thickness and potential are small. A schematic representation of the surface is given in Figure 3.1. Specifically adsorbed ions are located at the solid surface in the σ_o plane and the counter ions are placed at the σ_1 plane. The potential at the σ_1 plane, ψ_1 is assumed to be zero. The relationship between the surface charge σ_o and surface potential ψ_o is given by

$$\sigma_o = C\psi_o \qquad (3.12)$$

where the capacitance C is a constant. In this model all

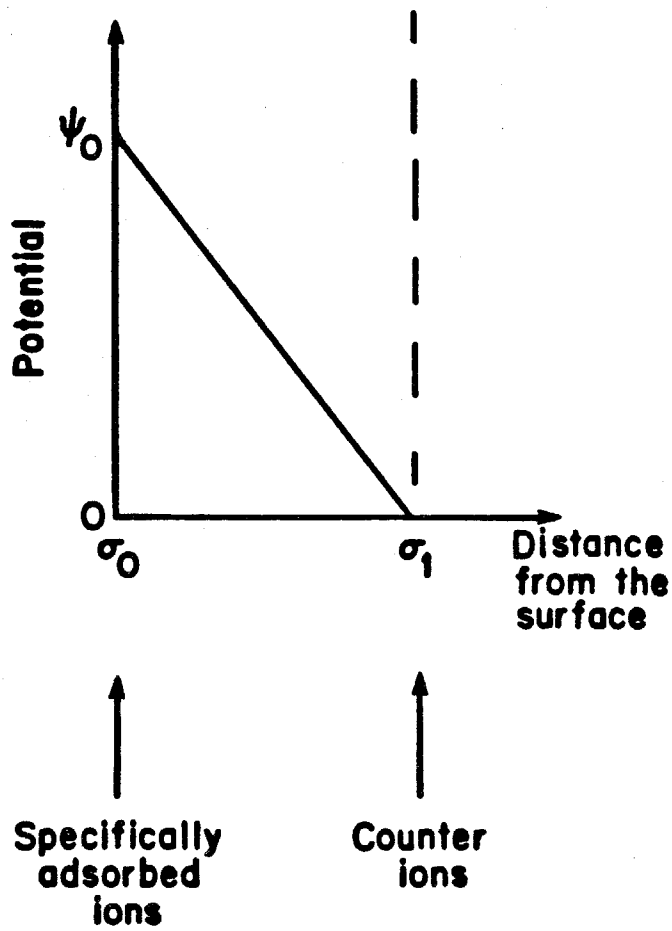

Figure 3.1. Schematic representation of the potential distribution at the metal oxide-water interface.

bound ions are assigned to the same mean plane of adsorption, so, $\psi_{H^+} = \psi_{Mn^{2+}} = \psi_o$.

Since formation of complexes between surface groups and the background electrolyte ions are not considered in the model, surface hydrolysis constants must be determined for each electrolyte concentration of interest. No generality in applying the model is lost by neglecting the interaction between surface groups and the electrolyte, since the constants obtained are necessarily "conditional constants", valid only in the electrolyte in which they were obtained because the activity coefficients for surface species are unknown. The constants in another electrolyte can only be expressed by a new set of conditional constants.

3.2. Results and discussion

3.2.1. Titration

From the titration data the surface charge at each point on the titration curve can be calculated using the charge balance equation:

$$\sigma_o(eq/L) = C_A - C_B + [H^+] - [OH^-] \qquad (3.13)$$

$$= (<\equiv SOH_2^+> - <\equiv SO^->) \cdot a \qquad (3.14)$$

where,

σ_0 = surface charge in eq/L

C_A = moles/L of strong acid added

C_B = moles/L of strong base added

a = solids concentration in g/L.

$[H^+]$ and $[OH^-]$ are calculated from the pH measurements using activity corrections calculated from the Davies equation ($\gamma_{H^+} = \gamma_{OH^-} = 0.774$).

The total concentration of surface sites S_T is given by

$$S_T \text{ (moles/L)} = a \times E.C. \tag{3.15}$$

where,

E.C. = exchange capacity (see section 2.4.2 for definition).

$$S_T = [\equiv SOH] + [\equiv SOH_2^+] + [\equiv SO^-] \tag{3.16}$$

The pH_{zpc} is the pH at which $[\equiv SOH_2^+] = [\equiv SO^-]$.

At pH $<<$ pH_{zpc}, $\sigma_o \sim [\equiv SOH_2^+]$, thus

$$[\equiv SOH] = S_T - \sigma_o \tag{3.17}$$

At pH $>>$ pH_{zpc}, $\sigma_o \sim -[\equiv SO^-]$ and

$$[\equiv SOH] = S_T + \sigma_o \tag{3.18}$$

Using these approximations, the acidity constants can be calculated from equations 3.3 and 3.4. A plot of pK_{ai} against surface charge is linear except near pH_{zpc} (see Figure 3.2). By extrapolating the linear portion of these plots to the zero point of charge the values of the intrinsic hydrolysis constants can be obtained. The specific capacitance C is given by

$$C = \frac{F}{2.303RT} \cdot \frac{1}{b} \cdot \frac{F}{a \cdot A} \tag{3.19}$$

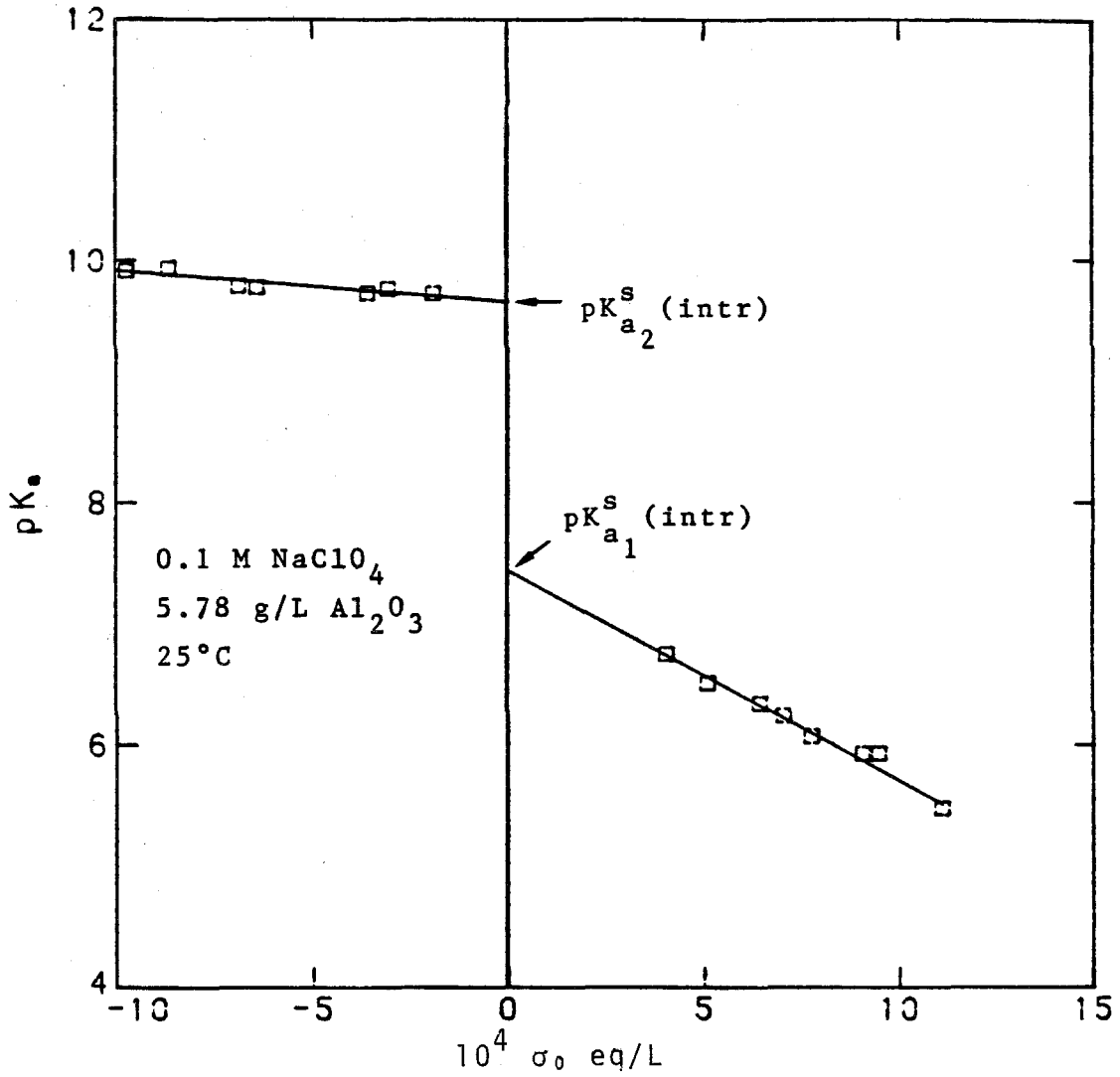

Figure 3.2. A plot $pK^s_{a_1}$ as a function of surface charge σ_o. Extrapolation to zero charge gives the intrinsic acidity constants.

where b is the slope of the plot pK_{ai} vs. σ_o and A is the specific surface area (in m^2/g).

The capacitance for the positively charge surface is C_+ and the capacitance for the negatively charged surface is C_- .

The intrinsic constants, pH_{zpc}'s, and capacitances for α-FeOOH, γ-FeOOH, and δ-Al_2O_3 obtained from the titration data are given in Table 3.1. The data for each solid agree well with each other and with other published data for these oxides. The cited data are selective, representing published values for the properties of these solids in similar electrolytes.

For all three oxides, C_+ is less than C_-. Since the ClO_4^- is larger than the Na^+ ion, it is reasonable that the double layer on the positively charged surface is thicker than on the negatively charged surface.

Figure 3.3 shows that for a typical data set, the curve calculated using the constants obtained from the experimental titration data fits the data reasonably well.

The data obtained by Young (1981) for the Aerosil 200 surface were used in this work; these data are given in Table 3.2. In order to fit his data, Young found it necessary to consider the formation of a surface complex with Na^+.

Table 3.1 The acidity constants, pH_{zpc} and capacitances of α-FeOOH, γ-FeOOH and γ-Al_2O_3 surfaces.

Oxide	Electrolyte	$pK^s_{a_1}$	$pK^s_{a_2}$	pH_{zpc}	C_+, F/m^2	C_-, F/m^2	Reference
α-FeOOH	0.1 M $NaClO_4$	6.21	8.8	7.5	2.5	3.6	This work, Batch G1
	"	6.08	9.05	7.57	-	-	" " Batch G2
	"	6.33	8.93	7.63	-	-	" " Batch G2
	"	6.4	9.25	7.8	2.3*	3.8*	Sigg and Stumm (1981)
	0.1 M NaCl	-	-	7.5	-	-	Balistrieri and Murray(1981)
	0.1 M KCl	-	-	7.5	-	-	Atkinson et al. (1967)
	0.1 M NaCl	-	-	7.7	-	-	Hingston et al. (1968)
	0.1 M KNO_3	-	-	7.5	-	-	Yates and Healy (1975)
γ-FeOOH	0.1 M $NaClO_4$	6.4	8.32	7.23	2.8	3.9	This work, Batch L2
	"	6.05	8.14	7.10	2.2	3.7	" " Batch L2
	"	5.65	8.13	6.89	-	-	" " Batch L3
	0.7 M NaCl	-	-	6.77	-	-	Sung (1981)
	"	5.7	7.7	6.7	-	-	Waite (1983)
γ-Al_2O_3	0.1 M $NaClO_4$	7.64	9.7	8.6	2.0	13	This work
	"	7.4	10.0	8.7	1.3*	13*	Kummert and Stumm (1980)
	"	7.2	9.5	8.3	-	-	Hohl and Stumm (1976)

*Calculated from author's results.

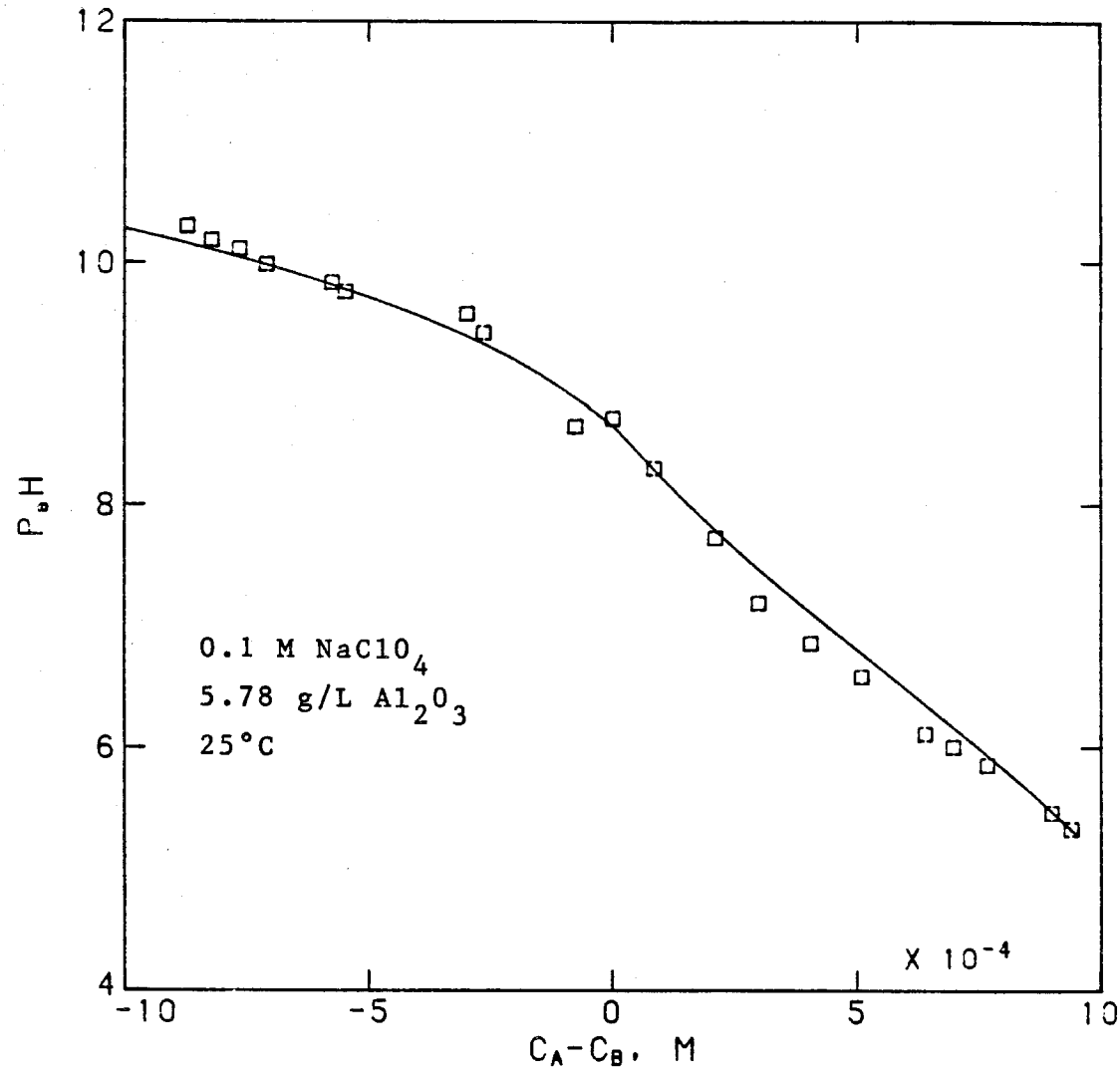

Figure 3.3. Titration data for γ-Al_2O_3. The solid curve is calculated using the constants given in Table 3.1.

Table 3.2 Physical and chemical properties of the Aerosil 200 surface (after Young, 1981).

Specific surface area	A	182 m^2/g
Capacitance	C	125 F/m^2
Site density		2.4 sites/nm^2
	$pK^s_{a_1}$	~ -3
	$pK^s_{a_2}$	7.8
	$p^*K^s_{1,Na}$	9.5

$$^*K^s_{1,Na} = \frac{\{\equiv SiO^-Na^+\}\ [H^+]}{\{\equiv SiOH\}\ [Na^+]}$$

3.2.2 Mn(II) adsorption

3.2.2.1 Kinetics of adsorption

The intial uptake of Mn(II) on the metal oxides is rapid (see Tables 3.3 -3.7 and Figure 3.4). After this the amount of Mn(II) in solution is either constant or decreases very slowly. The uptake of Mn(II) is too rapid to accurately measure the rate of uptake, but the half-life for adsorption reaction is less than five minutes. The continued slow uptake occurring in some cases may be due to slow adsorptive uptake or oxidation by residual oxygen.

3.2.2.2 Effect of pH on Mn(II) adsorption

As is shown in Tables 3.8 - 3.11 and Figure 3.5 the amount of Mn(II) adsorbed increases rapidly in a narrow pH range. Similar results were obtained by other workers for Mn(II) adsorption on lepidocrocite (Sung and Morgan, 1981), goethite (Grimme, 1968), and silica (Vydra and Galba, 1969).

It is possible to model the adsorption of Mn(II) using the framework outlined in Section 3.1. In these calculations the hydrolysed species is not considered. The reason for not considering both the hydrolysed and bidentate species simultaneously is that the concentration of both species have the same pH dependence, so it is impossible using the available data to make anything but an arbitrary choice about the relative proportions of each species. In these calculations the values given in Table 3.1 for the acid - base equilibria and the capacitance for the negatively

Table 3.3 Kinetics of adsorption of Mn(II) on goethite at pH 9.00.

Time (mins)	Filterable Mn µM
2	39.2
4	39.4
6	39.1
10	39.2
15.5	38.9
29	38.7
50	38.5

[α-FeOOH] = 0.449 g/L, 0.1 M $NaClO_4$, 25°C

pH = 9.00, pCO_2 = 324 ppm, pN_2 = 1.00 atm,

Mn_T = 50 µM.

Table 3.4. Kinetics of adsorption of Mn(II) on goethite at pH 8.05

Time (mins)	Filterable Mn µM
1.5	47.1
4	47.0
6	47.0
8	47.2
20	47.1
40	46.9
60	47.0

[α-FeOOH] = 0.445 g/L, 0.1 M $NaClO_4$, 25°C

pH = 8.05, pCO_2 = 324 ppm, pN_2 = 1.0 atm,

Mn_T = 50 µM.

Table 3.5. Kinetics of adsorption of Mn(II) on lepidocrocite.

Time (mins)	Filterable Mn μM
1.5	43.5
3.2	39.7
4.5	37.4
6	37.8
8	37.8
10	38.0
30	38.2
60	38.3

[γ-FeOOH] = 0.0899 g/L, 0.1 M $NaClO_4$, 25°C

pH = 8.52; pCO_2 = 324 ppm, pN_2 = 1.00 atm,

Mn_T = 50 μm.

Table 3.6. Kinetics of Adsorption of Mn(II) Aerosil 200.

Time (mins)	Filterable Mn μM
2	35.7
3.7	33.4
5	33.6
8	33.5
10	32.7
20	33.2
40	33.0
60	32.6

[SiO_2] = 0.0391 g/L, 0.1 M $NaClO_4$, 25°C

pH = 9.15, pCO_2 = 324 ppm, pN_2 = 1.00 atm,

Mn_T = 50 μM.

Table 3.7. Kinetics of adsorption of Mn(II) on alumina.

Time (mins)	Filterable Mn μM
2	40.2
4.5	38.9
7	38.9
10	38.8
20	38.3
40	39.0
60	38.5

$[\delta\text{-}Al_2O_3]$ = 0.503 g/L 0.1 M $NaClO_4$, 25°C

pH = 8.62, pCO_2 = 340 ppm, pN_2 = 1.00 atm,

Mn_T = 50 μM.

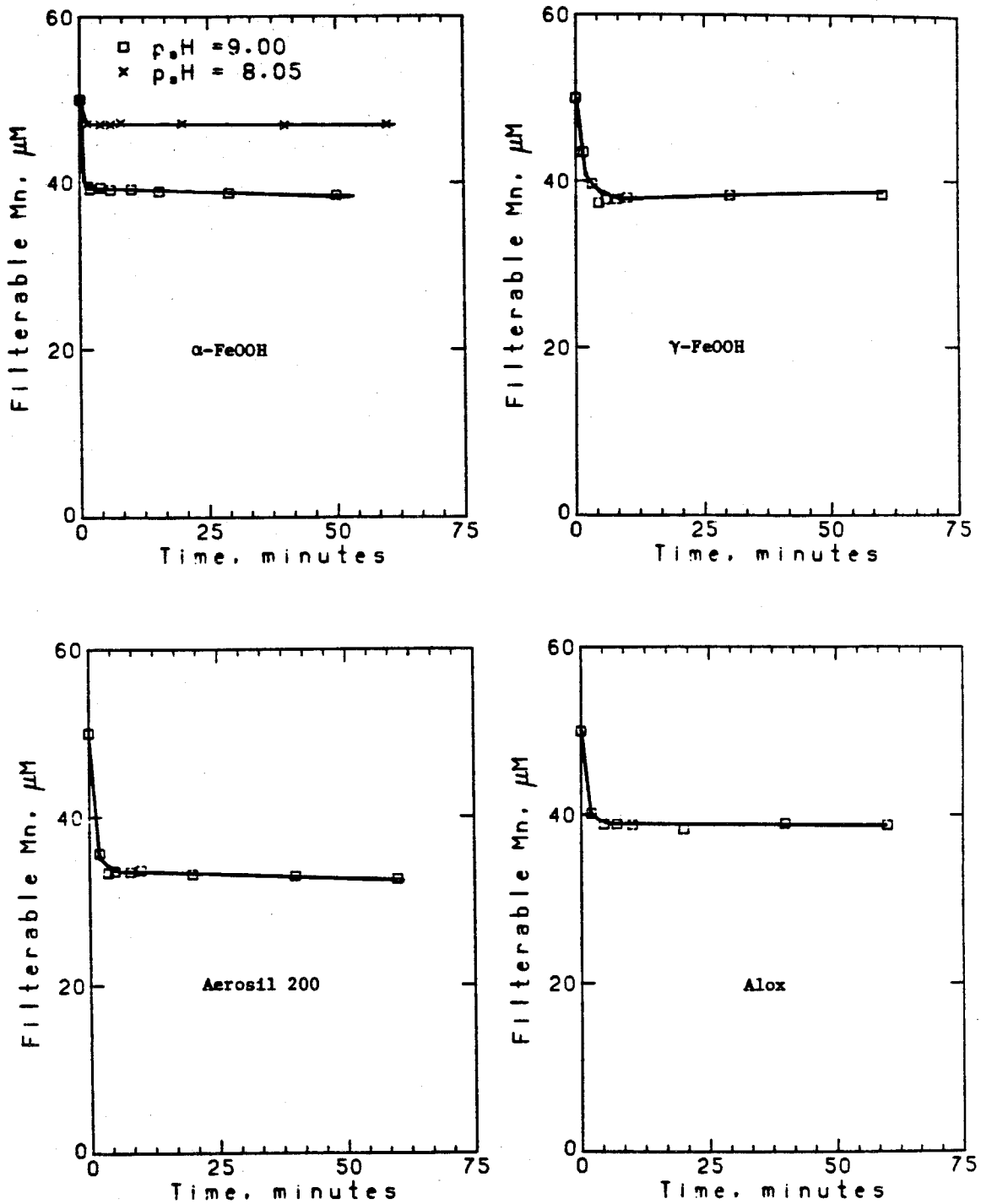

Figure 3.4. Kinetics of adsorption of Mn(II) on goethite, lepidocrocite, silica and alumina. The experimental conditions are given in Tables 3.3 - 3.7.

Table 3.8. Adsorption of Mn(II) on goethite as a function of pH.

pH	Adsorbed Mn, μM
8.02	2.4
8.15	3.6
8.25	5.7
8.28	6.4
8.36	9.8
8.44	12.5
8.49	13.5
8.60	19.9
8.63	22.4
8.72	28.7

0.89 g FeOOH/L (Batch G1) in 0.1 M $NaClO_4$

25°C, Mn_T 50 μM, pN_2 = 1.0 atm.

10 minute equilibration time.

Table 3.9. Adsorption of Mn(II) on lepidocrocite as a function of pH.

pH	Adsorbed Mn, μM
7.68	6.2
7.80	8.5
7.91	11.8
7.99	13.0
8.05	14.1
8.13	18.0
8.20	22.8
8.28	27.1
8.36	28.8
8.42	30.9
8.51	36.7
8.59	38.9
8.68	40.3
8.76	42.6
8.85	45.3
8.91	46.4

0.45 g FeOOH (Batch L2)/L in 0.1 M $NaClO_4$,

25°C, Mn_T 50 μM, pN_2 = 1.0 atm.

10 minute equilibration time.

Table 3.10. Adsorption of Mn(II) on silica as a function of pH.

pH	Adsorbed Mn, μM
8.07	0.5
8.23	1.5
8.41	3.2
8.53	4.4
8.68	5.0
8.85	8.1
8.95	8.1
9.05	11.6
9.22	14.0

0.5 g SiO_2/L in 0.1 M $NaClO_4$

25°C, Mn_T 50 μM, pN_2 = 1.00 atm.

10 minute equilibration time.

Table 3.11. Adsorption of Mn(II) on alumina as a function of pH.

pH	Adsorbed Mn, μM
8.04	1.6
8.16	2.6
8.26	2.8
8.33	4.3
8.52	4.7
8.57	5.4
8.67	6.7
8.70	7.2
8.78	9.6
8.86	12.4
8.93	15.5
9.03	19.9
9.09	22.5

0.5 g Al_2O_3/L in 0.1 M Na ClO_4

25°C, Mn_T 50 μM, pN_2 = 1.00 atm.

10 minute equilibration time.

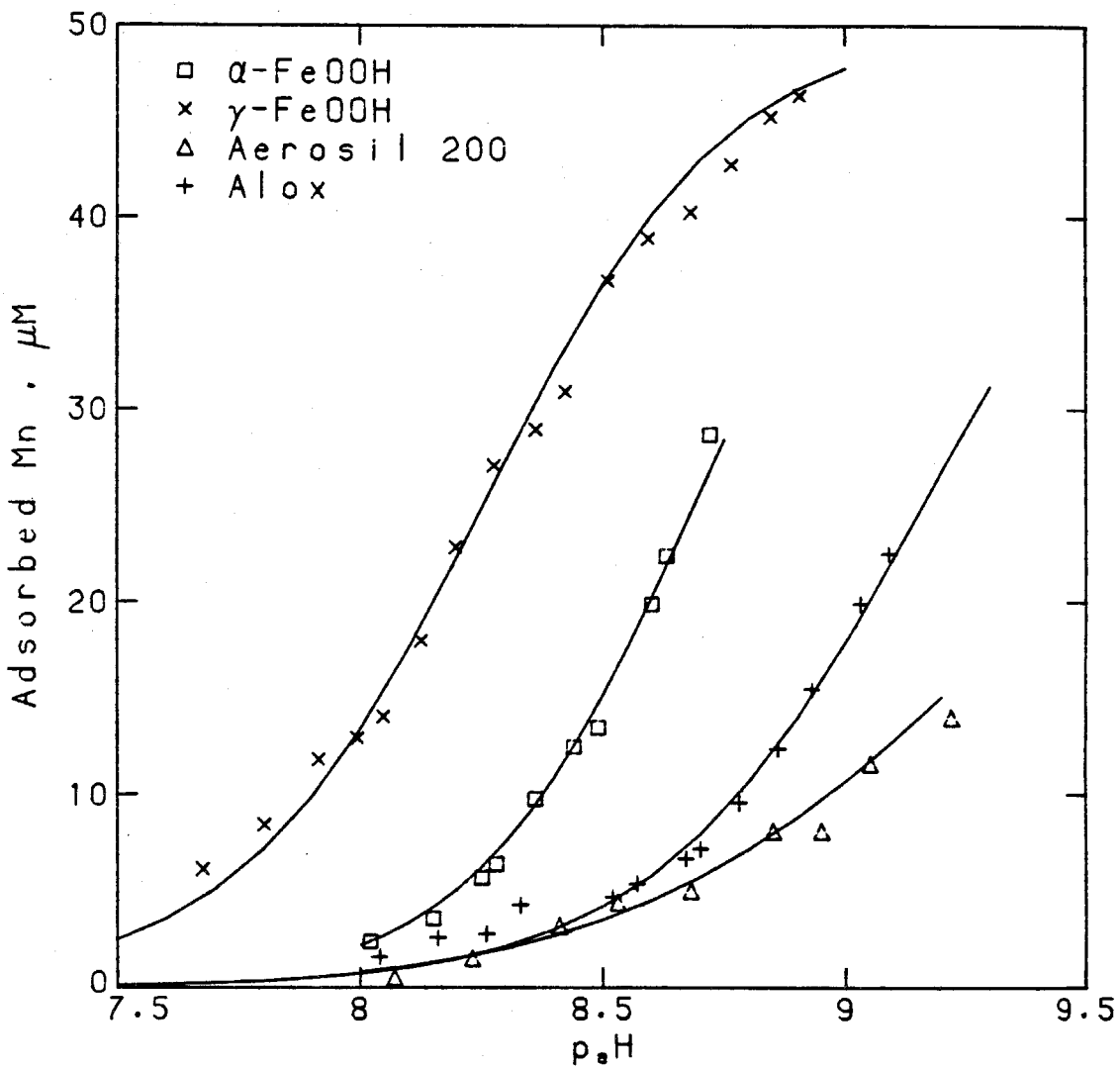

Figure 3.5. Mn(II) adsorption as a function of pH. The solid lines are calculated using the constants given in Tables 3.1 and 3.12. The experimental conditions are given in Tables 3.8 - 3.11.

charged surface C_- were used. The constants found for the Mn(II) adsorption reactions are given in Table 3.12. They were obtained by adjusting the constants to give the best fit by eye to the adsorption data. As is shown in Figure 3.5 the model fits the data very well. For the silica surface the monodentate surface complex was not considered, since its inclusion did not improve the fit to the adsorption data.

3.3 Speciation on the metal oxide surface

It was shown in the previous section that the model outlined in Section 3.1 can describe the adsorption behaviour of Mn(II), at least under the conditions studied (i.e. low adsorption densities). Using this model one can calculate the distribution of species as a function of pH. Figure 3.6 shows the calculated distribution of surface species in the pH range of interest. The solids concentration used in these calculations is typical of that used in the oxidation experiments. In these calculations, the hydrolysed surface species is not considered. If one were to include the hydrolysed species, rather than bidentate species in these calculations, the results would be similar, for the surface is in considerable excess ($S_T >> Mn_T$), so whether the bound Mn occupies one or two surface sites is not particularly important.

The important Mn surface species on the lepidocrocite, goethite, and silica surface is the bidentate (or

Table 3.12. Stability constants for interaction of Mn(II) with metal oxide surfaces.

	$\log^{*}K_1^{s}$(intr)	$\log^{*}\beta_2^{s}$(intr)
γ-FeOOH	-6.1	-12.7
α-FeOOH	-6.8	-13.7
SiO_2	-	-13.9
δ-Al_2O_3	-6.1	-14.4

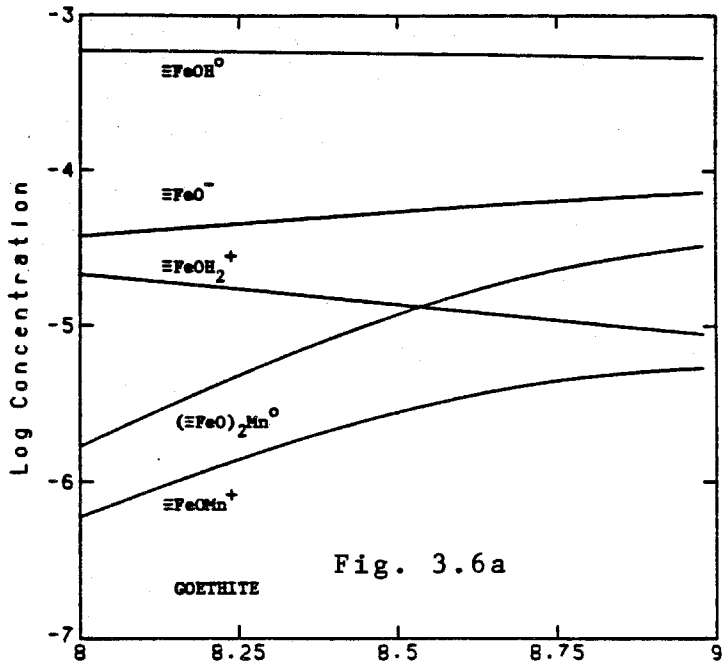

Fig. 3.6a

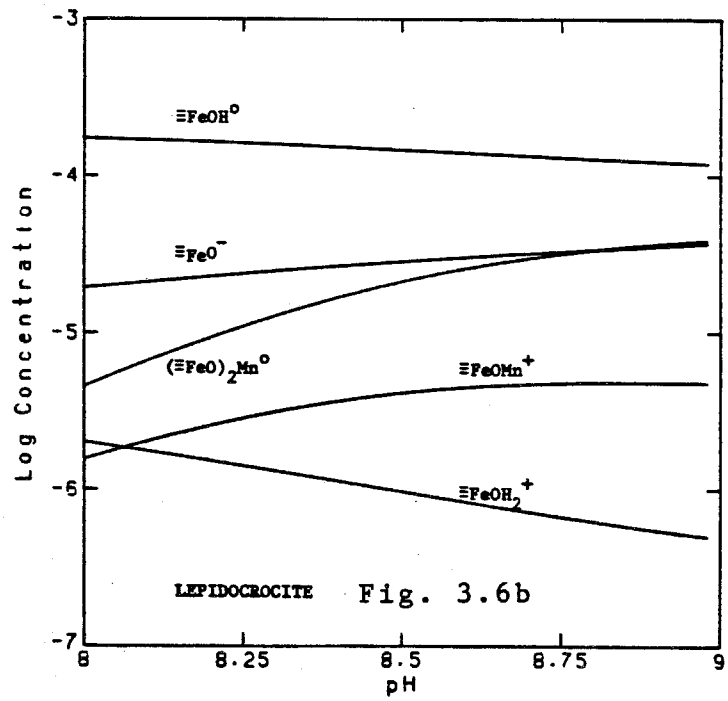

Fig. 3.6b

Figure 3.6. Calculated speciation on the metal oxide surface.

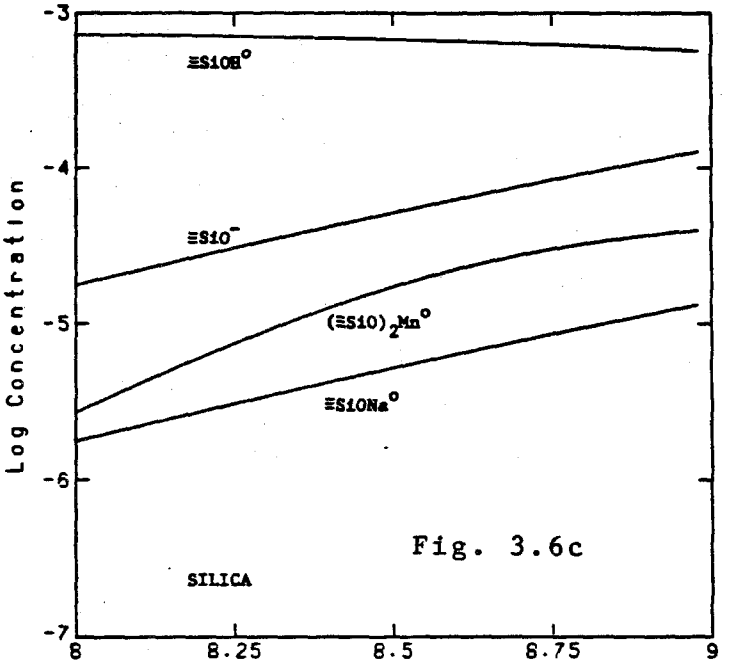

Fig. 3.6c

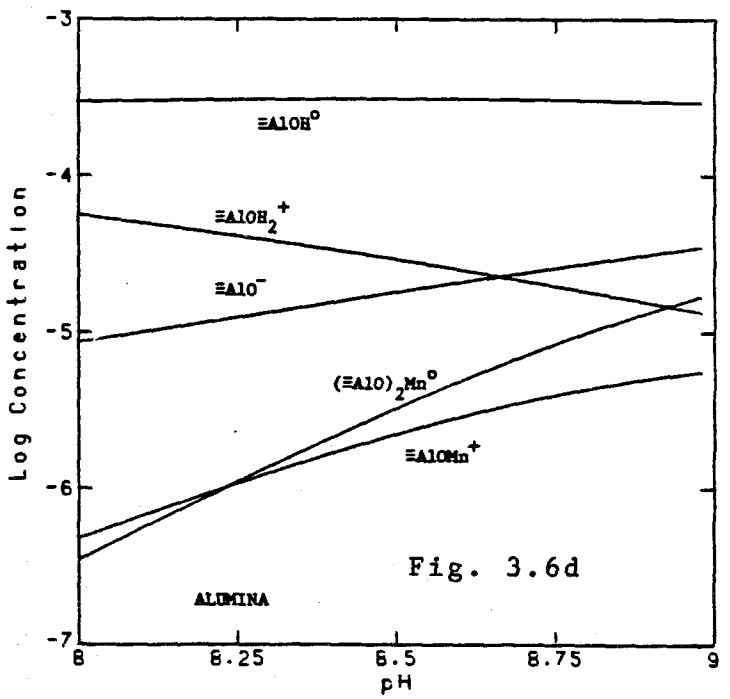

Fig. 3.6d

Figure 3.6 (continued) Calculated speciation on the metal oxide surface.

hydrolysed) complex. On the alumina surface the bidentate (or hydrolysed) complex is the important Mn species at pH >8.25. At pH <8.25 the monodentate complex is the more important Mn surface species on the alumina surface. In the pH range 8-9; goethite, lepidocrocite and silica surfaces are negatively charged. The alumina surface is positively charged below pH 8.7 and negatively charged above that pH.

CHAPTER 4

OXIDATION OF MN(II) IN THE PRESENCE OF METAL OXIDE SURFACES.

4.1 Introduction

This chapter discusses the oxidation of Mn(II) on four metal oxide surfaces; silica SiO_2, alumina δ-Al_2O_3, geothite α-FeOOH and lepidocrocite γ-FeOOH. The oxidation of Mn(II) on the iron oxide surfaces was considered in detail, since these surfaces were most effective in accelerating the oxidation. For the iron oxides, the effect of pH, oxygen partial pressure pO_2, solids concentration, temperature and light on the oxidation rate were studied. The influence of pH and solids concentration on the rate of oxidation on the silica surface was investigated. The effect of ionic strength and buffer composition on rate of Mn(II) oxidation was also investigated. Since preliminary investigations showed that the rate of Mn(II) oxidation on the alumina surface was very slow, this system was not investigated further.

4.2 Previous oxidation studies

The oxidation of Mn(II) in aqueous systems has been extensively studied (Nichols and Walton, 1942; Hem, 1963, 1981; Morgan, 1964, 1967; Michard, 1969; Brewer, 1975; Coughlin and Matsui, 1976; Wilson, 1980; Sung and Morgan, 1981). At constant pH and pO_2 the rate of oxidation in the absence of any added metal oxides can be described by the

expression:

$$\frac{-d[Mn(II)]}{dt} = k_1^*[Mn(II)] + k_2^*[Mn(II)][MnO_x] \qquad (4.1)$$

where $[MnO_x]$ is the concentration of oxidized Mn (Morgan, 1967). The first term in this rate expression describes the loss of Mn(II) due to homogeneous oxidation. The second term describes the loss of Mn(II) due to oxidation at the MnO_x surface. Morgan found that the reaction was first order in oxygen concentration and over the pH range he studied, second order in hydroxide ion concentration. Wilson (1980) found that above the pH at which the solution is saturated with respect to pyrochroite $Mn(OH)_2$, the oxidation rate is independent of pH. This result suggests that the oxidizable species is $Mn(OH)_2(aq)$, since in a system in equilibrium with pyrochroite, the concentration of this species is independent of pH.

It has been suggested that many surfaces including titanium, stannic, ferric, manganese(III) and manganese(IV) oxides, calcite, silica, clay minerals, and feldspars accelerate the oxidation of Mn(II) (Nichols and Walton, 1942; Hem, 1963, 1981; Morgan, 1964, 1967; Michard, 1969; Brewer, 1975; Coughlin and Matsui, 1976; Wilson, 1980; Sung and Morgan, 1981). Most of these previous investigations do not provide a quantitative description of the oxidation of Mn(II) on the surface(s) studied. The autocatalytic oxidation of Mn(II) has been extensively studied (Morgan,

1964, 1967; Brewer,1975). From these data the surface rate constants for Mn(II) oxidation on the MnO_x surface can be calculated (Sung,1981). Sung and Morgan (1981) studied the oxidation of Mn(II) in the presence of lepidocrocite, under conditions where the surface was in excess. The reaction kinetics are, at least in the early stages of the experiment, first order. They found that Mn(II) is more rapidly oxidized when the surface is present. In the presence of milli-molar levels of Fe(III) the initial oxidation rate could be described by the expression:

$$\frac{-d[Mn(II)]}{dt} = k_{Fe}[OH^-]^2\ Fe(III)_{total}[O_2(aq)][Mn(II)] \qquad (4.2)$$

where $Fe(III)_{total}$ is the total concentration of Fe(III) (i.e. the concentration of lepidocrocite) and k_{Fe} is the surface rate constant. The surface rate constant for the oxidation of Mn(II) on the lepidocrocite surface is of the same order of magnitude as that reported for the MnO_x surface. The surface rate constants discussed here are expressed on the basis of the concentration of the solid and not, as would be preferable, on the basis of either the concentration of surface sites available or the surface area of the metal oxide.

4.3 Interpretation of kinetic data

As is described in section 2.6, the rate of oxidation of Mn(II) was determined by following the loss of filterable Mn with time. In interpreting the results of these experi-

ments, it is assumed:

(i) no oxidized Mn passes through the filter,

(ii) that sorptive equilibrium is maintained during the course of the experiment,

(iii) the surface is not significantly altered during the course of the experiment,

(iv) the oxygen transfer rate is fast enough so that, except during the first few minutes of the experiment, the solution is saturated with oxygen, and

(v) no precipitation of Mn occurs.

The validity of these assumptions is discussed in the following section.

The experimental conditions are designed such that the expected rate of oxidation of Mn(II) is pseudo-first order in Mn(II), i.e.

$$\frac{-d[Mn(II)]}{dt} = k_1[Mn(II)] \tag{4.3}$$

If no precipitate is formed, then

$$[Mn(II)] = [Mn(II)]_{sol} + [Mn(II)]_{ads} \tag{4.4}$$

where $[Mn(II)]_{sol}$ is the concentration of soluble Mn(II) and $[Mn(II)]_{ads}$ the concentration of adsorbed Mn(II).

If adsorptive equilibrium is maintained, if the nature of the surface is not altered during the experiment, and if the pH is constant, then

$$[Mn(II)]_{ads} = K'[Mn(II)]_{sol} \tag{4.5}$$

where K' is the equilibrium constant for the reaction

$$Mn(II)_{sol} \rightleftharpoons Mn(II)_{ads} \cdot \tag{4.6}$$

Combining 4.4 and 4.5

$$[Mn(II)] = (1 + K')[Mn(II)]_{sol} \cdot \tag{4.7}$$

If there is no oxidized or precipitated Mn in the filtrate then

$$Mn_f = [Mn(II)]_{sol} \tag{4.8}$$

where Mn_f is filterable Mn.

Substituting 4.8 into 4.7 and differentiating, one obtains

$$\frac{-d[Mn(II)]}{dt} = (1 + K') \frac{dMn_f}{dt} \tag{4.9}$$

Substituting 4.9 into 4.3 and rearranging, it is found that

$$\frac{dMn_f}{dt} = \frac{k_1}{(1 + K')} [Mn(II)] = k_1 Mn_f \tag{4.10}$$

If this expression is integrated, then

$$\ln Mn_f = \ln Mn_{f,t=0} + k_1 t \tag{4.11}$$

A plot of log Mn_f versus time is linear if the kinetics are first order in Mn(II). The slope of this plot is $k_1/2.303$, where k_1 is the pseudo-first rate constant for the oxidation of Mn(II).

4.4 Results and Discussion

4.4.1 Validity of the interpretation of kinetic data

As was discussed in the previous section, a number of assumptions were made in order to interpret the results. In this section the validity of these assumptions is discussed.

The *first assumption made was that no oxidized Mn* passes through the filter. Frequent checks for the presence of oxidized Mn in the filtrate were made using the leuco crystal violet technique (Kessick et al., 1972). No detectable ($<10^{-7}$ M) oxidized Mn was found in the filtrate.

As shown in section 3.2.2.1, the half life for Mn(II) uptake on the solid is less than 5 minutes. Since the distribution coefficient ($[Mn(II)_{ads}]/[Mn(II)_{sol}]$) is generally less than 1, the desorption kinetics, at least for the predominant Mn surface species, must be quite fast. The Mn(II) and solid are intially equilibrated under N_2 for 30 minutes, which is long enough for them to come to sorptive equilibrium. As the adsorption/ desorption kinetics are fast compared to the oxidation kinetics, sorptive equilibrium is retained during the experiment.

The conditions of the experiment are chosen so that concentration of surface sites is much greater than the total Mn concentration. Under these conditions, the total number of reaction sites is nearly constant during the course of the experiment. It would be expected that the nature of the surface would only change during the course of

the experiment if the sites at which Mn was oxidized were more reactive than the original sites. This is not the case since if it were, the reaction would then be autocatalytic and not first order, as is observed. So the third assumption is also valid.

As is shown in Figure 4.1, the system is rapidly saturated with oxygen. The saturation concentration for oxygen shown in the figure was calculated using the data given in Standard Methods (1980) for NaCl solutions. The rate of oxygen transfer to solution is described by the equation:

$$\frac{dC}{dt} = K_L a \ (C_s - C) \qquad (4.12)$$

where dC/dt is the change in oxygen concentration,

$K_L a$ is the overall mass transfer coefficient,

C_s is the saturation concentration of oxygen in solution, and

C is the concentration of oxygen in solution (Metcalf and Eddy, Inc., 1979). In this system $K_L a = 0.148\ min^{-1}$ and the time taken to achieve 50% saturation is 5 minutes. If the rate of oxygen consumption due to Mn(II) oxidation is R, then:

$$\frac{dC}{dt} = K_L a \ (C_s - C) - R \qquad (4.13)$$

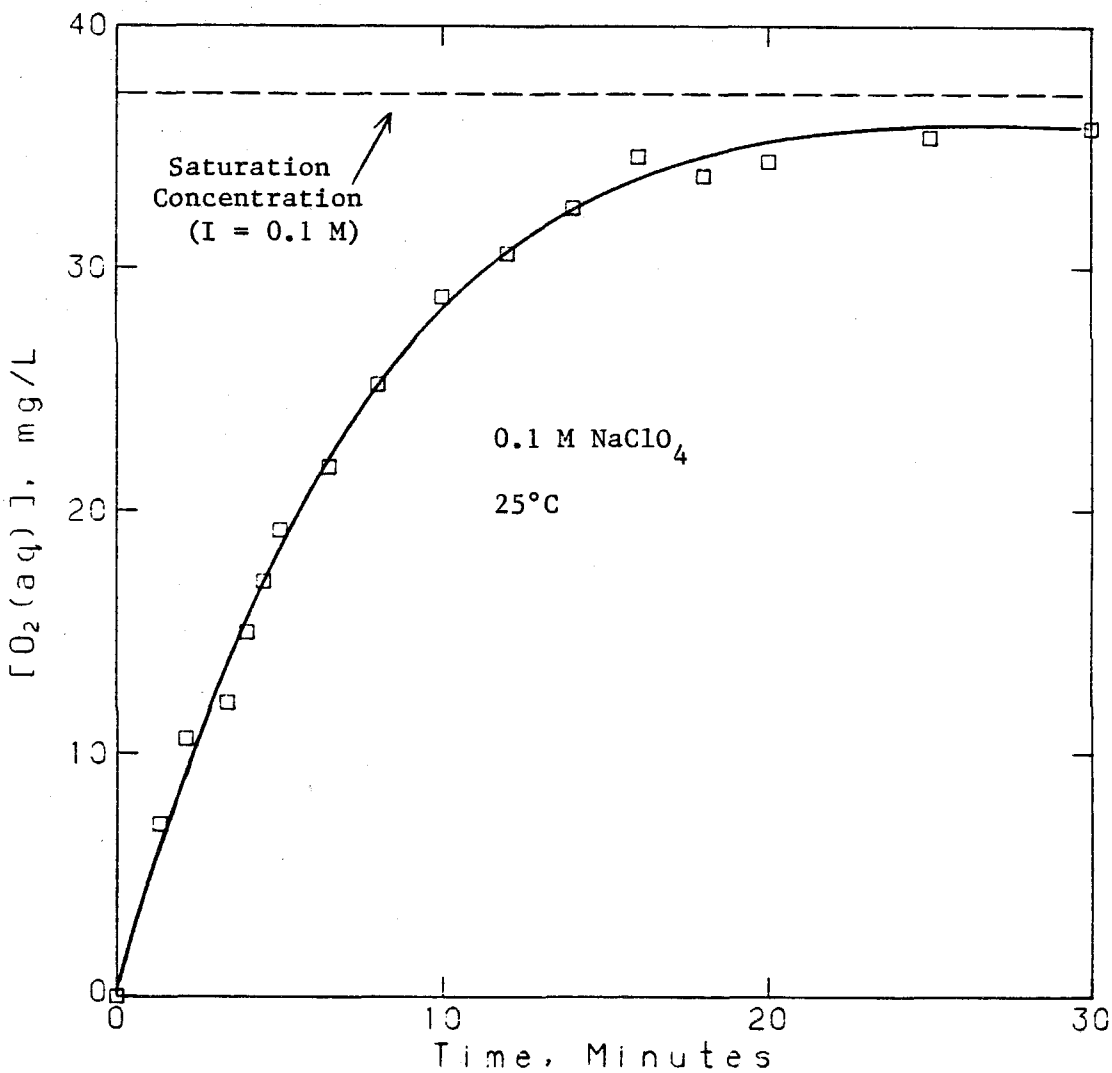

Figure 4.1 Oxygen concentration as a function of time.

Assuming a steady state,

$$K_L a = \frac{R}{C_s - C} \tag{4.14}$$

At 25°C the highest rate of Mn(II) oxidation found in these experiments was 1.5×10^{-6} M min^{-1}. If the reaction stoichiometry is

$$Mn^{2+} + \frac{1}{2} O_2 + H_2O \rightleftharpoons MnO_2 + 2H^+ \tag{4.15}$$

then the steady state concentration for $O_2(aq)$ is 99.6% of the saturation concentration. Thus the fourth assumption is valid.

Because the oxidation of Mn(II) is strongly pH dependent, it is most easily studied at constant pH. Buffers are the preferred method of pH control, since controlling the pH by adding base to the system will produce localized areas of high pH where rapid oxidation may occur. A carbonate buffer system was chosen, since it is the principal buffer in alkaline and neutral natural waters. A disadvantage of the carbonate buffer system is that rhodocrocite $MnCO_3(s)$ is sparingly soluble. In most of the oxidation experiments, the solution is supersaturated with respect to $MnCO_3(s)$. In the geothite and lepidocrocite experiments, the ratio of the ion activity product (IAP) to the solubility product K_{s0} is less than 10; but in the silica and alumina experiments the ratio IAP/K_{s0} is as high as 45. Figure 4.2 shows that there is no loss of filterable Mn from a solution that is supersaturated with respect to

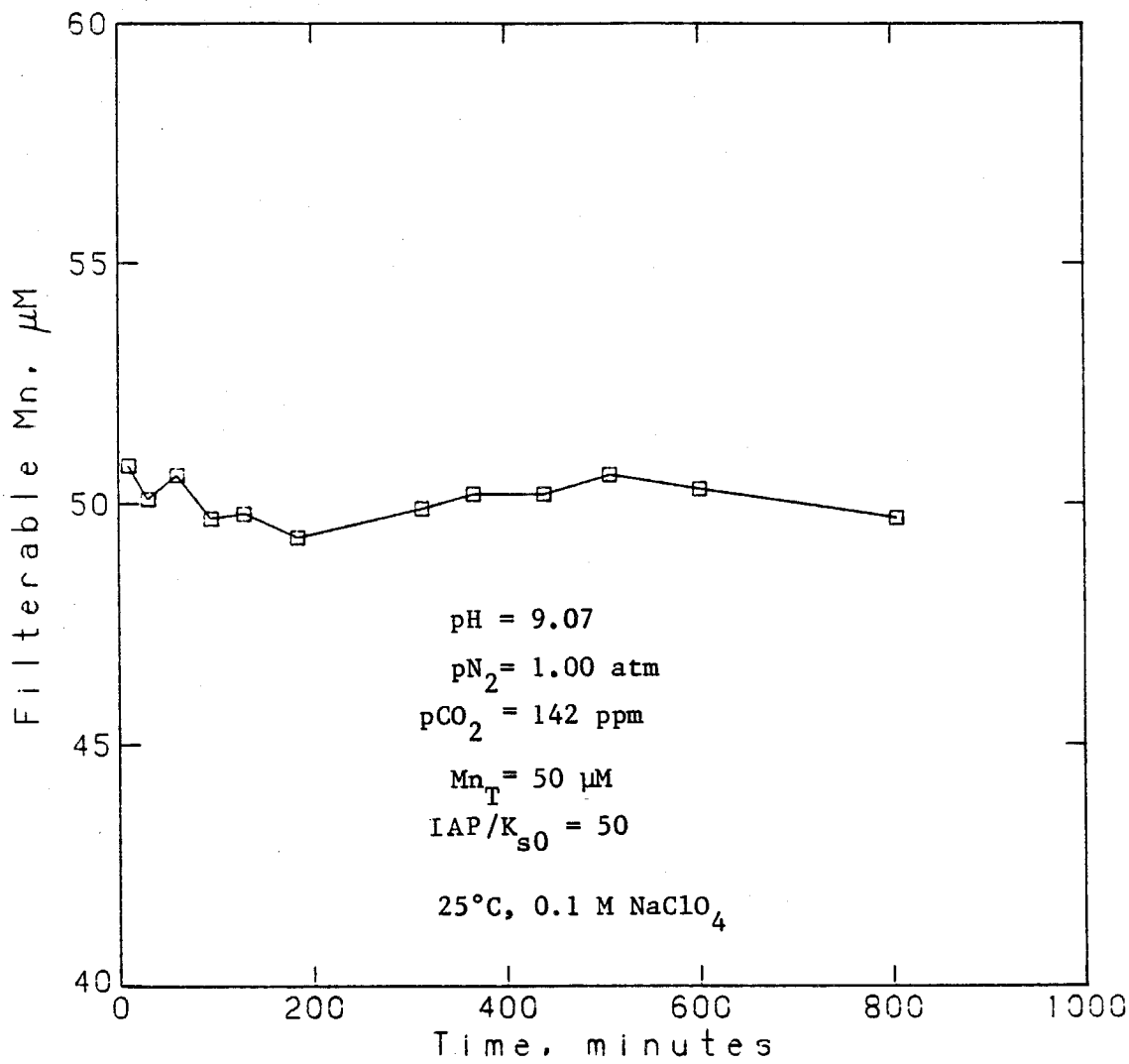

Figure 4.2 Filterable Mn as a function time in a system supersaturated with respect to $MnCO_3(s)$.

$MnCO_3(s)$ (IAP/K_{s0} = 50) over a period of several hours. Nuclepore 0.03 micron filters were used in this experiment, so if a precipitate was formed, it was not retained on even a 0.03 micron filter. It seems reasonable to infer from these results that the kinetics of precipitation of $MnCO_3(s)$ at pH 9.07 are so slow that the solid is not formed in this system. At lower pH, presumably the kinetics of precipitation are slower than at pH 9.07.

In systems where a metal oxide is present, $MnCO_3(s)$ could nucleate on the solid. Figure 4.3 shows the filterable Mn found in a system equilibrated with a 10 mM goethite suspension and an N_2 atmosphere containing approximately 350 ppm CO_2. In these experiments and in those illustrated in Figure 4.4, the usual equilibration time was 30 minutes, though in some cases longer equilibration times were used. The solid curve on this figure shows the calculated filterable Mn supposing that the system is in equilibrium with $MnCO_3(s)$ i.e. $MnCO_3$ is precipitated (assuming that adsorbed and precipitated Mn are non-filterable). The dashed line indicates the expected filterable Mn supposing that $MnCO_3(s)$ is not precipatated i.e. considering only removal due to adsorption. Clearly, the results indicate that either $MnCO_3(s)$ is not precipitated, or that the precipitate is filterable. Whilst the precipitate may be colloidal, it seems unlikely that none of this precipitate would be retained on the filter. Considering that Mn(II) was

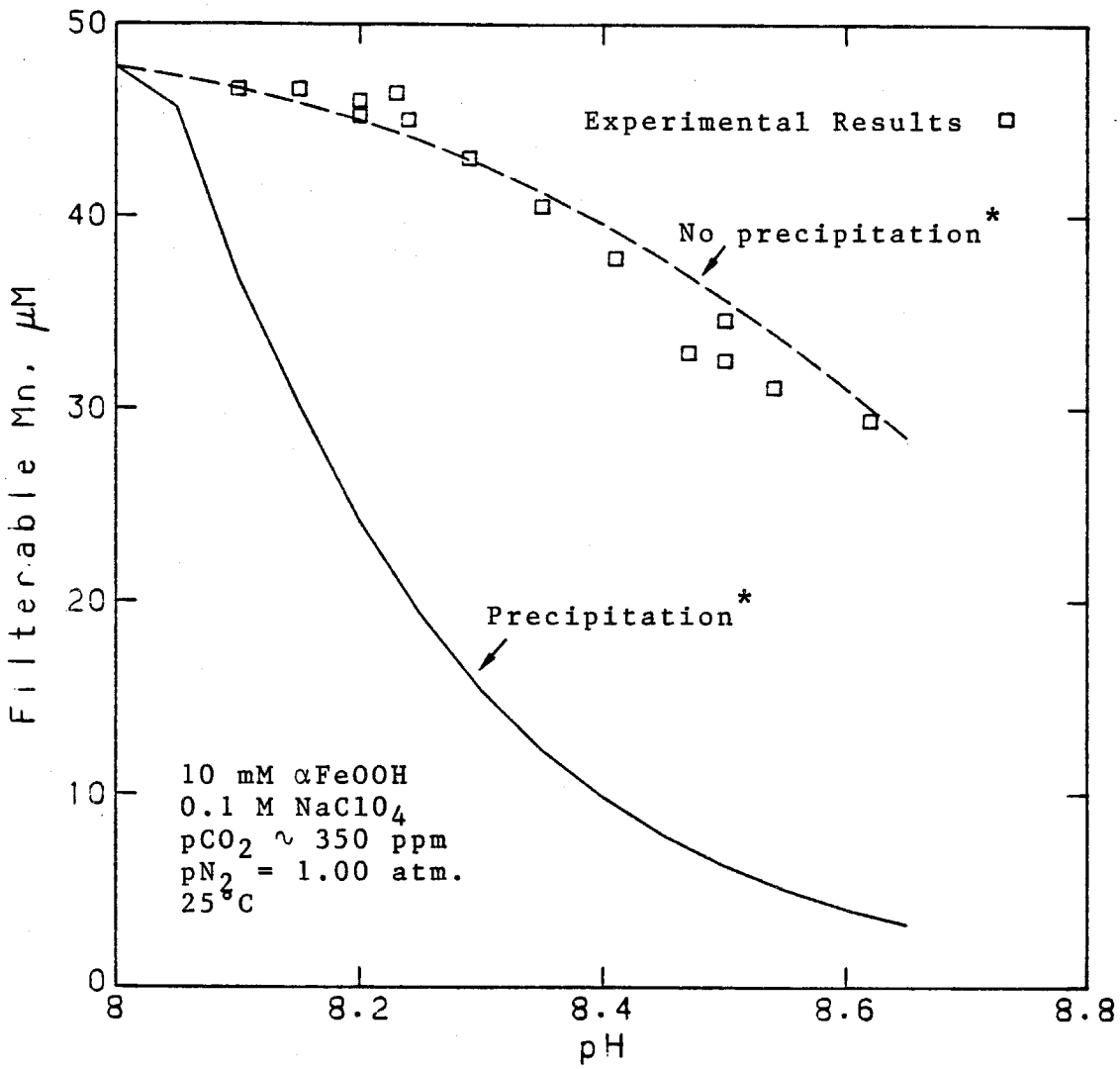

*see text for explanation of these terms.

Figure 4.3. Filterable Mn in αFeOOH suspension with carbonate present.

added to the suspension, it would be expected that if a precipitate formed, it would nucleate on the existing particles and it would be retained on the filter with these particles. If rhodocrocite precipitated as separate particles, it seems implausible that the filter could retain virtually all the metal oxide particles (which generally have dimensions of 50 nm or less) whilst retaining virtually none of the $MnCO_3$ particles. Figure 4.4 shows that for a system containing silica, at pH less than 9.0 the filterable Mn is close to that expected if no precipitation occurs. Above pH 9.0, some precipitation may occur, but the extent of precipitation is small. The results shown in Figures 4.3 and 4.4 are the measurements of filterable Mn taken in the oxidation experiments prior to oxygen bubbling. In these experiments, Mn(II) was usually equilibrated (under N_2) with the solid for 30 minutes, but the time taken for some oxidation experiments is several hours and it is possible that during this time, $MnCO_3(s)$ could precipitate. Figure 4.5 shows the filterable Mn found in a 0.5 g/L silica suspension (under N_2) as a function of time. After the intial rapid uptake, there is little decrease in the filterable Mn over a period of more than 18 hours, indicating that if the precipitation of $MnCO_3(s)$ does occur, the kinetics are very slow. The intial uptake is approximately that expected due to adsorption.

The preceding discussion shows that the assumptions

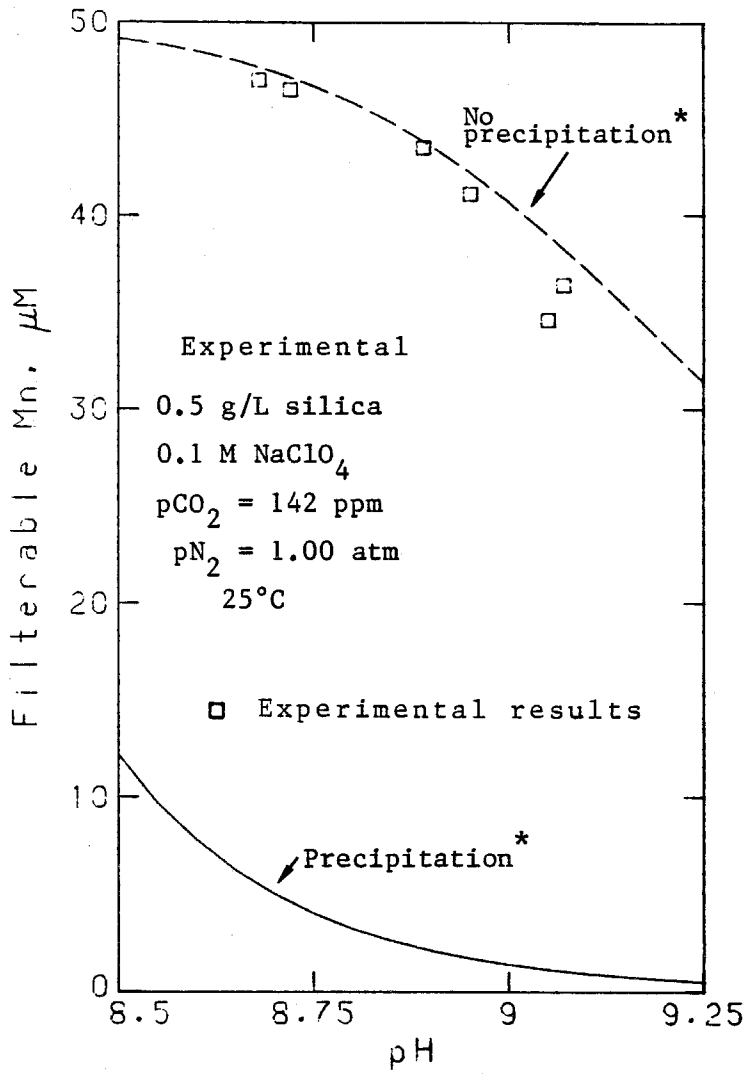

*see text for explanation of these terms.

Figure 4.4 Filterable Mn in a silica suspension with carbonate present.

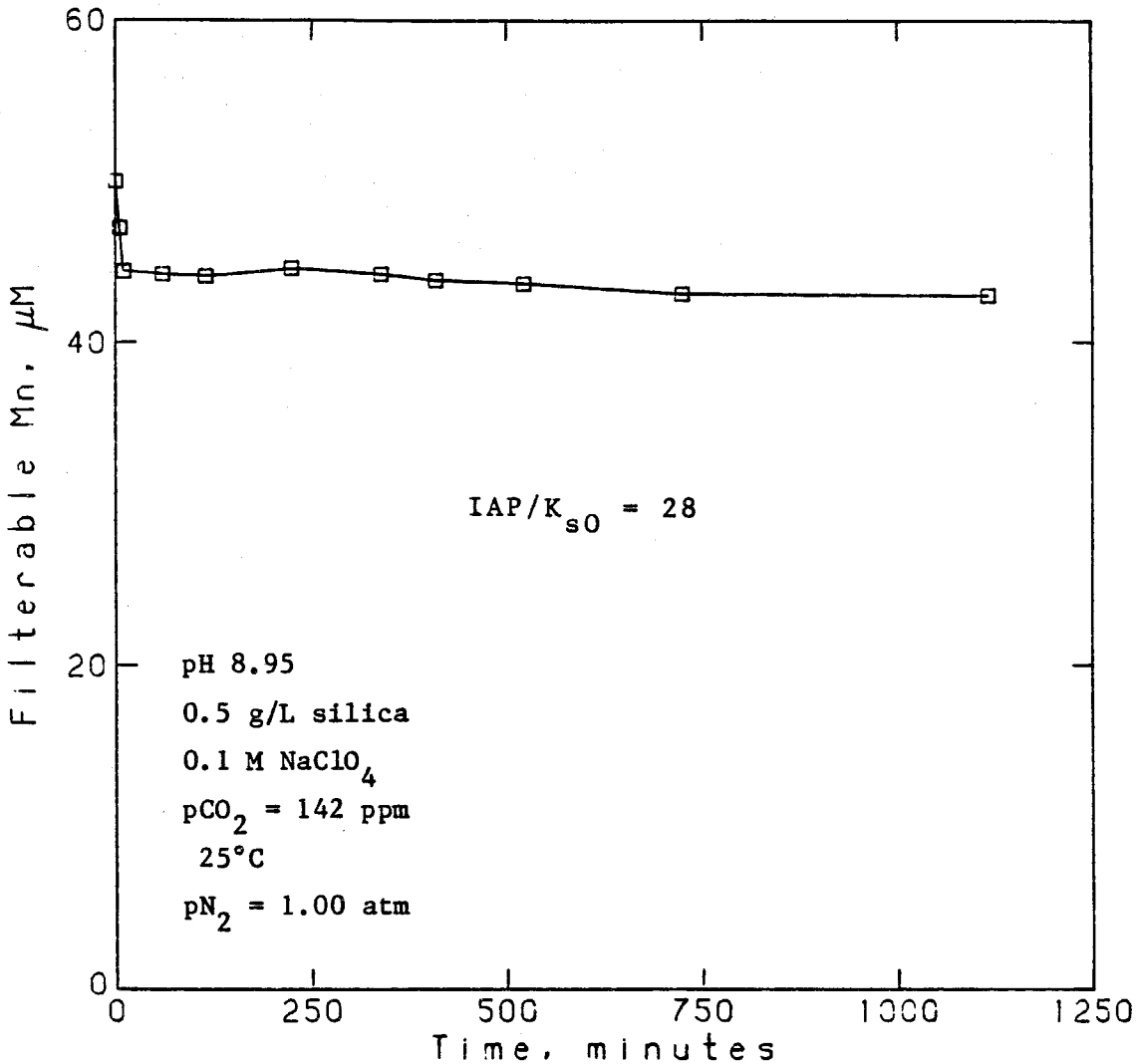

Figure 4.5 Removal of Mn from a silica suspension under N_2.

made in interpreting the data on the kinetics of loss of filterable Mn to obtain the rate of loss of Mn(II) are valid.

4.4.2 "Homogeneous" oxidation of Mn(II)

The oxidation of Mn(II) in systems were no metal oxides are present initially has been studied, in order to be able to take account of reactions not occurring on the metal oxide surface in experiments made in the presence of metal oxides.

As previously mentioned, the oxidation of Mn(II) in aqueous systems at constant pH and pO_2 can be described by an expression of the form:

$$\frac{-d[Mn(II)]}{dt} = k_1^*[Mn(II)] + k_2^*[Mn(II)][MnO_x] \qquad (4.16)$$

(Morgan, 1967).

If a metal oxide that accelerates the reaction is present, there will be a third term in the rate law. For example, the oxidation of Mn(II) in the presence of lepidocrocite at constant pH and pO_2 may be described by a rate law of the form:

$$\frac{-d[Mn(II)]}{dt} = k_1^*[Mn(II)] + k_2^*[Mn(II)] + k_{Fe}[Mn(II)]Fe(III)_{total} \qquad (4.17)$$

where $Fe(III)_{total}$ is the total Fe(III) concentration (Sung and Morgan, 1981).

Under the conditions used in these experiments the

second term in the above expression is negligibly small. The first is small, but not always negligble.

Figure 4.6 shows the loss of filterable Mn under N_2 and O_2. There is a small but significant decrease in filterable Mn in the system when oxygen is present; this loss is presumably due to oxidation of Mn(II). As shown in Figure 4.7, the kinetics of filterable Mn removal under O_2 are approximately first order. The dependence of the rate of oxidation of Mn(II) on pH is presented in Table 4.1. Also shown in this table is Morgan's (1964) data for the oxidation of Mn(II) in carbonate buffers (as reinterpreted by Sung(1981)). The rate of Mn(II) oxidation observed by Morgan is about 3 times faster than that found in this work. The C_T and ionic strength in these systems are not identical. The differences in C_T are probably not consequential. If the reaction shows a similar dependence on ionic strength to that observed for the homogeneous oxidation of Fe(II) by oxygen (Sung and Morgan, 1980), then results shown here and Morgan's(1964) results agree within 50%. For the data presented in this work, a plot of k_1 as a function of pH has a slope of 2.6 $\pm$0.8, not 2.1 as found previously by Morgan.

Recently, Diem and Stumm (1984) reported that at pH 8.4, in a 0.1 mM $NaHCO_3$ solution, no removal of filterable Mn(II) was observed over a period in excess of 7 years. This suggests that at pH 8.4 the rate of Mn(II) oxidation is at

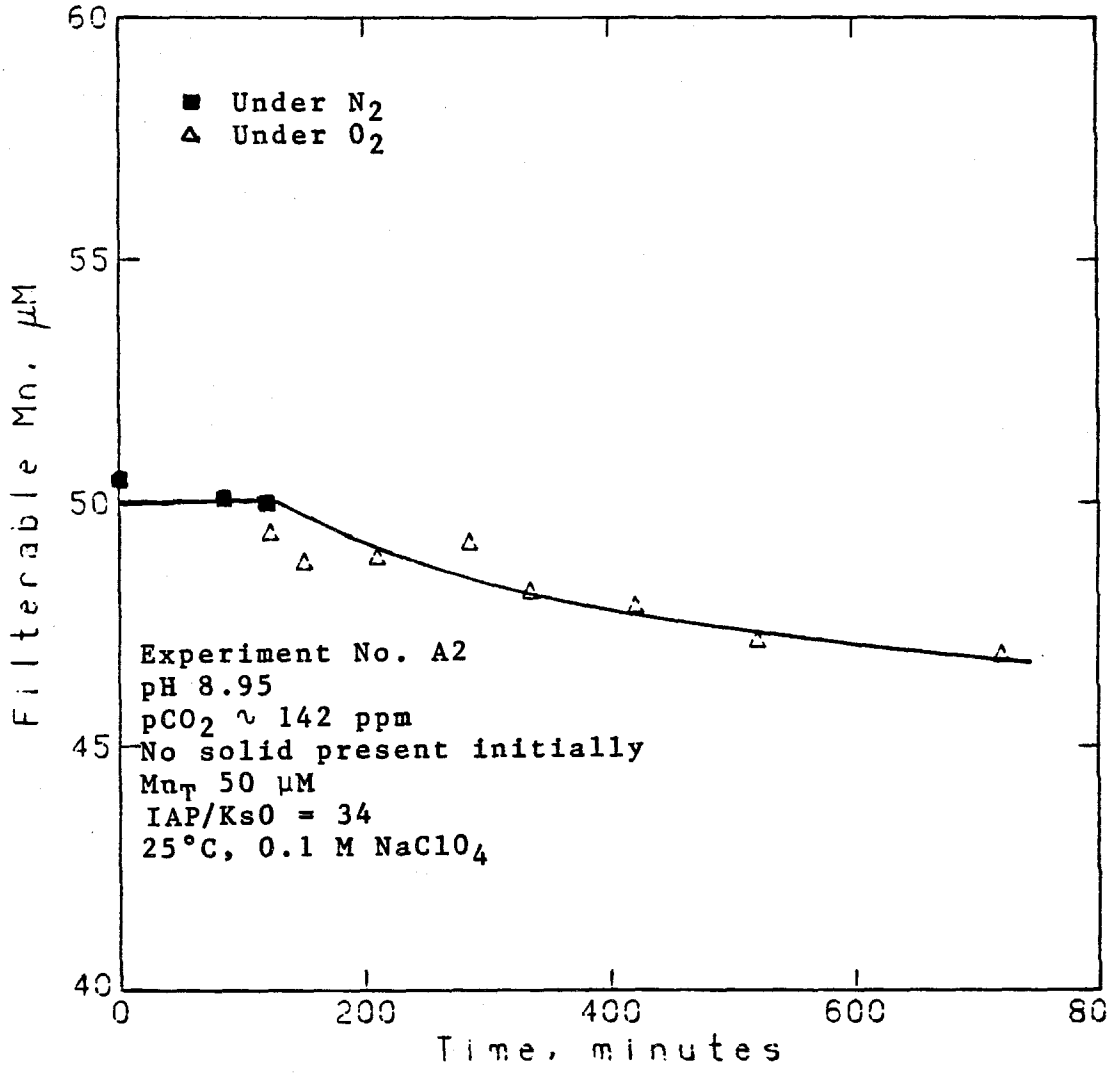

Figure 4.6. Loss of filterable Mn under N_2 and under O_2 with no solid present initially.

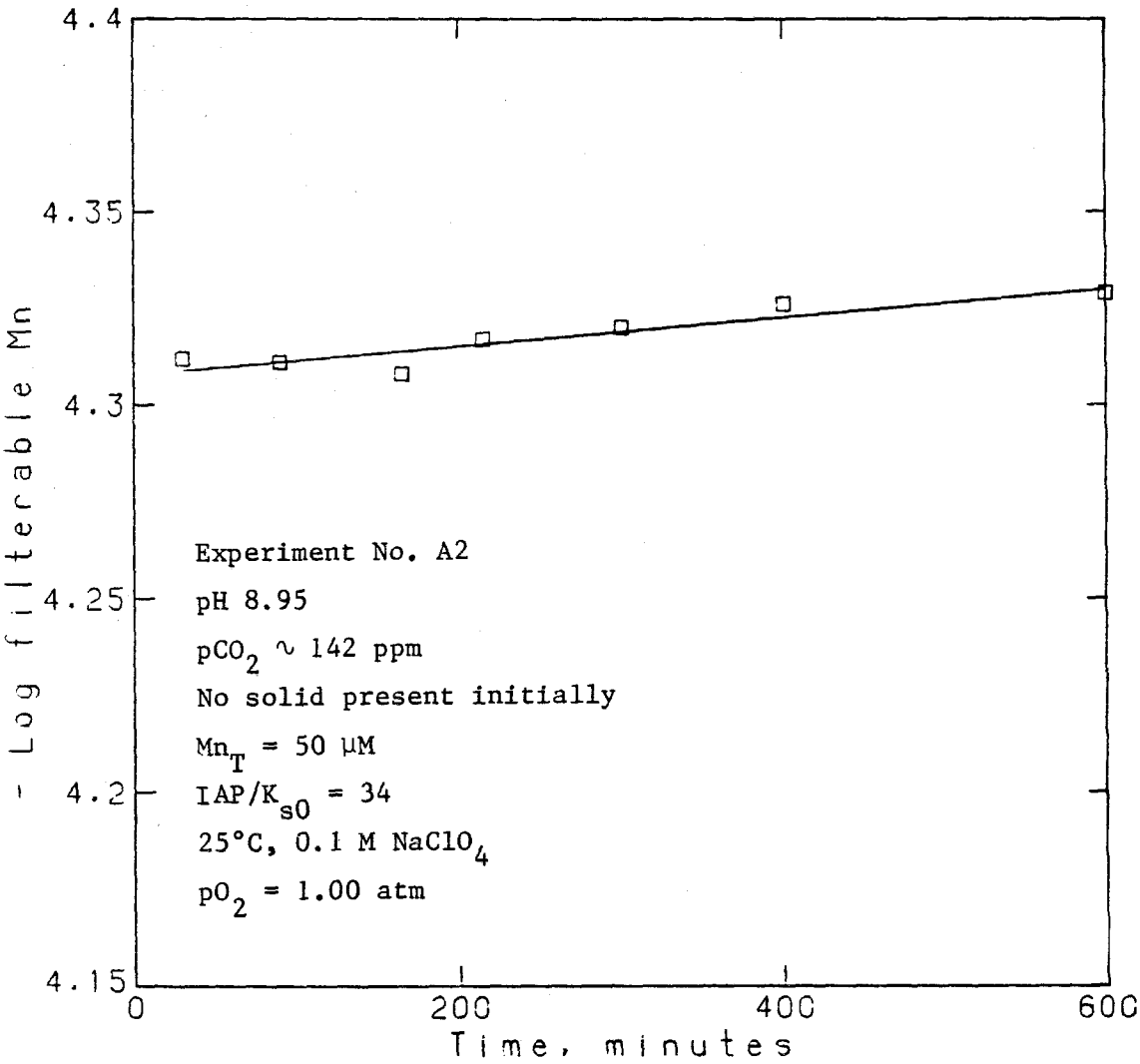

Figure 4.7 First order plot for removal of filterable Mn under O_2.

Table 4.1 Oxidation of Mn(II) in the absence of metal oxides

Expt. No.	pH	This work [1] k_1^* ± 95% conf. limits (min^{-1})	Morgan (1964)[2] pH	Morgan (1964)[2] k_1^* (min^{-1})
A1	8.35	$< 2 \times 10^{-6}$	9.0	3.6×10^{-4}
A2	8.95	$9 \times 10^{-5} \pm 2 \times 10^{-5}$	9.3	1.7×10^{-3}
A3	9.04	$1.7 \times 10^{-4} \pm 4 \times 10^{-5}$	9.5	4.2×10^{-3}
A4	9.25	$5.7 \times 10^{-4} \pm 4 \times 10^{-5}$		

[1] All experiments at 25°C in 0.1 M $NaClO_4$. pO_2 = 1.00 atm., Mn_T = 50 μM. In A1 pCO_2 = 348 ppm and in the other experiments pCO_2 = 142 ppm.

[2] All experiments at 25°C. pO_2 = 1.00 atm., Mn_T = 450 μM, $[HCO_3^-] + [CO_3^{2-}]$ = 1.6 mM.

least two orders of magnitude slower than the oxidation rate predicted by extrapolation of studies at higher pH to these conditions. At higher pH (pH 8.8), where the system is intially supersaturated with respect rhodocrocite (IAP/K_{s0} ~5), the rate of Mn(II) oxidation found by these workers is comparable to that observed in this and earlier (Morgan, 1964; Wilson, 1980) studies. Diem and Stumm claim that there is no evidence for Mn(II) oxidation in systems not over-saturated with respect to a Mn(II) solid. They infer that oxidation of Mn(II) at higher pH occurs on the rhodocrocite surface. As was shown in section 4.4.1, there is strong evidence that at pH < 9.1 rhodocrocite does not precipitate in the systems studied here. If this is the case, the results shown in Table 4.1 indicate that Mn(II) is oxidized in homogeneous systems. Morgan (1964) has shown that Mn(II) is oxidized in NH_4^+/NH_3 buffers that are not supersaturated with respect to any Mn(II) solid. These results suggest that Mn(II) can be oxidized in homogeneous systems, but they do not offer any explanation for the fact that in homogeneous solution, Mn(II) is very slowly oxidized at pH 8.4. Whatever the explanation for the behaviour of Mn(II) in these systems, this is not a significant point in this study, for the oxidation of Mn(II) on the metal oxides is considerably faster than that occurring when the solid is not present. The data for the oxidation of Mn(II) in the presence of metal oxides have been corrected for "homogeneous" oxidation

using the relation:

$$k_1 = k_{obs} - k_{hom} \qquad (4.18)$$

where k_{obs} is the observed rate constant,

k_1 is the rate constant for the reaction on the surface, and

k_{hom} is the rate constant for the "homogeneous" oxidation. k_{hom} is calculated using the equation:

$$k_{hom} = 1.25\ [OH^-]^{2.56} \qquad (4.19)$$

This equation was obtained by fitting a power function to the data given in Table 4.1.

4.4.3 Oxidation of Mn(II) in the presence of metal oxide surfaces

The results for a typical oxidation experiment in which a metal oxide solid was present are shown in Figure 4.8. There was an initial rapid uptake of Mn due to adsorption, then the filterable Mn was relatively constant until the system was switched to oxygen bubbling. Under oxygen, there is a steady decrease in filterable Mn. The plot of log Mn_f as a function of time (Figure 4.9) shows that except in the first 5 to 10 minutes of the oxidation experiment, the kinetics of removal of filterable Mn are first order. The "induction" period seen for this reaction corresponds approximately to the time required for the system to reach oxygen saturation.

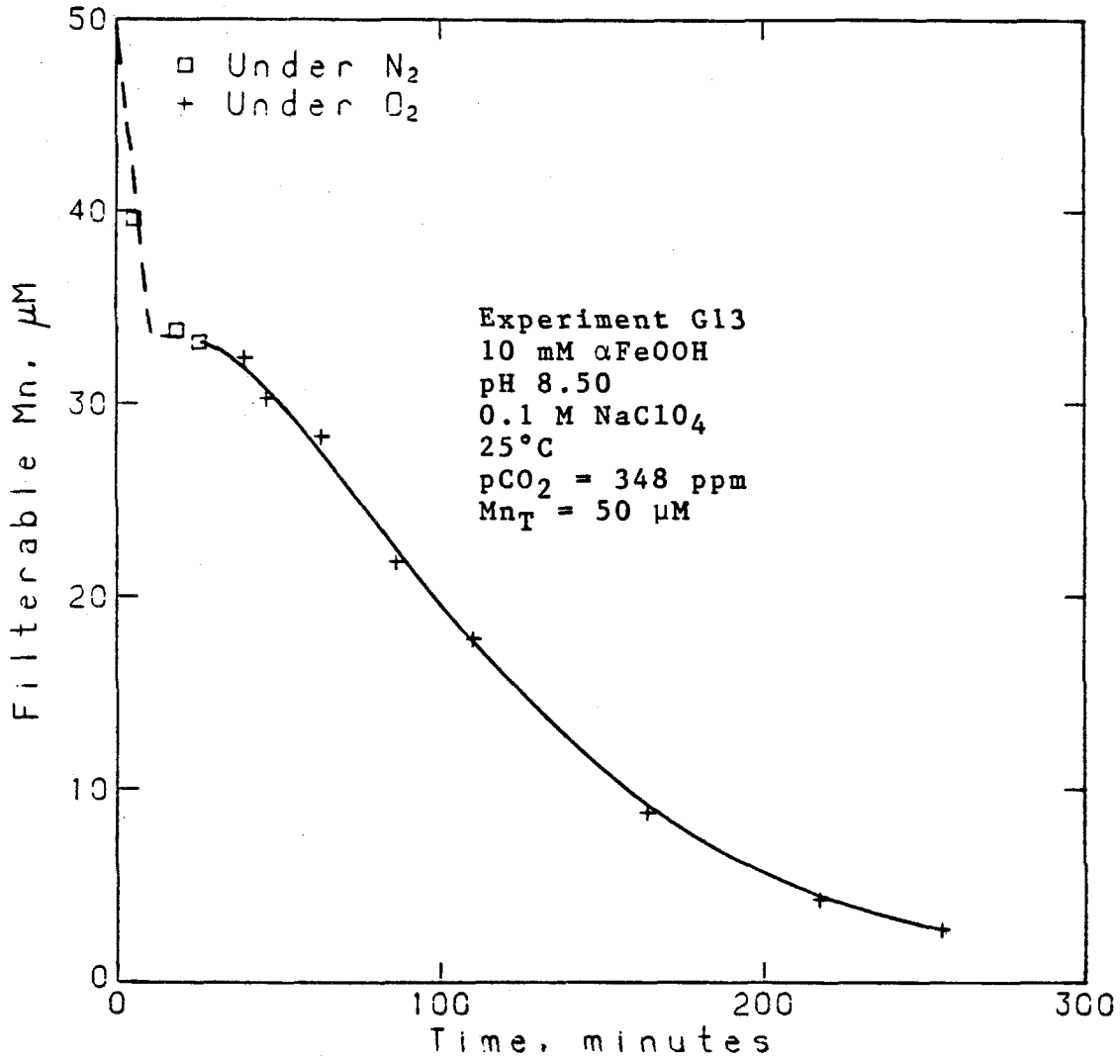

Figure 4.8. Typical oxidation experiment in presence of metal oxide.

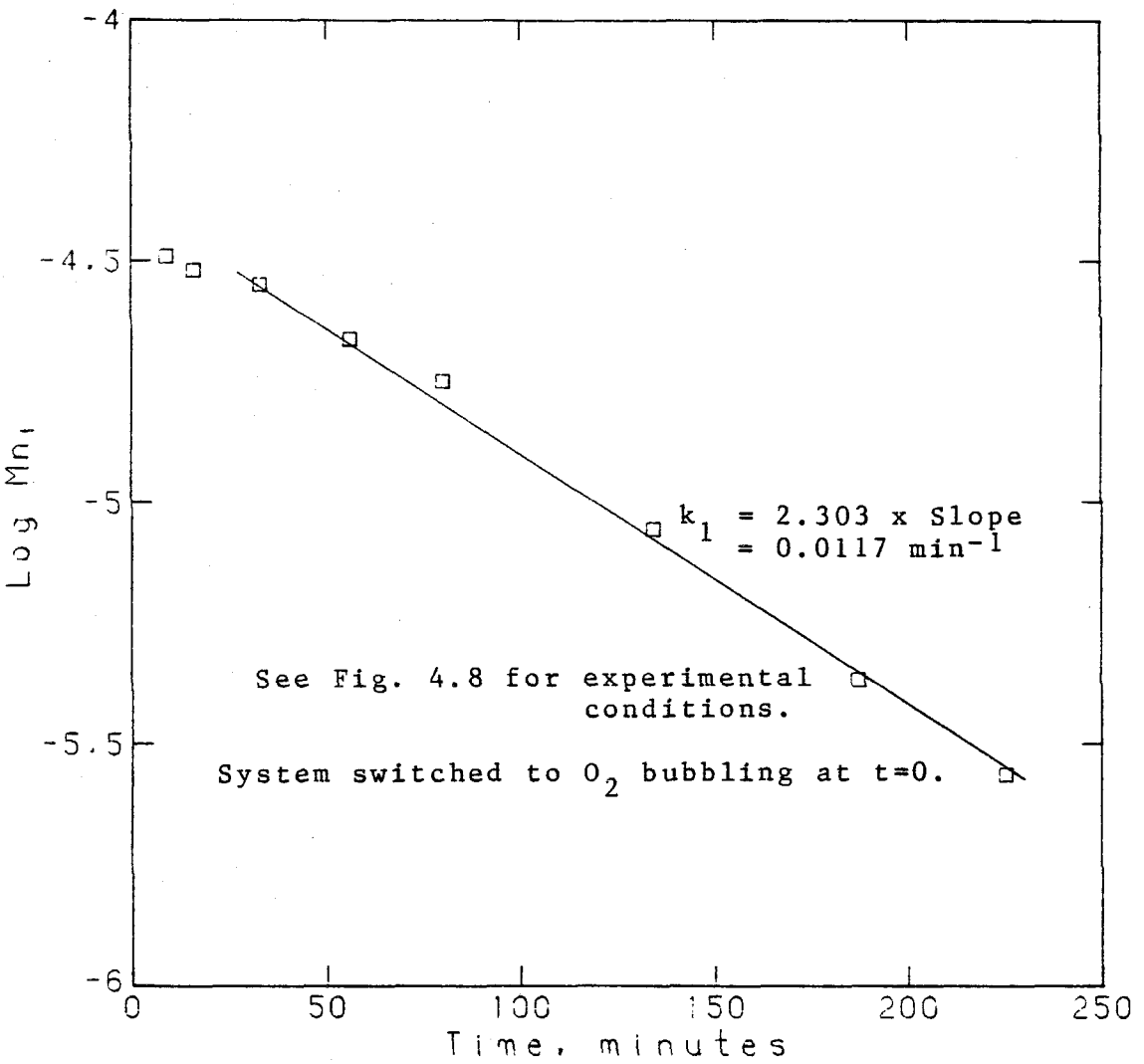

Figure 4.9 Log Mn_f as a function of time for system where metal oxide is present.

The experimental conditions used and results found in the experiments discussed in this section are summarized in Tables 4.2 - 4.5. The alumina data are discussed in section 4.4.3.8, because there are too few results to meaningfully discuss them separately.

4.4.3.1 Reproducibility

Tables 4.6 - 4.8 show the results for three sets of experiments made to determine the reproducibility of measurements of the rate constant k_1. The estimates of the relative standard deviation for measurements of k_1 vary between 1.3% and 7.3%. In an individual experiment, the confidence limits for the rate constant k_1 were calculated from the error in the slope of the regression line of a plot log Mn_f versus time. The factors contributing to this variability are unknown, but small errors in the pH measurements could account for much of the observed variability. For example, assuming (as is shown in section 4.4.3.2) that the reaction rate is dependent on $[OH^-]^2$, then at pH 8.32 the reaction rate is 10% faster than at pH 8.30.

4.4.3.2 The influence of pH

The pH dependence of the rate of oxidation of Mn(II) on silica, alumina, goethite and lepidocrocite is shown in Tables 4.2 - 4.5. The reaction shows a strong pH dependence. As shown in Figures 4.10a, 4.11a and 4.12a, a plot of log k_1 versus pH is approximately linear. For the oxidation of Mn(II) on the goethite, lepidocrocite, and silica surfaces,

Table 4.2. Results and experimental conditions for Mn(II) oxidation studies in the presence of goethite.

Expt. No.	pH	pO_2 (atm)	[α-FeOOH] (μM)	pCO_2 (ppm)	Mn_T (μM)	Initial Mn_{ads} (μM)	k_1 (min^{-1})
Batch G1							
G1	8.10	1.00	9.94	348	49.7	3.1	.00174
G2	8.20	1.00	10.0	348	50.0	4.8	.00171
G3	8.29	1.00	10.0	348	50.0	7.0	.0038
G4	8.47	1.00	9.72	348	48.6	15.7	.0104
G5	8.54	1.00	9.90	348	49.5	18.4	.0097
G6	8.62	1.00	10.0	348	50.0	20.6	.0127
Batch G2							
G7	8.15	1.00	10.0	348	50.0	3.4	.00237
G8	8.20	1.00	10.0	348	50.0	4.0	.0027
G9	8.23	1.00	10.0	348	50.0	3.6	.00333
G10	8.24	1.00	10.0	348	50.0	5.0	.00472
G11	8.35	1.00	10.0	348	50.0	9.5	.0046
G12	8.41	1.00	10.0	348	50.0	12.2	.0098
G13	8.50	1.00	10.0	348	50.0	16.4	.0117
G14	8.50	1.00	10.0	358	50.0	17.5	.0135
G15	8.50	0.209	10.0	358	50.0	16.9	.00296
G16	8.48	1.00	1.00	358	50.0	2.7	.00177
G17	8.50	1.00	2.00	358	50.0	4.5	.00295
G18	8.50	1.00	20.0	358	50.0	24.3	.0308
G19	8.64	1.00	10.0	358	50.0	18.6	.0124
G20	8.65	1.00	10.0	358	50.0	21.5	.0130
G21	8.65	1.00	10.0	358	50.0	19.9	.0153
G22	8.63	1.00	10.0	358	50.0	19.8	.0142
G23	8.64	1.00	10.0	358	50.0	20.2	.0138
G24	8.60	1.00	10.0	359	50.0	9.8	.00134
G25	8.58	1.00	10.0	359	50.0	17.2	.00991
G26	8.55	1.00	10.0	359	50.0	23.8	.0322
G27	8.68	1.00	10.0	359	50.0	32.1	.088

All experiments in 0.1 M $NaClO_4$. G1-G23 25°C, G24-G27 at temperatures indicated in Table 4.12.

Table 4.3 Results and experimental conditions for Mn(II) oxidation studies in the presence of lepidocrocite.

Expt. No.	pH	pO_2 (atm)	[γ-FeOOH] (μM)	pCO_2 (ppm)	Mn_T (μM)	Initial Mn_{ads} (μM)	k_1 (min^{-1})
Batch L2							
L1	8.00	1.00	1.00	348	50.4	4.3	.00349
L2	8.03	1.00	1.00	348	50.0	6.6	.00412
L3	8.04	1.00	1.00	348	50.0	6.8	.00452
L4	8.04	1.00	1.00	348	50.0	6.0	.00446
L5	8.08	1.00	1.04	348	52.5	7.2	.00574
L6	8.18	1.00	1.00	348	50.0	9.8	.00757
L7	8.18	1.00	1.00	348	50.0	11.6	.0080
L8	8.36	1.00	1.04	348	52.5	17.8	.0147
L9	8.42	1.00	1.00	348	50.0	20.6	.0176
L10	8.58	1.00	1.04	348	52.5	30.1	.028
Batch L3							
L11	8.01	1.00	1.04	359	52.5	4.7	.00430
L12	8.16	1.00	1.04	348	52.5	10.2	.00786
L13	8.29	0.209	1.04	359	52.5	12.6	.00224
L14	8.30	1.00	1.04	359	52.5	13.6	.0122
L15	8.29	1.00	1.00	358	50.0	13.8	.0115
L16	8.29	1.00	0.200	358	50.0	4.8	.00362
L17	8.30	1.00	2.00	358	50.0	22.8	.0184
L18	8.29	1.00	4.00	358	50.0	27.5	.0206
L19	8.39	1.00	1.00	358	50.0	16.4	.0127
L20	8.50	0.209	1.00	358	50.0	21.4	.00362
L21	8.52	1.00	1.00	358	50.0	21.2	.0183
L22	8.50	1.00	1.00	358	50.0	21.4	.0188
L23	8.51	1.00	1.00	358	50.0	22.0	.0182
L24	8.68	1.00	1.00	358	50.0	27.2	.0255
L25	8.60	1.00	5.00	359	50.0	19.8	.00713
L26	8.62	1.00	5.00	359	50.0	34.8	.0324
L27	8.68	1.00	5.00	359	50.0	38.7	.0471
L28	8.67	0.209	5.00	359	50.0	39.9	.0474
L29	8.65	0.209	5.00	359	50.0	48.2	.126
L30	8.28	1.00	1.00	358	50.0	6.5	.00276

All experiments except L30 in 0.1 M $NaClO_4$. L30 in 0.7 M $NaClO_4$. All experiments at 25°C except L25, L26, L28 and L29. The temperature for these experiments is indicated in Table 4.12.

Table 4.4 Results and experimental conditions for Mn(II) oxidation studies in the presence of silica.

Expt. No.	pH	pO_2 (atm)	$[SiO_2]$ (g/L)	pCO_2 (ppm)	Mn_T (μM)	Initial Mn_{ads} (μM)	k_1 (min^{-1})(1)
S1	8.23	1.00	0.507	358	50.7	1.5	.00008
S2	8.41	1.00	0.508	358	50.8	3.9	.00015
S3	8.68	1.00	0.500	142	50.0	3.0	.00054
S4	8.72	1.00	0.500	142	50.0	3.5	.00042
S5	8.95	1.00	0.500	142	50.0	8.9	.00100
S6	9.05	1.00	0.500	142	50.0	15.4	.0032
S7	9.07	1.00	0.300	142	50.0	13.6	.0023
S8	~9.07	1.00	0.500	*(2)	50.0	12.8	.0035

(1) Corrected for "homogeneous" oxidation.

(2) An NH_4^+/NH_3 buffer was used in this experiment.

All experiments at 25°C in 0.1 M $NaClO_4$.

Table 4.5 Results and experimental conditions for Mn(II) oxidation studies in the presence of alumina.

Expt. No.	pH	pO_2 (atm)	$[Al_2O_3]$ (g/L)	pCO_2 (ppm)	Mn_T (μM)	Initial Mn_{ads} (μM)	k_1 (min^{-1})(1)
AL1	8.58	1.00	3.02	358	50.0	25.5	.00050
AL2	8.95	1.00	0.500	142	50.0	7.5	.00033
AL3	9.00	1.00	0.500	142	50.0	9.5	.00059
AL4	9.08	1.00	0.500	142	50.0	15.6	.0035

(1) Corrected for "homogeneous" oxidation.

All experiments at 25°C in 0.1 M $NaClO_4$.

Table 4.6. Reproducibility of measurements of the rate of oxidation of Mn(II) in the presence of goethite at pH ~ 8.64.

Expt. No.	$k_1 \pm$ 95% confidence limits (min^{-1})	pH
G20	.0124 ± .0014	8.64
G21	.0130 ± .0005	8.65
G22	.0153 ± .0005	8.65
G23	.0142 ± .0018	8.63
G24	.0138 ± .0008	8.64

k_1 = 0.0137 min^{-1}. Relative standard deviation 8.2%.

The experimental conditions used in these experiments are given in Table 4.2.

Table 4.7 Reproducibility of measurements of the rate of oxidation of Mn(II) in the presence of lepidocrocite at pH ~ 8.04.

Expt. No.	$k_1 \pm$ 95% confidence limits (min^{-1})	pH
L2	.00412 ± .00032	8.03
L3	.00452 ± .00018	8.04
L4	.00446 ± .00021	8.04

k_1 = .00437 min^{-1}. Relative standard deviation 4.9%.

The experimental conditions used in these experiments are given in Table 4.3.

Table 4.8 Reproducibility of measurements of the rate of oxidation of Mn(II) in the presence of lepidocrocite at pH ~ 8.51.

Expt. No.	$k_1 \pm$ 95% confidence limits (min^{-1})	pH
	.0183 ± .0010	8.52
L22	.0188 ± .0017	8.50
L23	.0182 ± .0016	8.51

k_1 = 0.0184 min^{-1}. Relative standard deviation 1.7%.

The experimental conditions used in these experiments are given in Table 4.3.

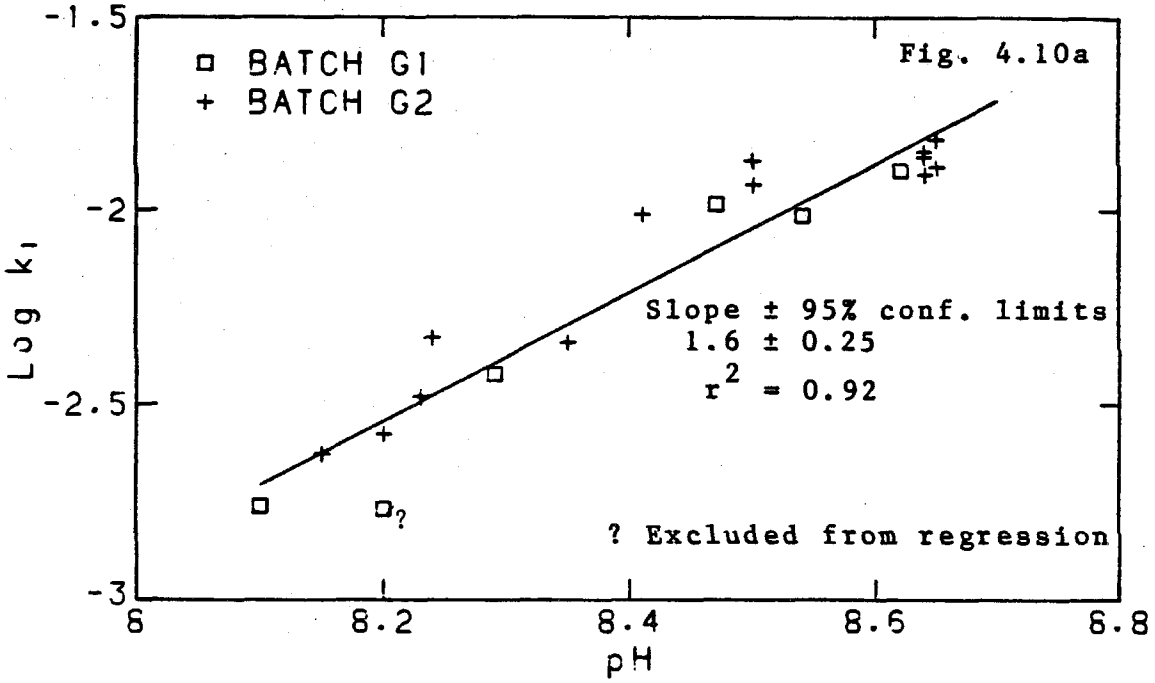

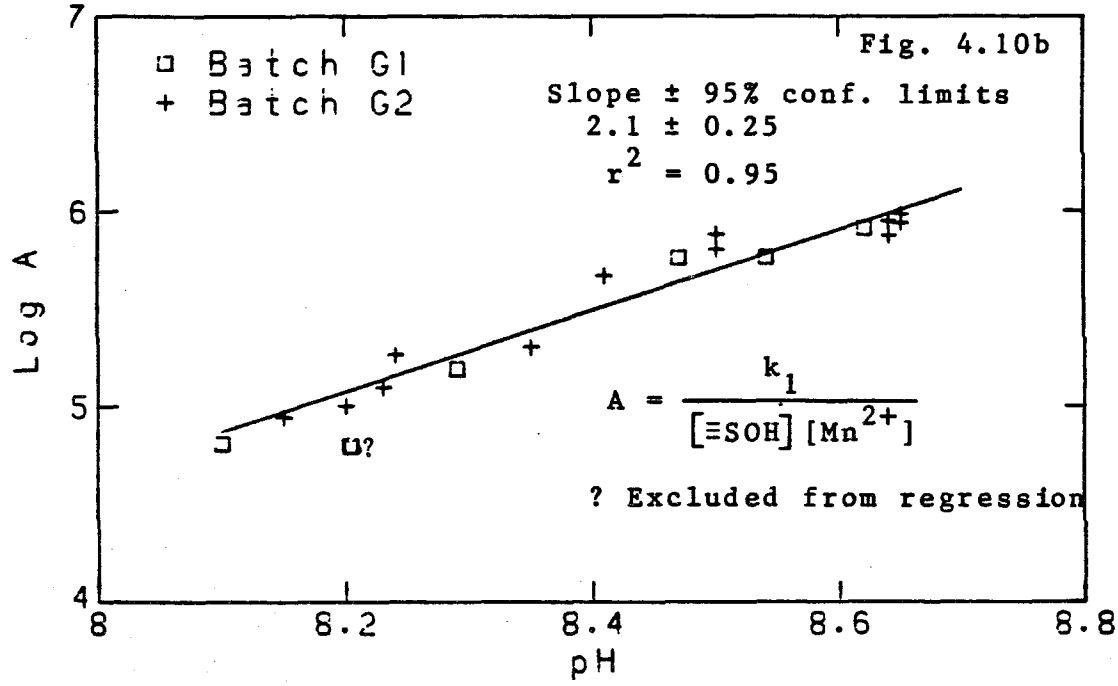

Figure 4.10 Log k_1 vs. pH and Log A vs. pH for the goethite data. Experiments G1-G14, G20-G24. Experiment G2 excluded from regression.

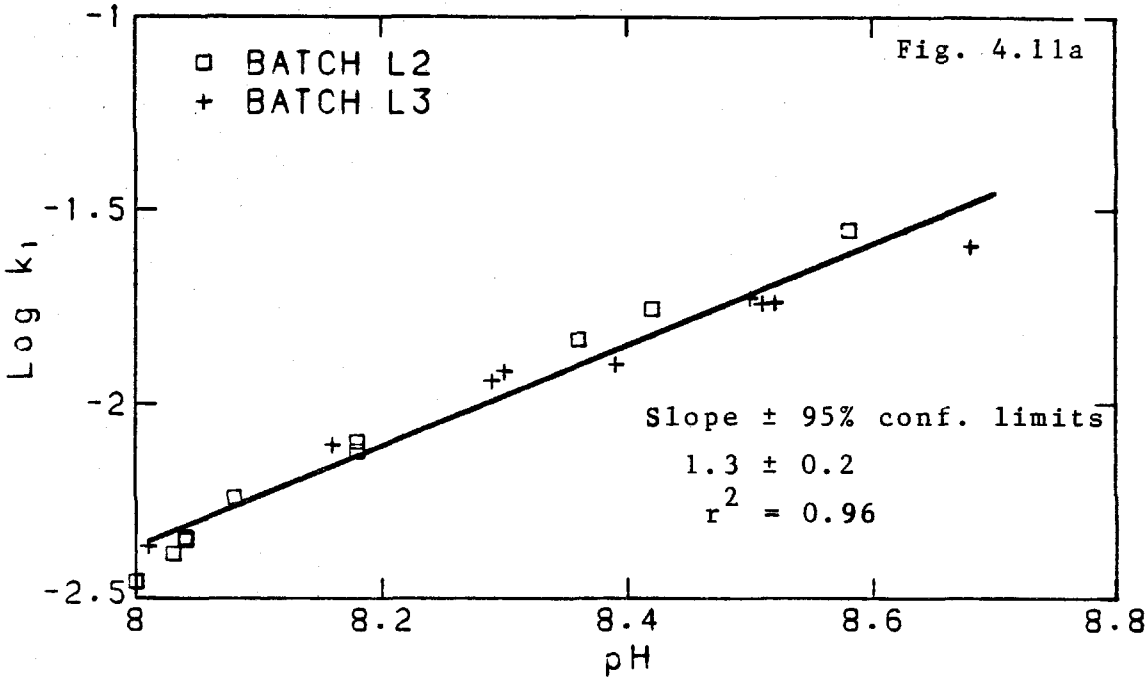

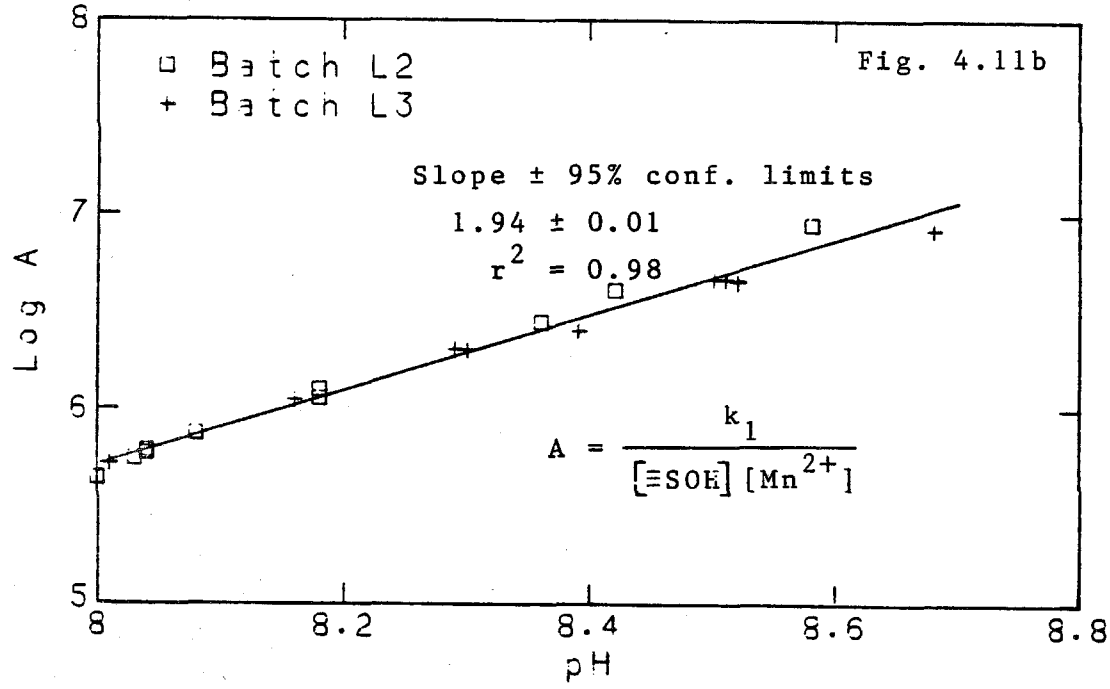

Figure 4.11 Log k_1 vs. pH and log A vs. pH for the lepidocrocite data. Experiments L1-L15 and L21-L24.

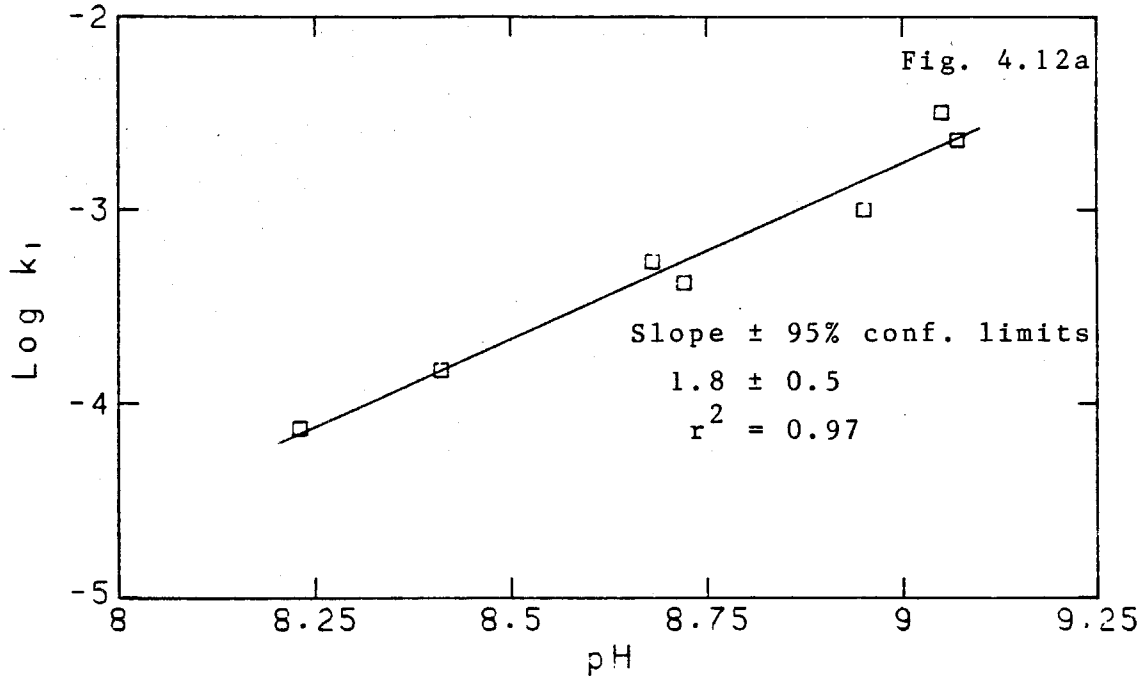

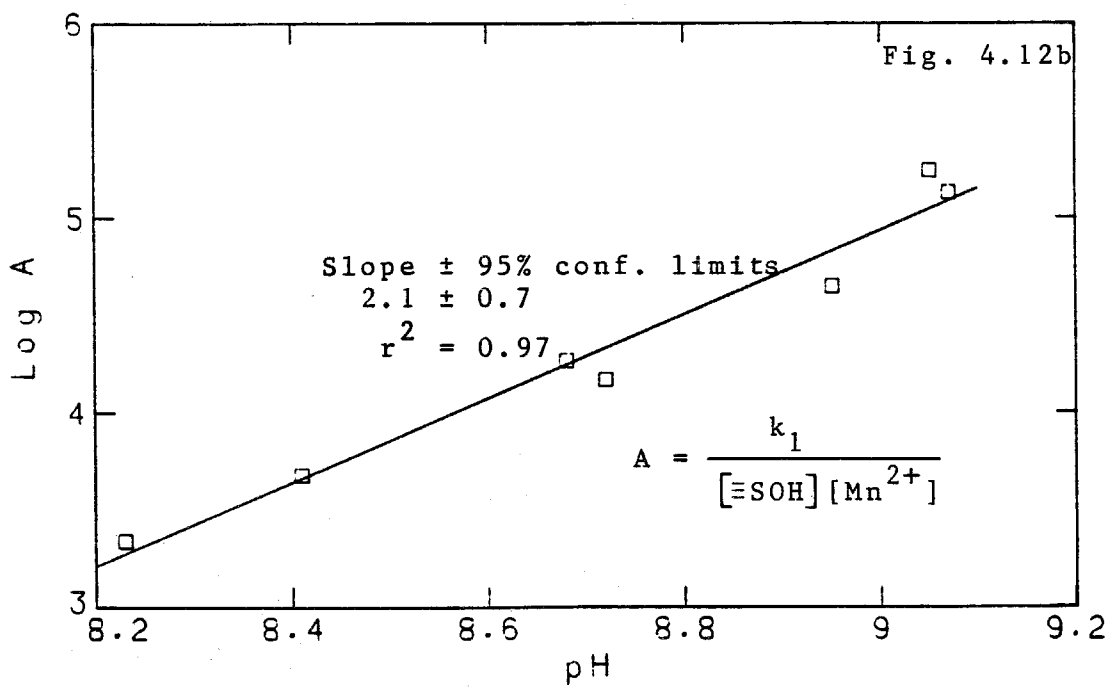

Figure 4.12 Log k_1 vs. pH and log A vs. pH for the silica data. Experiments S1-S6.

the slopes of the regression lines are 1.6 ± 0.25, 1.3 ± 0.2, and 1.8 ± 0.5 respectively. It is suggested in section 4.4 that the oxidation kinetics can be described by a rate law of the form

$$\frac{-d[Mn(II)]}{dt} = k'' \cdot a \cdot \langle (\equiv SO)_2 Mn \rangle \tag{4.20}$$

where

$$\langle (\equiv SO)_2 Mn \rangle = {}^{*}\beta_2 \frac{\langle \equiv SOH \rangle [Mn^{2+}]}{2 [H^+]^2} \tag{4.21}$$

Then at constant ionic strength and pO_2, a plot of log A versus pH should be linear with a slope of 2, where

$$A = \frac{k_1}{[\equiv SOH]\,[Mn^{2+}]} \tag{4.22}$$

The ≡SOH concentration is calculated using the surface equilibrium constants determined in chapter 3. The Mn^{2+} concentration is calculated using the relation

$$[Mn^{2+}] = Mn_f \cdot \alpha_{Mn^{2+}} \tag{4.23}$$

where

$$\alpha_{Mn^{2+}} = \left(1 + {}^{c*}K_1/[H^+] + {}^{c}K_1[HCO_3^-]\right)^{-1} \tag{4.24}$$

Figures 4.10b, 4.11b and 4.12b show that for the goethite, lepidocrocite, and silica data this plot is approximately linear and the slopes of the regression lines are 2.1 ± 0.25, 1.94 ± .01, and 2.1 ± 0.7 respectively. For the oxidation of

Mn(II) on goethite and lepidocrocite, the data fit the plot log A versus pH slightly better than they do a plot log k_1 versus pH. However, using Fisher's z' transformation (Goulden, 1939) to test the difference in the correlation coeffecients at the 95% confidence level, this difference is not significant. For the oxidation of Mn(II) on silica, the fit is equally good for either plot.

Figure 4.10 shows that there is little, if any, difference in the rate of oxidation of Mn(II) on the two batches of goethite used in these experiments. The same is also the true for the two batches of lepidocrocite used in these experiments (see Figure 4.11).

4.4.3.3 Influence of oxygen

As is shown in Table 4.9, the rate of oxidation of Mn(II) on goethite and lepidocrocite is approximately five times faster under oxygen than under air (pO_2 = 0.21 atm.), indicating that the reaction is probably first order in oxygen concentration.

4.4.3.4 Influence of solids concentration

The rate of oxidation of Mn(II) on goethite, lepidocrocite and silica increases with increasing solids concentration (see Tables 4.2-4.4). As shown in Figure 4.13, a plot of log k_1 versus log solids concentration is approximately linear. The slopes of the regression lines through the data for the oxidation of Mn(II) on goethite and lepidocrocite are 0.9 ± 0.2 and 0.6 ± 0.4 respectively.If the

Table 4.9 Mn(II) oxidation in the presence of goethite or lepidocrocite as a function of oxygen concentration.

Expt. No.	pO_2 (atm)	pH	k_1 (min^{-1})
Geothite			
G13	1.00	8.50	.0117
G14	1.00	8.50	.0135
G15	0.209	8.50	.00296
Lepidocrocite			
L13	0.209	8.29	.00224
L14	1.00	8.30	.0122
L15	1.00	8.29	.0115
L20	0.209	8.50	.00362
L21	1.00	8.52	.0183
L22	1.00	8.50	.0188
L23	1.00	8.51	.0182

The experimental conditions used in these experiments are given in Tables 4.2 and 4.3.

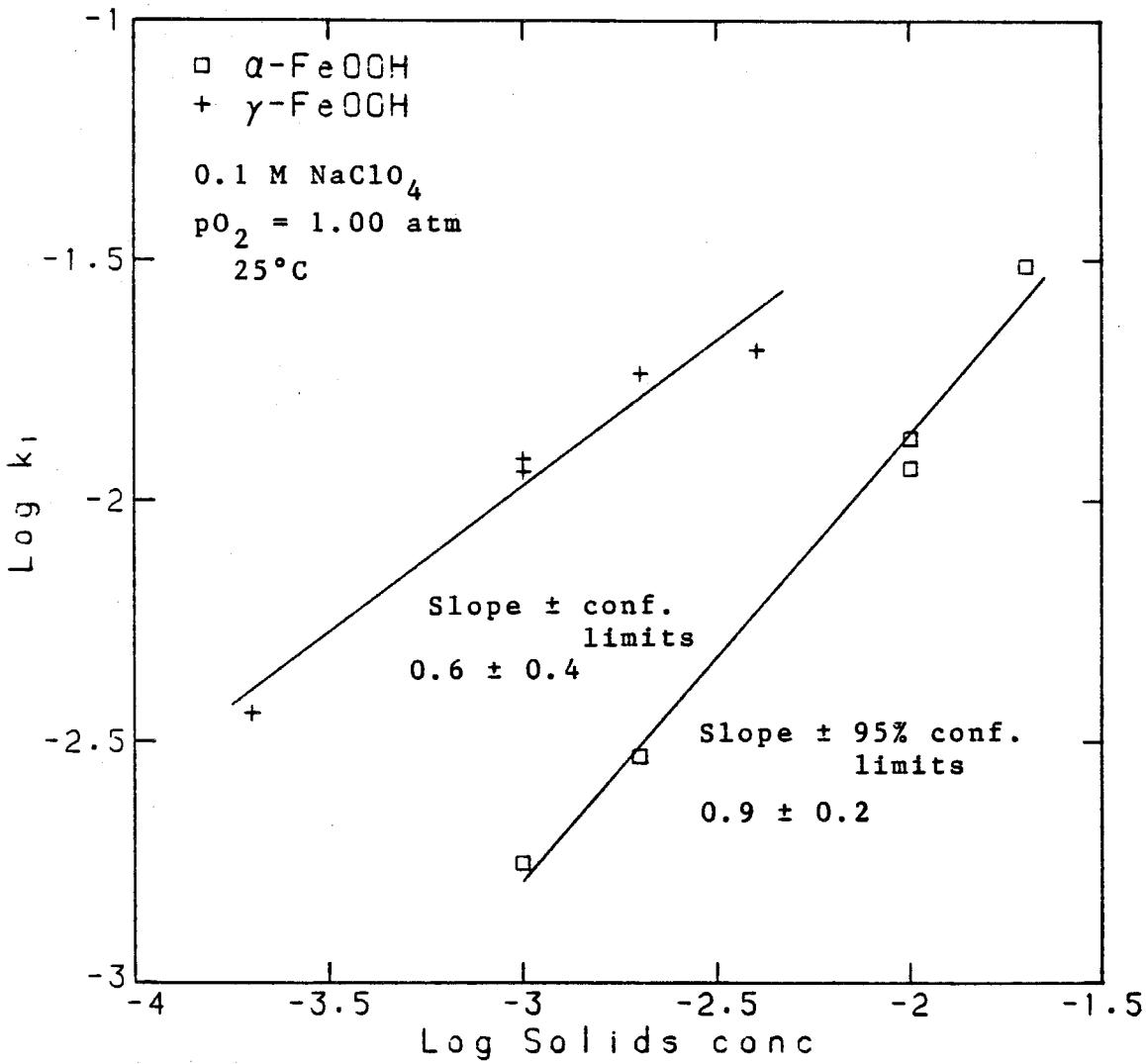

Figure 4.13 Log k_1 as a function of solids concentration for the oxidation of Mn(II) in the presence of geothite or lepidocrocite. Experiments G13, G14, G16-G18 and L14-L18.

rate of the reaction is described by equation 4.20, then a plot of $\log(k_1/[Mn^{2+}])$ versus log [≡SOH] should be linear with slope 1. Figure 4.14 shows that for Mn(II) oxidation on the goethite or lepidocrocite surface, this plot is approximately linear. The slopes of the regression lines 1.13 ± 0.26 and 1.14 ± 0.34 respectively. The rate of oxidation of Mn(II) is faster in a suspension containing 0.5 g/L silica than in a suspension containing 0.3 g/L silica (see Table 4.4, Experiments S6 and S7). For these data the slope of the plot of $\log(k_1/[Mn^{2+}]$ versus log solids concentration is 0.7.

4.4.3.5 Effect of ionic strength

As is shown in Table 4.10, the rate of oxidation of Mn(II) on lepidocrocite is about 4 times slower in 0.7 M $NaClO_4$ than in 0.1 M $NaClO_4$. The concentration of adsorbed Mn is about 2 times lower at the higher ionic strength. It is apparent that the increase in ionic strength shifts the surface equilibria significantly. However, it is not possible to quantify these effects. Changes in ionic strength will not only affect the activity of solution species, but will alter the electrical aspects of the solid-water interface and may, if the ions in the support electrolyte are adsorbed on the surface, alter site availibility. Neither the electrostatic effects nor the site availibility can be quantified in this system with the available information.

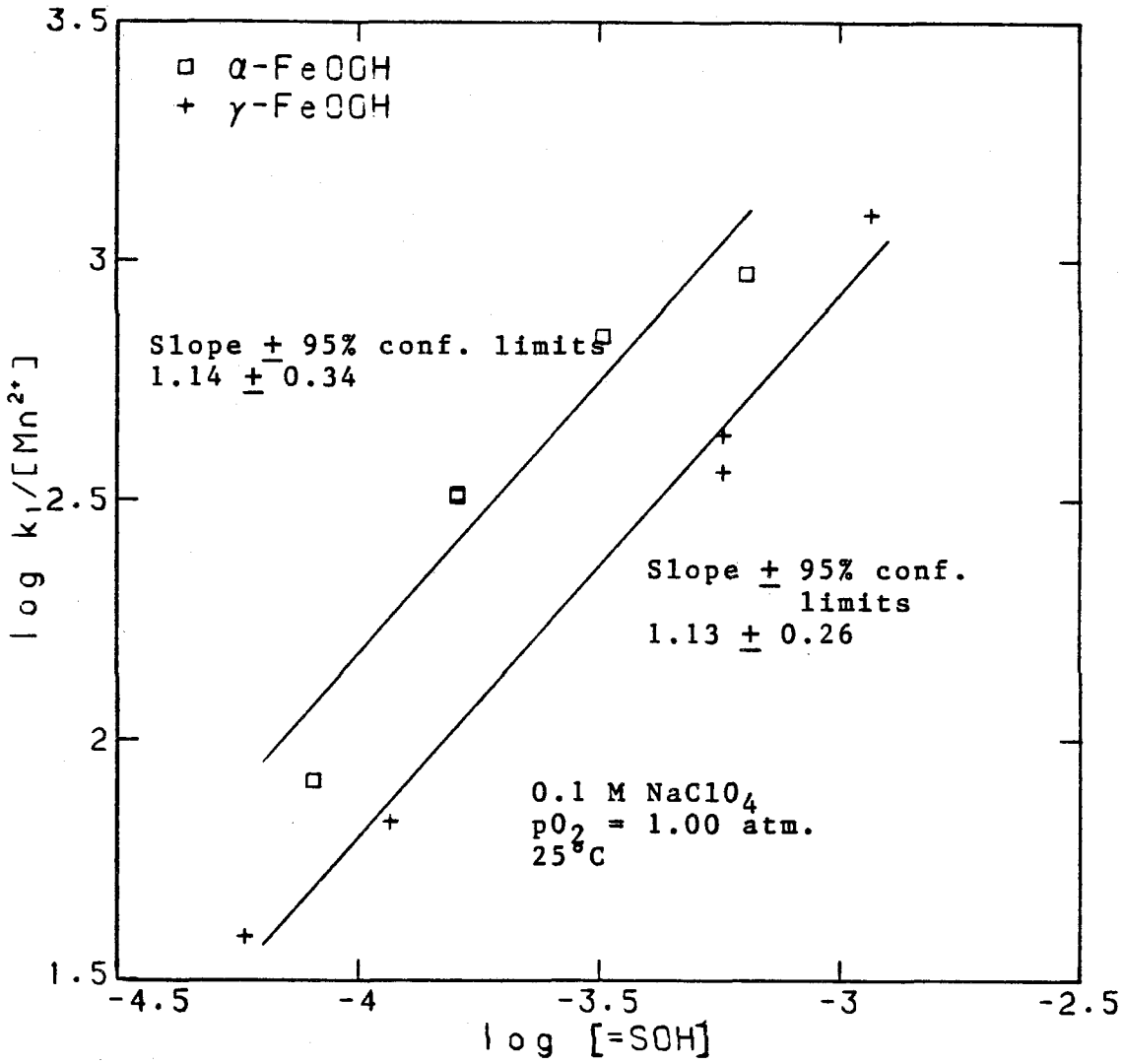

Figure 4.14. Log ($k_1/[Mn^{2+}]$) as a function of log [≡SOH] for the oxidation of Mn(II) in the presence of goethite or lepidocrocite.

Table 4.10 Mn(II) oxidation in the presence of lepidocrocite as a function of ionic strength.

Expt. No.	Ionic Medium	pH	k_1 (min^{-1})
L14	0.1 M $NaClO_4$	8.30	.0122
L15	"	8.29	.0115
L3	0.7 M $NaClO_4$	8.28	.00276

The experimental conditions used in these experiments are given in Table 4.3.

4.4.3.6 Effect of light

Two experiments were conducted to assess the effect of normal laboratory lighting on the rate of Mn(II) oxidation. The first part of this experiment was conducted in "darkness"; during this part of the experiment the reaction vessel was covered in aluminium foil and the laboratory fluorescent lights were turned off. The only lighting in the room was a darkroom light. In the second part of the experiment the foil was removed and the fluorescent lights turned on. As shown in Figure 4.15, normal laboratory lighting has no effect on the rate of Mn(II) oxidation in the presence of goethite or lepidocrocite. The purpose of these experiments was to establish whether normal laboratory lighting affects the the rate of Mn(II) oxidation. One cannot from the results of these experiments preclude the possibilty that light of greater intensity or shorter wavelength could effect the rate of Mn(II) oxidation.

4.4.3.7 Effect of buffer composition

As was pointed out previously, a buffer is necessary in these experiments. Ideally the buffer should have no effect on the rate of Mn(II) oxidation. A carbonate buffer system has been used in these experiments for the reason that it is the principal buffer in neutral and alkaline natural waters. The possible disadvantage of this buffer is that rhodocrocite, $MnCO_3(s)$ is only sparingly soluble. However, as is discussed in section 4.4.1 rhodocrocite does not appear to

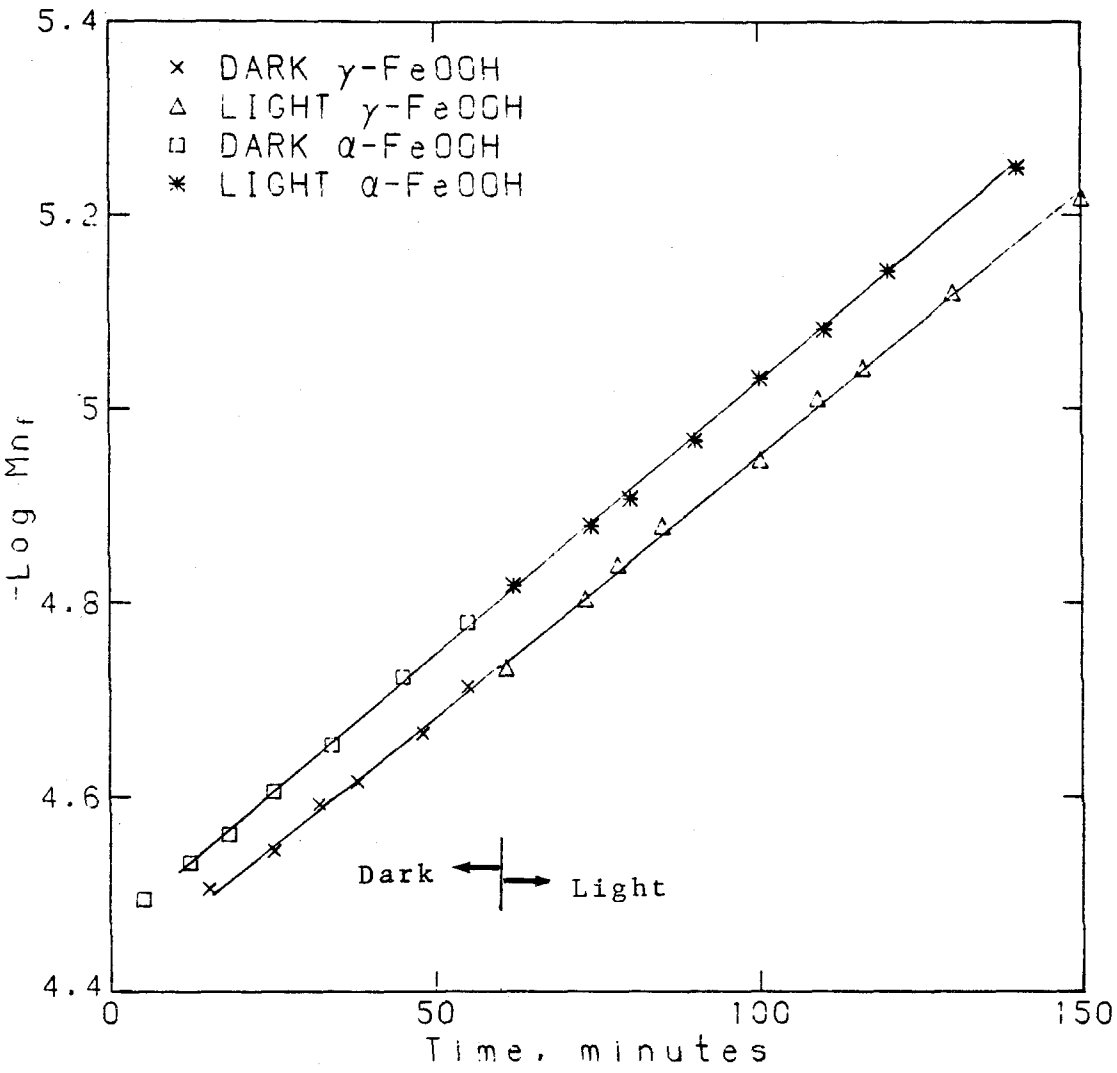

Figure 4.15 The effect of light upon Mn(II) oxidation in the presence of goethite or lepidocrocite.

form rapidly in the systems studied in these experiments. Ideally a buffer should not interact with Mn(II) at all, but all buffers are to some extent complexing agents. In the systems studied here less than 10% of the soluble Mn(II) is present as $MnHCO_3^+$. Though the amount of $MnHCO_3^+$ is small, if this complex were rapidly oxidized then this would affect the rate of Mn(II) oxidation. However, as was shown in section 4.4.2, in carbonate buffers the "homogeneous" oxidation of Mn(II) is slow compared to the rate of oxidation of Mn(II) on the surfaces studied in this work. It would also be desirable if the buffer did not affect the binding of Mn(II) to the metal oxide surface. As was shown in Figures 4.3 and 4.4, the presence of HCO_3^-/CO_3^{2-} does not influence the adsorption behaviour of Mn(II) appreciably. Also, Balistrieri and Murray (1982) found that HCO_3^-/CO_3^{2-} did not affect the binding of Zn(II) and Cd(II) on goethite.

As is shown in Table 4.4 (Experiments S6 and S7), the rate of oxidation of Mn(II) in carbonate and NH_3/NH_4^+ buffers is similar. This experiment shows that either the bicarbonate and ammonical buffers have little effect on the rate of Mn(II) oxidation or if they do affect the oxidation rate, they do so in about the same degree. The NH_3/NH_4^+ is in one way more suitable than the carbonate buffer, because Mn(II) is soluble in this buffer. The disadvantages of this buffer are that the buffer is not an important one in natural waters and that the pH of the system is not well

controlled because of NH_3 volatilization.

In summary, the carbonate buffer appears not to significantly influence the rate of Mn(II) oxidation and is a suitable buffer for studying this reaction.

4.4.3.8 Oxidation of Mn(II) on the alumina surface

The results obtained for the oxidation of Mn(II) on the alumina surface are shown in Table 4.5. The rate of oxidation of Mn(II) in the presence of alumina is considerably slower than that on the other metal oxide surfaces studied. There is some reason to doubt whether the rate of Mn(II) oxidation is actually as fast as that indicated in Table 4.5. Non-oxidative removal may be significant in these experiments. The removal of filterable Mn under nitrogen was only monitored for 30 -60 minutes, which is insufficient time to determine if the rate of non-oxidative removal is significant in an oxidation experiment which takes several hours. If significant non-oxidative removal (due either to continued adsorptive uptake or to $MnCO_3(s)$ precipitation) occurs in these experiments then the results given in Table 4.5 would overestimate the rate of oxidation of Mn(II) in the presence of alumina. This question was not investigated further, since the rate of oxidation of Mn(II) in the presence of alumina is so slow that it is not of interest in natural waters.

4.4.3.9 Temperature dependence

The temperature dependence of the rate of oxidation of Mn(II) on goethite and lepidocrocite is shown in Table 4.11. Mn(II) was so strongly adsorbed on the lepidocrocite surface at 40°C that the rate of oxidation could not be measured accurately. Also, at this temperature the assumption that the system is in sorptive equilibrium may no longer be valid unless the adsorption/desorption kinetics are also considerably faster at higher temperatures. The apparent activation energies for the reaction on the goethite and lepidocrocite surface are 100 ± 30 kJ/mol and 90±40 kJ/mol respectively (see Figure 4.16). If these activation energies are corrected for the temperature dependence of oxygen solubility (assuming first order dependence on oxygen concentration), then the apparent activation energies for the oxidation on the goethite and lepidocrocite surfaces are 120 kJ/mol and 110 kJ/mol respectively. These activation energies are high, indicating the reaction is strongly temperature dependent.

The intial adsorbed Mn and pH in these experiments are also indicated in Table 4.11. The pH in these experiments varies, because the pH of the suspension was adjusted to 8.3 at 25°C, and then the temperature was adjusted to the desired value. The extent of Mn(II) adsorption increases greatly with temperature. It is interesting to ask what influence this has on the temperature dependence of the rate

Table 4.11 Mn(II) oxidation in the presence of goethite or lepidocrocite as a function of temperature.

Expt. No.	Temp. K	pH	pO_2 (atm)	Initial Mn_{ads} (μM)	k_1 (min^{-1})
Goethite					
G20	283.2	8.60	1.00	9.8	.00134
G24	293.0	8.58	1.00	17.2	.00991
G25	298.2	8.65	1.00	21.5	.0130
G26	303.2	8.55	1.00	23.8	.0322
G27	313.2	8.68	1.00	32.1	.088
Lepidocrocite					
L25	279.4	8.60	1.00	19.8	.00713
L26	293.2	8.62	1.00	34.8	.0324
L27	298.2	8.68	1.00	38.7	.0471
L28	303.1	8.67	0.209	39.9	.0474
L29	313.8	8.65	0.209	48.2	.126

The experimental conditions used in these experiments are given in Tables 4.2 and 4.3.

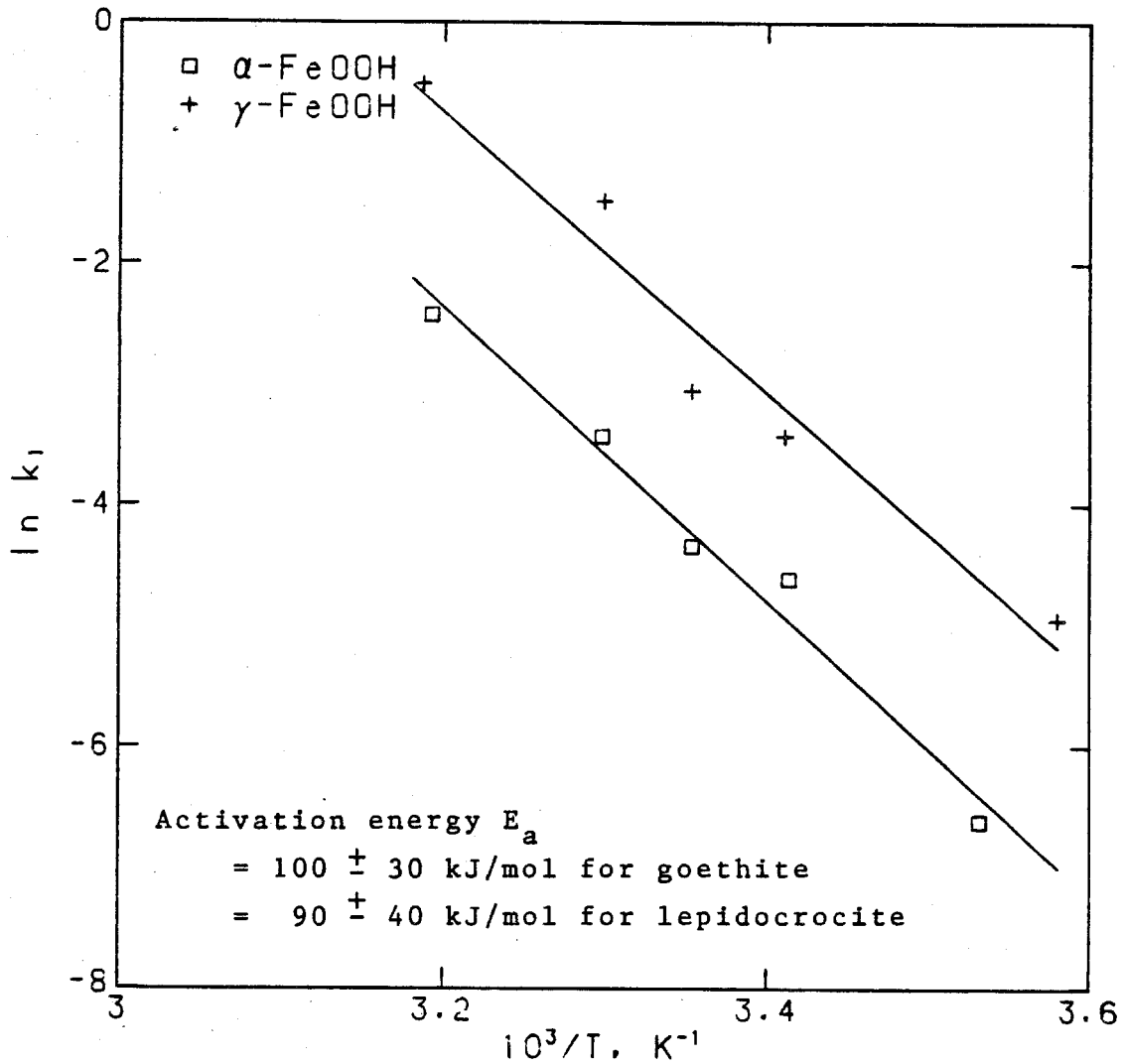

Figure 4.16. Ln k_1 as a function of 1/T for the oxidation of Mn(II) in the presence of goethite or lepidocrocite. Experiments G20, G24-27 and L25-29.

of Mn(II) oxidation. The enthalpy of adsorption ΔH_{ads} for the reaction

$$Mn^{2+}(aq) \rightleftharpoons Mn_{ads} \qquad (4.25)$$

on the goethite surface is approximately 50 kJ/mol. For this reaction on the lepidocrocite surface, ΔH_{ads} is about 55 kJ/mol. If, as is suggested in the following section, the rate of oxidation is proportional to the concentration of $(\equiv SO)_2Mn$ on the surface and if one assumes that the enthalpy for the reaction

$$Mn^{2+} + \begin{matrix} =SOH \\ | \\ =SOH \end{matrix} \rightleftharpoons \begin{matrix} =SO \\ | \\ =SO \end{matrix} \!\!\diagdown\!\!\diagup Mn + 2H^+ \qquad (4.26)$$

is similar to ΔH_{ads} (which is not unreasonable, because $(\equiv SO)_2Mn$ is the principal manganese surface species, so the enthalpy for reaction 4.26 should dominate ΔH_{ads}), then the apparent activation energies for the oxidation of Mn(II) on the goethite and lepidocrocite surfaces are 50 kJ/mol and 35 kJ/mol respectively. That is, about half the measured activation energy can be attributed to the temperature dependence of the adsorption process. The other half can be attributed to the temperature dependence of the other reactions proceeding the rate controlling step and to the activation energy for the rate controlling step.

4.5 Rate law formulation and mechanism

In the previous section the dependence of the rate of Mn(II) oxidation on pH, oxygen concentration and solids concentration was discussed. Based on purely statistical

considerations, the order of the reaction with respect to either solids concentration or oxygen concentration is not known to any great degree of certainty, because they are based on few data. But it seems reasonable on the basis of chemical considerations to suggest that the order of the reaction is integral and that it is first order with respect to <≡SOH> and oxygen concentration. Given that the reaction occurs at the surface, it is reasonable that the reaction rate would be proportional to the concentration of the reactive species on the surface. The concentration of both Mn surface species under the conditions used in these experiments is proportional to <≡SOH>, so any reasonable mechanism would be consistent with a first order dependence on <≡SOH>. It is less certain that the reaction is first order in oxygen concentration, but this finding is consistent with the findings of Morgan(1964) and Brewer(1975) for the autocatalytic oxidation of Mn(II). Morgan's conclusions are based on a limited data set so they must be regarded as tentative. Brewer does not present the data on which his conclusions were based, so it is impossible to assess the uncertainty associated with his results.

The reaction is first order in Mn_f and, as was shown in sections 4.3 and 4.4.3.1, this means that under the conditions of these experiments the reaction is first order in Mn(II).

For the oxidation of Mn(II) on goethite and lepidocrocite the experimental data are consistent with a rate law of the following form:

$$\frac{-d[Mn(II)]}{dt} = k^* \frac{<\equiv SOH>[Mn^{2+}]}{[H^+]^2} \cdot a \cdot pO_2 \qquad (4.27)$$

where k^* has the units M min^{-1} atm^{-1}.

The oxygen dependence of the rate of oxidation of Mn(II) on silica was not investigated, but assuming the reaction is first order in oxygen concentration, the data for Mn(II) oxidation on silica are consistent with 4.27.

The oxidation of Mn(II) on these solids is a surface process. It might reasonably be expected to depend on the concentration of the reactive surface species. The pH dependence of the reaction rate suggests that the reactive surface species might be the bidentate complex $(\equiv SO)_2Mn$ (or the hydrolysed complex $\equiv SOMn\text{-}OH$). If the initial concentration of this species is plotted against the observed initial rate, normalized with respect to oxygen concentration, then for the results for the silica, goethite and lepidocrocite systems there is a strong correlation between these parameters (see Figure 4.17). For the reaction where alumina is present there are too few data to draw a conclusion, but if the one outlying point indicated on Figure 4.17 is not considered, the data show that the enhancement of the oxidation rate on alumina is less than that on the other solids studied in this work. This

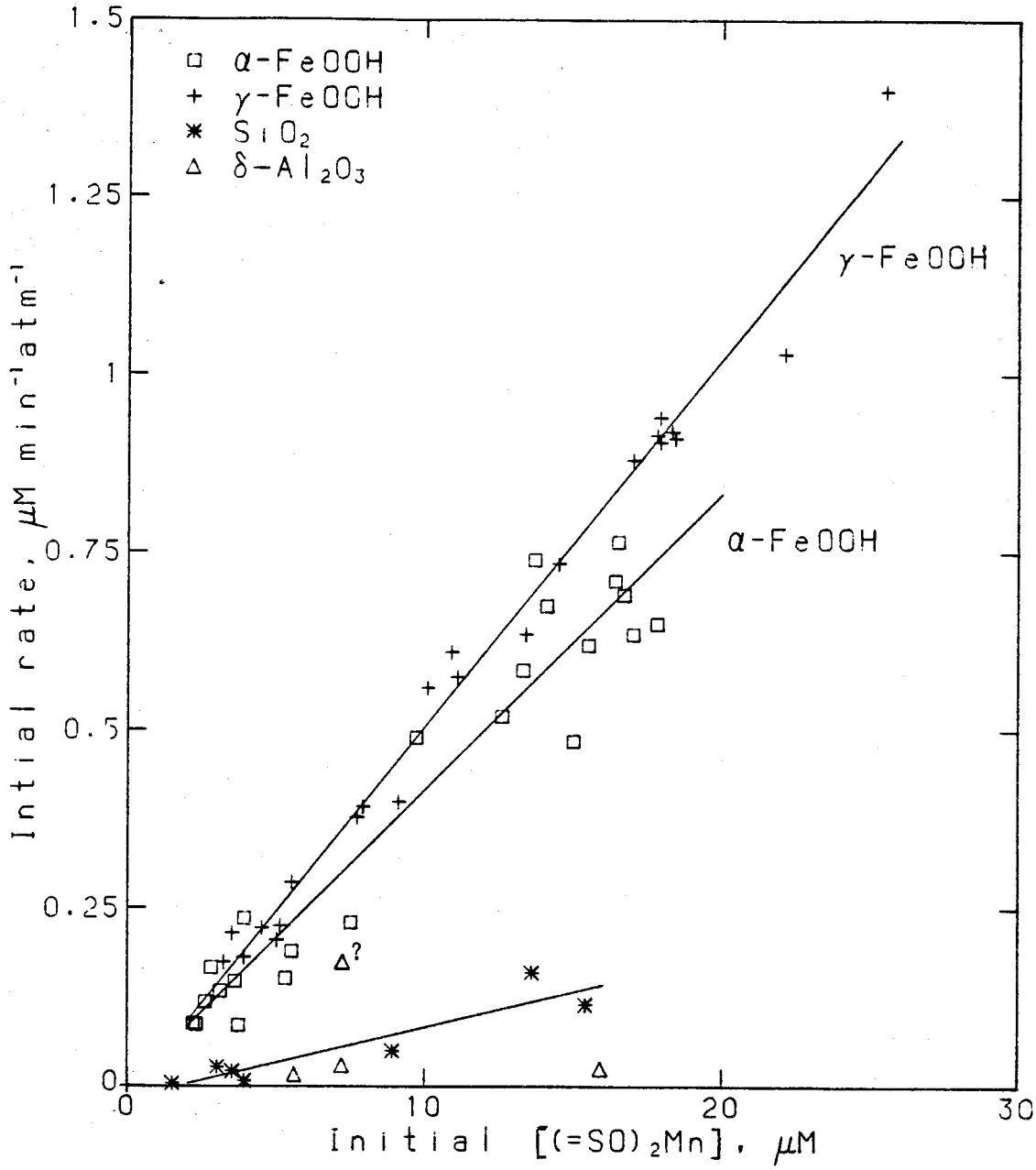

Figure 4.17. Initial oxidation rate as a function of initial $(\equiv SO)_2$ Mn concentration.

correlation suggests an alternative formulation of the rate law:

$$\frac{-d[Mn(II)]}{dt} = k'' \cdot a \cdot \langle(\equiv SO)_2Mn\rangle \; pO_2 \qquad (4.28)$$

The values for the rate constant k" are shown in Table 4.12.

To calculate k" for the silica and alumina surface, it is assumed that the reaction is first order in oxygen concentration and $\langle(\equiv SO)_2Mn\rangle$. The k" decrease in the order

lepidocrocite ~ goethite > silica > alumina.

The similarity of the the constant k" for goethite and lepidocrocite is striking and suggests that the immediate coordinative environment of the adsorbed Mn(II) is important in determining the enhancement of the oxidation of Mn(II), rather than the crystal structure of the solid.

An interpretation of the above reactivity sequence is not immediately apparent. One might speculate that a plausible mechanism for the reaction is as shown in Figure 4.18. In this mechanism the accelerated oxidation of Mn(II) on the surface, compared to that in solution, could be explained in terms of the energetics of the reaction Mn(II) $\longrightarrow$ Mn(III). The energetics of the reaction

$$Mn^{2+} \rightleftharpoons Mn^{3+} + e^- \qquad (4.29)$$

are unfavourable (log K = -25, Stumm and Morgan, 1980). Because of this, the oxidation of $Mn^{2+}(aq)$ to $Mn^{3+}(aq)$ is

Table 4.12 k" for the oxidation of Mn(II) on goethite, lepidocrocite, silica and alumina.

Solid	k" (min^{-1} atm^{-1})
αFeOOH	.042
γFeOOH	.052
SiO_2	.010
δAl_2O_3	<.005

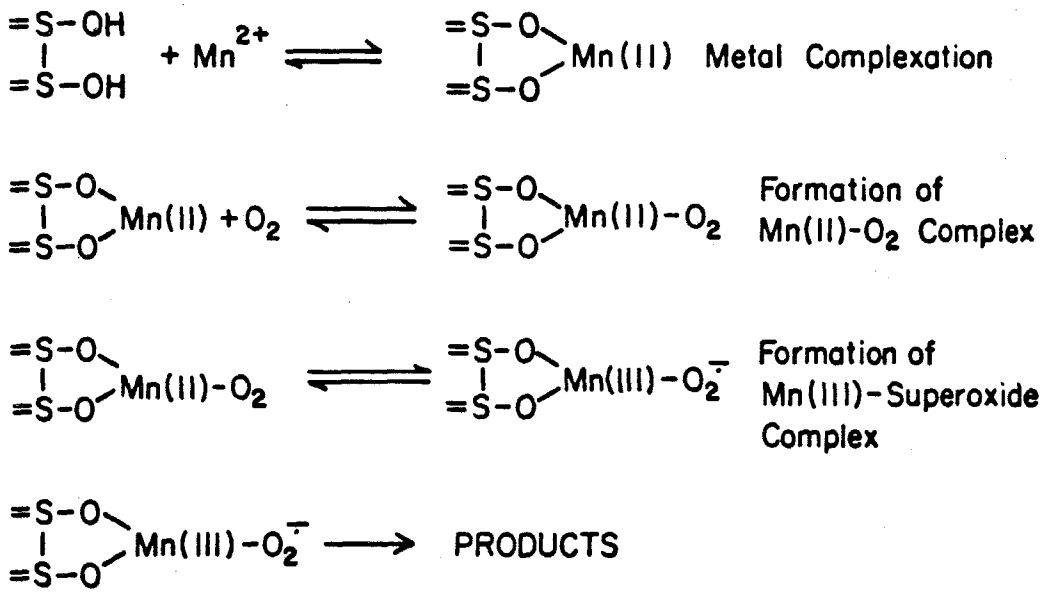

Figure 4.18. Possible mechanism for the oxidation of Mn(II) on a metal oxide surface.

likely to be very slow. The energetics of the reaction Mn(II) $\longrightarrow$ Mn(III) are more favourable at higher pH. For the reactions

$$Mn^{3+} + H_2O \rightleftharpoons MnOH^{2+} + H^+ \qquad (4.30)$$

$$Mn^{2+} + H_2O \rightleftharpoons MnOH^{+} + H^+ \qquad (4.31)$$

log K are ~0 (Sillen and Martell, 1971) and -10.0 (see Appendix A) respectively. Combining 4.29, 4.30, and 4.31, one obtains

$$MnOH^{+} \rightleftharpoons MnOH^{2+} + e^- \quad K=10^{-15} \qquad (4.32)$$

showing that at higher pH the reaction Mn(II) $\longrightarrow$ Mn(III) is more energetically favourable. The reaction is still more favourable if Mn(III) is present in a solid form. For the reaction

$$Mn^{2+} + 2H_2O \rightleftharpoons MnOOH(s) + 3H^+ + e^- \qquad (4.33)$$

log K = -25.3 (Stumm and Morgan, 1980). At pH 8.5, pε 12.3

$$\frac{\{MnOOH(s)\}}{\{Mn^{2+}\}} = 10^{12.5} \qquad (4.34)$$

Under these conditions the oxidation of Mn(II) is energetically favourable. It seems not unreasonable to suggest that if manganese is bound to a solid the activation energy for the electron transfer step shown in Figure 4.18 might be lowered, because the product $(\equiv SO)_2Mn(III)-O_2^{\bullet}$ is

stabilized when Mn(III) is bound to the solid. The sequence of reactivity is not easily explained. The reactivity of the surface complex does decrease as the electronegativity of the metal ion in the solid (Fe(III), Si(IV) or Al(III)) decreases, suggesting that possibly the activation energy for the electron transfer is lowered if manganese is bound to an electron withdrawing group. Another possible explanation is that the reactivity of the surface complex is influenced by steric factors. If manganese is bound to the surface as a bidentate complex, then the distance between the two surface groups to which it is bound could influence the reactivity of the surface complex.

An alternative explanation for the accelerated oxidation of manganese on the surface is that the binding of dioxygen to Mn(II) is stronger when Mn(II) is bound to the surface. Fallab (1967) has suggested that the binding of Fe(II) to dioxygen is enhanced if the Fe(II) is complexed to another ligand that is a π-donor. If the surface can act as a π- donor, then Mn(II) could more effectively bind dioxygen when it is adsorbed on the surface. This should enhance the rate of oxidation of Mn(II).

It is possible that on the iron oxide surface, Mn(II) is oxidized by Fe(III) to give Mn(III) and Fe(II) (Hem, 1981). No reduced iron was found in solution, but at pH 8-9, Fe(II) would be rapidly removed from solution (Sung and Morgan, 1980). This mechanism does not explain the enhanced

oxidation of Mn(II) on silica or alumina, since neither Si(IV) nor Al(III) has an accessible lower oxidation state.

CHAPTER 5

THE EFFECT OF OTHER IONS ON MN(II) OXIDATION IN THE PRESENCE OF LEPIDOCROCITE.

5.1 Introduction

This chapter discusses the effect of other ions on the rate of oxidation of Mn(II) in the presence of lepidocrocite (γ-FeOOH). Lepidocrocite was chosen for these experiments, because of the four metal oxides studied it was the most effective in enhancing Mn(II) oxidation.

Since the rate of oxidation of Mn(II) is enhanced when Mn(II) is bound to the surface, the displacement of Mn(II) from the surface will inhibit the oxidation of Mn(II). The adsorption of other cations will displace Mn^{2+} from the surface by occupying the surface sites. The adsorption of anions may either decrease or enhance the binding of Mn(II). The adsorption of an anion decreases the number of sites available, but it also decreases the charge on the surface. The decrease in surface charge enhances the binding of positively charged species, which can outweigh the effect of decreasing the number of sites available. If the other anions present are ligands, the formation of solution complexes will displace Mn(II) from the surface (Davis and Leckie, 1968; Vuceta and Morgan, 1968).

The model discussed in Chapter 3 may be generalized to consider the interactions of the lepidocrocite surface with

other cations M^{z+}

$$\equiv FeOH + M^{z+} \rightleftharpoons \equiv FeOM^{z-1} + H^{+} \quad (5.1)$$

$$\equiv FeOH + M^{z+} + H_2O \rightleftharpoons \equiv FeOMOH^{z-2} + 2H^{+} \quad (5.2)$$

and with anions A^{z-}

$$\equiv FeOH + A^{z-} + H^{+} \rightleftharpoons \equiv FeA^{(z-1)-} + H_2O \quad (5.3)$$

$$\equiv FeOH + A^{z-} + 2H^{+} \rightleftharpoons \equiv FeHA^{(z-2)-} + H_2O \quad (5.4)$$

The formation of solution complexes can be described by the equation

$$Mn^{2+} + A^{z-} + nH^{+} \rightleftharpoons MnAH_n^{(n+2-z)+} \quad (5.5)$$

The Mn(II) complexes may be bound to the surface as "ternary" complexes (Bourg and Schindler, 1978; Bourg et al., 1979; Benjamin and Leckie, 1981) . These complexes may be bound to the surface via the metal (Type I)

$$\equiv S\text{-}O\text{-}Mn\text{-}A$$

or through the ligand (Type II)

$$\equiv S\text{-}O\text{-}A\text{-}Mn$$

In addition to the effects that other ligands have on the binding of Mn(II) to the surface, it is necessary to consider whether any metal complexes formed in the system are readily oxidizable.

In this work, the effect of Ca^{2+}, Mg^{2+}, Cl^{-}, SO_4^{2-}, phosphate, silicate, phthalate and salicylate on the oxidation of Mn(II) on lepidocrocite have been considered. Ca^{2+}, Mg^{2+}, Cl^{-}, and SO_4^{2-} are major components of natural waters Previous studies have shown that these ions bind to iron oxide surfaces (Balistrieri and Murray, 1979; Sigg and Stumm, 1981). The effect of the other major ions in natural waters (Na^{+}, K^{+} and HCO_3^{-}/CO_3^{2-}) was not studied. Na^{+} and K^{+} do not interact strongly with the iron oxide surface (Balistrieri and Murray, 1979; Sigg and Stumm, 1981). The extent of binding of HCO_3^{-}/CO_3^{2-} to the goethite surface has been estimated to be small at pH's above 7.5 (Sigg and Stumm, 1979; Balistrieri and Murray, 1981). Phosphate and silicate both interact strongly with iron oxide surfaces (Sigg and Stumm, 1979). Salicylate and phthlate were chosen as simple models for naturally occurring organics found in aquatic systems. Natural organic matter (Parfitt et al., 1977a; Davis, 1980; Davis and Gloor, 1981; Tipping et al.,1981a, 1981b) and polar organic compounds (Parfitt et al., 1977b, Davis and Leckie, 1978) have been shown to bind to iron oxide surfaces.

5.2 Results and discussion

5.2.1 Adsorption studies

This section considers the adsorption of Ca^{2+}, Mg^{2+}, Cl^{-}, SO_4^{2-}, phosphate, silicate, phthalate and salicylate on the lepidocrocite surface.

It is assumed that for the systems containing Ca^{2+}, Mg^{2+}, Cl^{-}, SO_4^{2-}, phosphate, and silicate, the surface species found on the lepidocrocite surface are the same as those found on the goethite surface (Balistrieri and Murray, 1979; Sigg and Stumm, 1981). At the pH used in the oxidation experiments (pH ~8.3), the important surface species are those indicated in Table 5.1. It is assumed that the possible salicylate and phthlate complexes on the surface are $\equiv$Fe-AH and $\equiv FeA^{-}$ (where A=salicylate or phthlate). The acidity constants for the lepidocrocite surface have been previously determined (see Chapter 3). Knowing the surface acidity constants, it is in theory possible to determine the surface binding constant for an ion which forms a single surface species by measuring the extent of adsorption of the ion at a single pH. If the ion forms two surface complexes then it is necessary to measure the extent of adsorption at two pH's to determine the two surface binding constants. The results obtained are adequate to make a semi-quantitative estimate of the binding of these ions to the surface in the experimental systems studied and in natural waters.

The experimental conditions used and results found in the experiments discussed in this section are given in Table 5.2. The experimental conditions were chosen so that the amount of the ion adsorbed could be determined by measuring the concentration of the ion in the filtrate, after equilibrating the solution with the solid. For this reason,

Table 5.1 Interactions of anions, Ca^{2+} and Mg^{2+} with the lepidocrocite surface.

	log $K^{(1)}$
$\equiv FeOH + Ca^{2+} + H_2O \rightleftharpoons \equiv FeOCaOH + 2H^+$	-14.5
$\equiv FeOH + Mg^{2+} + H_2O \rightleftharpoons \equiv FeOMgOH + 2H^+$	-13.7
$\equiv FeOH + sal^{2-} + 2H^+ \rightleftharpoons \equiv FesalH + H_2O$	23.7
$\equiv FeOH + sal^{2-} + H^+ \rightleftharpoons \equiv Fesal^- + H_2O$	15.6
$\equiv FeOH + phth^{2-} + 2H^+ \rightleftharpoons \equiv phthH + H_2O$	17.2
$\equiv FeOH + phth^- + H^+ \rightleftharpoons \equiv Fephth^- + H_2O$	<9.5
$\equiv FeOH + SO_4^{2-} + H^+ \rightleftharpoons \equiv FeSO_4^- + H_2O$	8.4
$\equiv FeOH + PO_4^{3-} + 2H^+ \rightleftharpoons \equiv FePO_4H^- + H_2O$	25.7
$\equiv FeOH + H_2SiO_4^{2-} + H^+ \rightleftharpoons \equiv FeSiO_4H_2^- + H_2O$	18.2
$\equiv FeOH + H_2SiO_4^{2-} + 2H^+ \rightleftharpoons \equiv FeSiO_4H_3 + H_2O$	25.1

sal^{2-} salicylate

$phth^{2-}$ phthalate

(1) K is the intrinsic constant at 25°C in 0.1 M $NaClO_4$

Table 5.2 Adsorption of anions, Ca^{2+}, and Mg^{2+} on the lepidocrocite surface.

Ionic Medium	pH	% X_{ads}
10^{-3}M $Ca(ClO_4)_2$ in 0.1 M $NaClO_4$	8.30	11.3
10^{-3} M $Mg(ClO_4)_2$ in 0.1 M $NaClO_4$	8.30	39.5
10^{-3} M salicylate in 0.1 M $NaClO_4$	8.29	15.2
" " " " "	7.02	7.0
10^{-3} M phthalate in 0.1 M $NaClO_4$	8.30	<2
" " " " "	7.00	75
10^{-3} M Na_2SO_4 in 0.1 M $NaClO_4$	8.31	5
10^{-3} M Na_2HPO_4 in 0.1 M $NaClO_4$	8.32	80.1
10^{-3} M silicate in 0.1 M $NaClO_4$	8.3	35
" " " " "	7.0	57

All experiments in 10 mM FeOOH at 25°C.

% X_{ads} is the percentage of X adsorbed, where
X = Ca^{2+}, Mg^{2+}, sal^{2-}, $phth^{2-}$, SO_4^{2-}, phosphate or silicate.

the conditions chosen for these experiments sometimes differ from those used in the oxidation experiments.

The constants obtained from these studies are given in Table 5.1. The surface equilibrium constant for the binding of the species $\equiv Fephth^-$ could not be determined, since the only successful fit to the adsorption data presumed that the concentration of this species is small (< 2% of the total phthlate) at both pH 7.0 and pH 8.3.

5.2.2 Oxidation studies

The results and experimental conditions used in the oxidation experiments are shown in Tables 5.3 and 5.4.

To determine if any of the ligands used in these experiments form complexes which are oxidizable at pH 8.3, the oxidation of Mn(II) in the absence of lepidocrocite was studied. As shown in Table 5.3, the rate of Mn(II) oxidation in these systems was very slow, showing that at pH 8.3, none of the solution complexes formed are readily oxidizable.

As shown in Table 5.4, in the system where lepidocrocite is present, all the ions studied, except phthlate, inhibit the rate of Mn(II) oxidation to some degree. The relative extent to which the ions affect the rate of Mn(II) oxidation is as follows

10^{-2}M Mg^{2+} > 10^{-3}M silicate ~ $5x10^{-3}$M salicylate > 10^{-3}M phosphate ~ 10^{-3}M salicylate ~ 0.7 M NaCl ~ 10^{-2}M Ca^{2+} > 0.0333M Na_2SO_4 >10^{-4}M phosphate > 10^{-3} M phthlate

Table 5.3 Oxidation of Mn(II) in the presence of other ions.

Expt. No.	Ionic Medium	k_1 (min^{-1})	pH
B1	10^{-2}M $Ca(ClO_4)_2$ in 0.1 M $NaClO_4$	$<7\times10^{-6}$	8.28
B2	10^{-2}M $Mg(ClO_4)$ in 0.1 M $NaClO_4$	$<1\times10^{-5}$	8.28
B3	10^{-3}M salicylate in 0.1 M $NaClO_4$	$<9\times10^{-6}$	8.35
B4	10^{-3}M phthalate in 0.1 M $NaClO_4$	$<2\times10^{-5}$	8.29
B5	0.0333 M Na_2SO_4	$<1\times10^{-5}$	8.25
B23	1.0×10^{-3}M silicate in 0.1 M $NaClO_4$	$<4\times10^{-5}$	8.32
B6	2.5×10^{-3}M Na_2HPO_4 in 0.1 M $NaClO_4$	$<2\times10^{-5}$	9.29
B7	0.7 M $NaClO_4$	$<2\times10^{-5}$	8.30
B8	0.7 M NaCl	$<3\times10^{-5}$	8.31

All experiments at 25°C.

Table 5.4 Oxidation of Mn(II) in the presence of lepidocrocite and other ions.

Expt. No.	Ionic Medium	pH	[γ-FeOOH] 10^{-3} M	k_1 (min^{-1})
B9	0.1 M $NaClO_4$	8.30	1.00	.0094
B10	" " "	8.31	1.00	.0104
B11	10^{-2}M $Ca(ClO_4)_2$ in 0.1 M $NaClO_4$	8.30	1.00	.0035
B12	10^{-2}M $Mg(ClO_4)_2$ in 0.1 M $NaClO_4$	8.29	1.00	.0007
B13	10^{-3}sal in 0.1 M $NaClO_4$	8.32	1.00	.0036
B14	$5x10^{-3}$sal in 0.1 M $NaClO_4$	8.30	1.00	.0013
B16	10^{-3}M phth in 0.1 M $NaClO_4$	8.33	1.00	.0110
B25	0.1 M $NaClO_4$	8.30	0.98	.0107
B24	10^{-4} M Na_2HPO_4 in 0.1 M $NaClO_4$	8.33	0.98	.0082
B17	10^{-3}M Na_2HPO_4 in 0.1 M $NaClO_4$	8.32	0.98	.0034
B18	10^{-3}M silicate in 0.1 M $NaClO_4$	8.33	0.98	.0012
B19	0.1 M $NaClO_4$	8.29	2.50	.0278
B20	0.0333 M Na_2SO_4	8.28	2.50	.0190
B21	0.7 M $NaClO_4$	8.30	10.0	.0098
B22	0.7 M NaCl	8.30	10.0	.0035

All experiments at 25°C.

In the previous chapter it was shown that the rate of oxidation could be described by the equation

$$\frac{-d[Mn(II)]}{dt} = k'' \cdot \langle(\equiv SO)_2Mn\rangle \cdot a \cdot pO_2 \qquad (5.6)$$

The rate of oxidation is also described by the equation

$$\frac{-d[Mn(II)]}{dt} = k_1 [Mn(II)] \qquad (5.7)$$

Equating 5.6 and 5.7 and rearranging, one obtains

$$k_1 = \frac{k'' \cdot \langle(\equiv SO)_2Mn\rangle \cdot a \cdot pO_2}{[Mn(II)]} \qquad (5.8)$$

If one assumes that the effects of changing the ionic composition of the support electrolyte are relatively minor, then for the systems where the ionic strength is ~0.1 M, the concentration of the $(\equiv SO)_2Mn$ in the system can be calculated using the surface equilibrium model and the constants given in Appendix A and Tables 3.1, 3.12 and Table 5.1. Using equation 5.8, the predicted pseudo-first order rate constant can be calculated. It was shown in the previous chapter that increasing the ionic strength of medium shifts the surface equilibria significantly, so no attempt has been made to model the speciation in 0.7 M NaCl or 0.7 M $NaClO_4$.

In Table 5.5 the ratio $k_1/k_{1,control}$ for the experimental results and those calculated from the model are compared. The control is the experiment in 0.1 M $NaClO_4$ at the same lepidocrocite concentration. The control

experiments were conducted during the course of these experiments. By comparing the ratio $k_1/k_{1,control}$ rather than the absolute values of k_1, one hopes to minimize the influence of any changes in the properties of the suspension during the course of time. The suspension used in these experiments was over 10 months old. The rate of oxidation of Mn(II) in the controls was about 20% slower than in corresponding experiments described in the previous chapter.

As shown in Table 5.5, the ratio $k_1/k_{1,control}$ calculated using the model and this ratio found in the experiments where Ca^{2+}, Mg^{2+}, salicylate, phosphate or silicate are present are not equal. In the experiments where sulfate and phthlate are present, these ratios are not significantly different. Realizing that the model has limitations (Stumm et al., 1980; Benjamin and Leckie, 1981), namely that (i) the equilibrium constants cannot be determined accurately, (ii) the constants vary with changes in surface coverage, concentration of adsorbate and adsorbent, (iii) surface equilibrium is attained very sluggishly, and at best, a meta-stable equilibrium is attained, (iv) the elucidation of effect of the electrical properties of the solid-water on the surface equilibria is difficult, particularly in electrolytes of different ionic composition, and (v) the model (as used in this work) does not consider the possibility that ternary complexes may exist on the surface, the predictions of the model should be

Table 5.5 Comparison of experimental and calculated values for the ratio $k_1/k_{1,control}$.

Expt. No.	Ionic Medium[1]	$\frac{k_1}{k_{1,control}}$ Experimental	Calculated
B11	10^{-2} M Ca^{2+}	0.35	0.73
B12	10^{-2} M Mg^{2+}	0.07	0.28
B13	10^{-3} M sal	0.36	0.80
B14	$5x10^{-3}$ M sal	0.13	0.64
B15	10^{-3} M phth	1.11	1.00
B24	10^{-4} M phosphate	0.77	0.60
B17	10^{-3} M phosphate	0.32	0.17
B18	10^{-3} M silicate	0.12	0.56
B20	0.0333 M sulfate	0.68	0.73

(1) See Table 5.4 for details of composition of ionic medium.

B9 and B10 are controls for B11-B15.

B25 is control for B17, B18, and B24.

B19 is control for B20.

regarded as semi-quantitative, so it is not surprising that the predicted and observed behaviour are not in quantitative agreement.

It should also be pointed out that the ratios $k_1/k_{1,control}$ obtained from the experimental data are based on very limited data, so they are subject to considerable uncertainty. Based on the results presented in section 4.4.3.1, the expected relative standard deviation for these measurements would be about ±7%. At the 95% confidence level the relative confidence interval would be about ±20%.

Despite the limitations of the model, it generally does predict qualitatively the order of reactivity expected in the systems studied. The model predicts that the effect of the added ions on the rate of Mn(II) oxidation should be

$$10^{-3}M \text{ phosphate} > 10^{-2}M\ Mg^{2+} >$$
$$5\times10^{-3}M \text{ salicylate} \sim 10^{-4}M \text{ phosphate} \sim 10^{-3}M \text{ silicate} >$$
$$10^{-2}M\ Ca^{2+} \sim 0.0333M\ SO_4^{2-} >$$
$$10^{-3}M \text{ salicylate} > 10^{-3}M \text{ phthlate},$$

which, except for the results obtained in phosphate solutions, is virtually the same order as found by experiment. This suggests that generally speaking the conceptual basis of the model is realistic and that the effect these ions have on the rate of oxidation of Mn(II) can be explained, qualitatively, in terms of the effects they have on the binding of Mn(II) to the surface.

The model predicts the effect of phosphate on the rate of Mn(II) oxidation is more significant than that found by experiment. A possible explanation for this discrepancy is that the phosphate adsorption is not described by the model used in this work. Using a similar model, Gupta (1976) found that at pH 9 the model did not describe the adsorption of phosphate on lepidocrocite. As the apparent binding constant for phosphate decreased as the adsorption density increased, the breakdown of the model was believed to be a consequence of lateral interactions between adsorbed phosphate groups. Another possible explanation for the breakdown of the surface complexation model is that phosphate may form a precipitate on the surface. Ligands such as phosphate which interact strongly with surfaces may form precipitates on the surface (Corey, 1981).

Whatever the explanation for the discrepancy between the predicted and actual rate of oxidation of Mn(II) in systems where phosphate is present, the effect of phosphate on the rate of oxidation of Mn(II) is, at concentrations less than 10^{-4}M, rather small. In 10^{-4}M phosphate the rate of oxidation of Mn(II) at pH 8.3 is only 20% slower than when no phosphate is present. As shown in Chapter 6, at the concentrations of phosphate found in natural waters the predicted effect of phosphate on the rate of Mn(II) oxidation is minimal.

Based on the model calculations, one can say that the

inhibition of Mn(II) oxidation in the system where sulphate is present is due largely to the formation of $MnSO_4$ complexes. The extent of binding of sulfate to the surface is too small to have any significant effect on the rate of Mn(II) oxidation. The model predicts that Mg^{2+}, Ca^{2+} and saliyclate inhibit the oxidation of Mn(II) largely because the adsorption of these ions displaces Mn(II) from the surface. Salicylate does complex Mn(II) to some extent, but the extent of complexation (<15%) is too small to have any great effect on the rate of Mn(II) oxidation. It is not surprising that phthlate has no effect on the rate of oxidation, for at pH 8.3, it neither binds strongly to the surface, nor forms any Mn(II) complexes.

The results obtained in 0.7 M NaCl and 0.7 M $NaClO_4$ are difficult to interprete with the available information. The amount of adsorbed Mn is about one third less in the chloride solution than in the perchlorate solution. However, the rate of oxidation of Mn(II) is about 3 times slower in 0.7 M NaCl than in 0.7 M $NaClO_4$, so the simple-minded idea that rate of the reaction should be roughly proportional to the amount of adsorbed Mn is not valid in this case. The experimental results can be reconciled with the predictions of the model if one presumes that the speciation on the surface is different in chloride and perchlorate media. Whilst this presumption is not unreasonable, it cannot be justified, because the speciation on the surface is unknown.

The oxidation of Mn(II) in 0.7M NaCl in the presence of lepidocrocite has been studied by Sung and Morgan (1981). Sung and Morgan found that at p_cH 8.55 (p_aH ~8.68), in 10mM γ-FeOOH, under pure oxygen, the half-life for Mn(II) oxidation was 58 minutes. Assuming the rate of oxidation of Mn(II) is proportional to $[OH^-]^2$, then Sung and Morgan's results predict that in this system at p_aH 8.3, the half-life for Mn(II) oxidation is about 330 minutes. In this work the half-life for the oxidation of Mn(II) under these conditions is 200 minutes, which is in reasonable accord with Sung and Morgan's results.

CHAPTER 6

MN(II) OXIDATION IN NATURAL WATERS: IMPLICATIONS OF EXPERIMENTAL STUDIES

6.1 Introduction

In the experimental studies described previously the particular conditions chosen for the experiment were often motivated by considerations of experimental convenience, so the conditions used may differ considerably from those found in natural waters. For example, the solids concentrations used in these experiments were much higher than that found in most natural waters. The reasons for using such a high solids concentration were two-fold; firstly so that the reaction would proceed at an easily measurable rate and secondly, so that the surface was in excess ($S_T >> Mn_T$). In this chapter the implications of the experimental studies for Mn(II) oxidation in natural waters are considered. This discussion aims to indentify the important factors influencing the kinetics of Mn(II) oxidation on metal oxide surfaces and to estimate the time scales for Mn(II) oxidation on these solids in natural waters.

6.2 Comparison of the rate of Mn(II) oxidation on different metal oxides

To compare the rate of Mn(II) oxidation on the different solids studied, consider the example outlined in Table 6.1. In this example it is assumed that (i) the total suspended solids concentration is 10 mg/L, (ii) the

Table 6.1 Input data for surface equilibria calculations *1.A comparison of metal oxides.*

	A m^2/g	Γ moles/m^2	a g/L	S_T mole/L
Goethite	250	1.6×10^{-5}	3.8×10^{-4}	1.5×10^{-6}
Lepidocrocite	250	1.6×10^{-5}	3.8×10^{-4}	1.5×10^{-6}
Silica	50	8.0×10^{-6}	6.1×10^{-3}	2.4×10^{-6}
Alumina	50	8.0×10^{-6}	1.8×10^{-3}	7.2×10^{-7}

p_cH 8.0

A - specific surface area

Γ - site density (calculated using data given in Table 2.7)

a - solids concentration

The appropriate constants from Tables 3.1 and 3.12 and Appendix A are used in these calculations.

elemental composition of the solid is that estimated by Martin and Whitfield (1983) for riverine suspended solids. (iii) the initial Mn(II) concentration is 0.2 μM, which is approximately the dissolved manganese concentration estimated by Martin and Whitfield for river waters, and (iv) 50% of the particulate iron in natural waters is present as oxide surface coatings (this estimate is based on Gibbs (1977)). Assuming the thickness of the coating is 1 nm, then the specific surface area of the iron oxide is about 250 m^2/g. Using the conditions indicated in Table 6.1, the concentration of $(\equiv SO)_2Mn$ on the goethite, lepidocrocite, silica and alumina surface can be calculated. According to equation 4.28

$$-\frac{d[Mn(II)]}{dt} = k''<(\equiv SO)_2Mn>\cdot a\cdot pO_2 \qquad (6.1)$$

Under the conditions considered here the reaction should be approximately first order. Then

$$t_{\frac{1}{2}} = \frac{\ln 2}{k_1} \qquad (6.2)$$

where k_1 is the pseudo-first order rate constant for the reaction and $t_{\frac{1}{2}}$ is the reaction half-life. Therefore the half-life for the oxidation is given by

$$t_{\frac{1}{2}} = \frac{\ln 2\ [Mn(II)]_0}{k''<(\equiv SO)_2Mn>_0\cdot a\cdot pO_2} \qquad (6.3)$$

where $[Mn(II)]_0$ is the intial Mn(II) concentration and

$<(\equiv SO)_2Mn>_0$ is the intial $(\equiv SO)_2Mn$ concentration (in moles/g solid).

The calculated half-lives for the oxidation under the conditions stated in Table 6.1 are as follows:

	$t_{\frac{1}{2}}$
goethite	210 days
lepidocrocite	34 days
silica	2.1 years
alumina	>50 years

It is clear that under the conditions pertaining in natural waters the iron oxides enhance the rate of oxidation of Mn(II) much more effectively than do either silica or alumina. In subsequent calculations only the oxidation of Mn(II) in the presence of lepidocrocite is considered.

In nature, silicon and aluminium are not usually found as oxides (SiO_2 or Al_2O_3), but as silicates (e.g. feldspars) or aluminosilicates (e.g. clay minerals). Whilst these solids have structural similarities to the oxides studied, it is possible that they may differ in their ability to enhance the rate of Mn(II) oxidation. Wilson (1980) found that goethite enhanced the rate of Mn(II) oxidation more effectively than the clay minerals, montmorillonite and kaolinite, which seems to bear out the findings reported here for simple metal oxides.

6.3 Factors influencing Mn(II) oxidation kinetics in natural waters

Influence of solids concentration and pH

The influence of solids concentration and pH on Mn(II) oxidation kinetics is illustrated in Figure 6.1. Under conditions that differ greatly from those studied in the laboratory, the rate of Mn(II) oxidation can only be estimated. The lines for $t_{\frac{1}{2}} > 1$ year are dashed to indicate that under these conditions it is only possible to estimate the rate of Mn(II) oxidation. The range of iron concentrations indicated on the figure is approximately that found in natural waters. The pH found in surface waters ranges from about pH 4-10; in Figure 6.1 an intermediate range is considered. The influence of both pH and solids concentration on the kinetics of Mn(II) oxidation is profound. Over the pH range 6-9 the predicted rate of Mn(II) oxidation varies by more than 5 orders of magnitude. Over the range of iron oxide concentration considered the rate of Mn(II) oxidation varies by nearly three orders of magnitude. Below pH 7.5 the reaction is slow ($t_{\frac{1}{2}} > 100$ days), even at high iron oxide concentrations. At the iron oxide concentration used in the example discussed in the previous section, $t_{\frac{1}{2}}$ varies between 1 day at pH 9 and 100 years at pH 6.

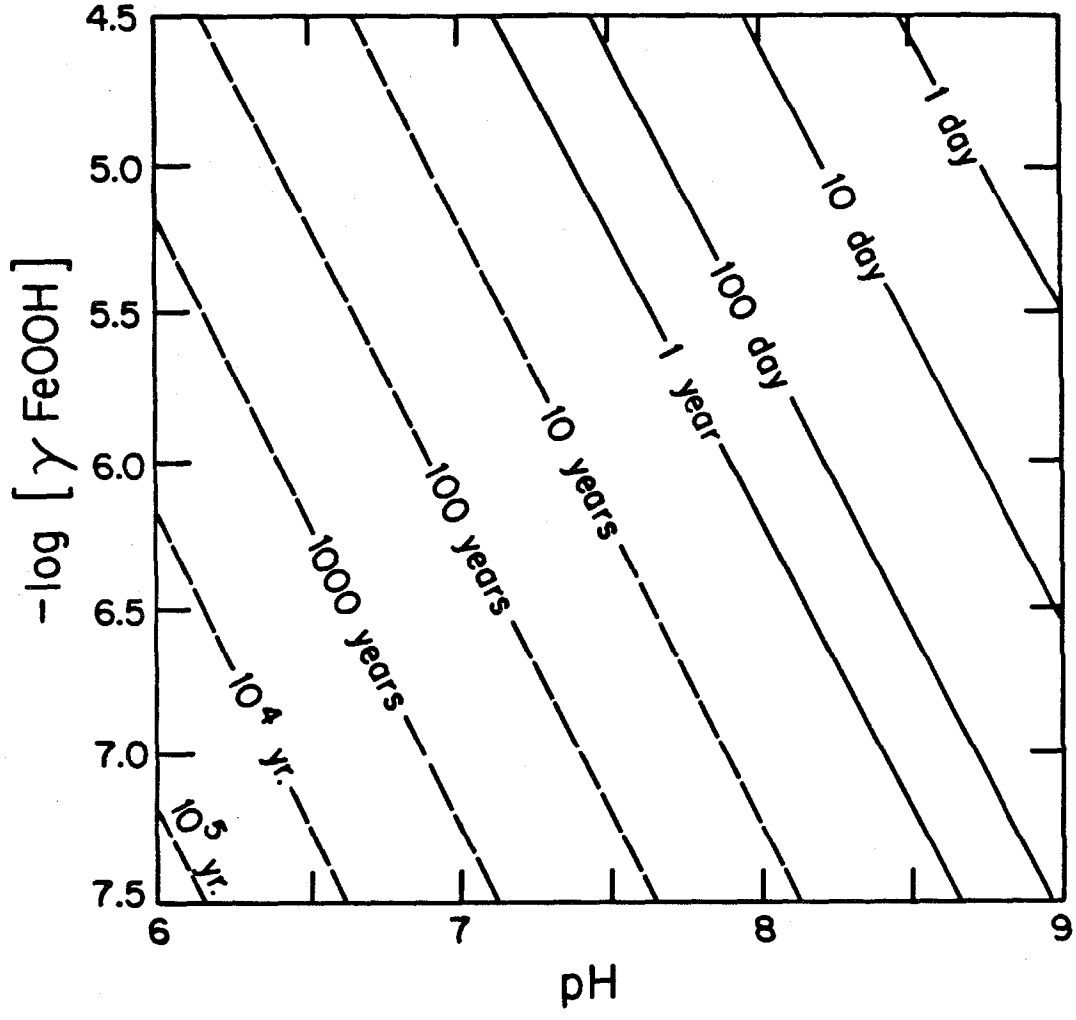

Figure 6.1 Half-life for Mn(II) oxidation on lepidocrocite. Mn_T = 0.2 μM, pO_2 = 0.21 atm., A = 250 m^2/g and $\Gamma = 1.6 \times 10^{-5}$ mole/m^2.

Influence of other ions

Three examples are considered to illustrate the importance of other ions on the kinetics of Mn(II) oxidation. In the first example the ionic composition of the solution is typical of that which might be found in a fresh-water environment. In the second example the ionic composition of the solution is typical of that found in the low salinity region of an estuary (the ionic strength of this solution is approximately 0.1 M). The composition of these solutions is shown in Table 6.2. In the third example the oxidation of Mn(II) in 0.1 M $NaClO_4$ is considered. In these calculations the surface equilibrium constants are considered to be independent of ionic strength or the ionic composition of the solution. Using equation 6.3, the predicted half-life for Mn(II) oxidation in these systems is as shown in Table 6.3. Since the rate of the reaction is proportional to $[\equiv FeOH][Mn^{2+}]$, the factors influencing the rate of Mn(II) oxidation can be identified by looking at the speciation of Mn(II) in solution and the species present on the surface.

As shown in Table 6.3, in fresh-water the presence of other ions has relatively little effect on the rate of Mn(II) oxidation. The effect of other ions on the rate of Mn(II) oxidation increases with increasing pH. But, even at pH 8.5 the presence of other ions does not decrease the rate of oxidation of Mn(II) by more than a factor of 2. It can be

Table 6.2 Input data for surface equilibrium calculations 2. *Influence of other ions.*

Component	X_T, moles/L	
	'Fresh water'	'Estuarine water'
Na^+	4.0×10^{-3}	7.0×10^{-2}
Ca^{2+}	1.0×10^{-3}	1.5×10^{-3}
Mg^{2+}	2.0×10^{-4}	8.3×10^{-3}
Cl^-	5.0×10^{-3}	8.5×10^{-2}
SO_4^{2-}	1.0×10^{-4}	4.3×10^{-3}
PO_4^{3-}	1.0×10^{-6}	1.0×10^{-6}
$H_2SiO_4^{2-}$	5.0×10^{-5}	5.0×10^{-5}
CO_3^{2-}	1.0×10^{-3}	1.0×10^{-3}
sal^{2-}	5.0×10^{-5}	5.0×10^{-5}
Mn^{2+}	2.0×10^{-7}	2.0×10^{-7}
$\equiv SOH$	2.0×10^{-6}	2.0×10^{-6}

The appropriate constants from Tables 3.1 and 3.12 and Appendix A are used in these calculations.

X_T - total concentration of the component

Table 6.3 Predicted half-lives for Mn(II) oxidation at 25°C in fresh-water, estuarine-water, and 0.1 M $NaClO_4$.

	$t_{1/2}$, days		
p_cH	Freshwater	Estuarine-water	0.1 M $NaClO_4$
7.5	290	470	240
8.0	31	94	25
8.5	4.6	57	2.7

seen from Table 6.4 that inhibition of Mn(II) oxidation at higher pH is due largely to the displacement of Mn(II) from the surface by Mg^{2+} (and to a lesser extent, Ca^{2+}). At lower pH some phosphate is adsorbed, but this has little effect on the extent of Mn(II) adsorption.

In the estuarine-water the effect of other ions is more significant. At pH 8.5 the predicted rate of Mn(II) oxidation is 20 times slower in the estuarine-water than in 0.1 M $NaClO_4$. Again, the inhibition of Mn(II) oxidation is largely due to Mg^{2+} adsorption. Complexation of Mn(II) by Cl^- also decreases the extent of Mn(II) adsorption. If the lower values for the stability constants for Mn(II)-chloro complexes found by Carpenter (1983) are used in these calculations then the predicted effect of Cl^- on the rate of Mn(II) oxidation is small.

Presumably in sea-water the effect of other ions on the kinetics of Mn(II) oxidation is significant, but it is difficult to quantify this effect. A rough calculation (neglecting any effects that ionic strength may have on surface equilibria) indicates that (under otherwise identical conditions) in sea-water the rate of oxidation of Mn(II) is of the order of 100 times slower than in a fresh-water environment.

As indicated in the previous chapter, both temperature and ionic strength have a significant influence on the rate of Mn(II) oxidation. At the ionic strength of seawater

Table 6.4 Calculated speciation in fresh-water, estuarine-water and 0.1 M $NaClO_4$.

p_cH 7.5

	% S_T		
	Fresh-water	Estuarine-water	0.1 M $NaClO_4$.
Surface species			
$\equiv FeOH$	83	69	92
$\equiv FeOH_2^+$	3	3	2
$\equiv FeO^-$	3	2	7
$\equiv FeOMgOH$	-	10	-
$\equiv FeH_2PO_4^-$	9	12	-
Mn species			
Mn^{2+}	90	66	100
$MnHCO_3^+$	5	2	-
$MnSO_4$	-	6	-
$MnCl^+$	4	25	-
$MnCl_2$	-	1	-

(Table 6.4 continued)

p_cH 8.0

	% S_T		
	Fresh-water	Estuarine-water	0.1 M $NaClO_4$.
Surface species			
$\equiv FeOH$	80	36	89
$\equiv FeOH_2^+$	1	-	1
$\equiv FeO^-$	7	4	10
$\equiv FeOMgOH$	3	53	-
$\equiv FeOCaOH$	3	1	-
$\equiv FeH_2PO_4^-$	3	4	-
$\equiv FeH_3SiO_4^-$	2	3	-
Mn species			
Mn^{2+}	90	66	99
$MnHCO_3^+$	5	2	-
$MnSO_4$	-	6	-
$MnCl^+$	4	25	-
$MnCl_2$	-	1	-

(Table 6.4 continued)

p_cH 8.5

	% S_T		
	Fresh-water	Estuarine-water	0.1 M $NaClO_4$.
Surface species			
$\equiv FeOH$	54	6	85
$\equiv FeO^-$	10	4	15
$\equiv FeOMgOH$	21	86	-
$\equiv FeOCaOH$	10	3	-
$\equiv FeH_3SiO_4^-$	3	3	-
Major Mn species			
Mn^{2+}	89	66	97
$MnOH^+$	1	-	1
$MnHCO_3^+$	3	2	-
$MnSO_4$	-	6	-
$MnCl^+$	4	25	-
$MnCl_2$	-	1	-
$(\equiv FeO)_2Mn$	1	-	2

(I=0.7 M) the rate of oxidation of Mn(II) is about 4 times slower than at an ionic strength of 0.1 M. The rate of Mn(II) oxidation doubles if the temperature is raised 5°C.

6.4 Mn(II) oxidation in natural waters : A comparison with predictions based on laboratory data

The removal of filterable manganese from natural waters has been studied by a number of workers. The rates of manganese removal found or estimated in some natural waters are summarized in Table 6.5. The estimates for the removal times for manganese range from periods of a few days, to several decades in the open ocean.

It is difficult to compare the predicted rates of Mn(II) oxidation, on the basis of laboratory studies with the rates of manganese removal measured in natural waters. In natural waters the relative importance of oxidative removal of manganese from solution, non-oxidative removal of manganese (adsorption, biological uptake) and reductive dissolution of manganese oxides is generally unknown. Also, the estimates for the rate of Mn(II) oxidation rates in natural waters based on experimental studies are subject to considerable uncertainty. This uncertainity is not only because of the limitations of the model, as discussed in the previous chapter, but also because of lack of data, such as the composition and concentration of the solids found in particular natural waters.

Whilst it is not possible in the field studies to

Table 6.5 Removal times for manganese in natural waters

Source of water	Temperature °C	pH	Approximate* Half-life for Removal (days)	Reference
Groundwater	30	6.9-8.25	10-40	Handa (1969/1970)
Lake Mendota	22	8.5	12	Deltino and Lee (1971)
Lake Greifensee (filtered)	20	8.8	100	Stumm and Giovanoli (1976)
Black Sea	8.5	7.7	2000	Murray and Brewer (1977)
Open ocean	Ambient	8.1	10^4	Weiss (1977)
Scheldt estuary	20	~7.5	3-8	Wollast et al. (1979)
Tamar estuary	20	~7.5	5-30	Morris et al. (1982)
Onieda Lake	18	8.0-8.4	1-4	Chapnick et al. (1982)
Saanich Inlet	9	7.4	2	Emerson et al. (1982)
MERL microcosm	Ambient	~8	4	Hunt (1983)
Esthwaite Water	10	6.5-7.5	1-2	Tipping et al.(1984)

* These estimates are obtained by various means and are not necessarily directly comparable. The half-lives given serve as an indication of the rate of manganese removal.

clearly distinguish manganese removal due to oxidation from removal due to sorptive processes or to assess the importance of reductive dissolution of manganese oxides, if the net removal of manganese in a particular environment and the predicted rate of Mn(II) oxidation are comparable, then this suggests that removal of Mn(II) by oxidation on iron oxides is an important process in this environment. It is necessary to exercise some caution in this regard and to consider not only the removal times, but any other available information. For example, in some studies (e.g. Emerson et al., 1982) it has been shown that bacterial poisons inhibit the rate of Mn(II) oxidation, which suggests the reaction is bacterially mediated.

The observed rates of manganese removal found in some systems (e.g. Lake Mendota) compare favourably with the rates of oxidative manganese removal predicted by equation 6.3. But in other cases the predictions of the model are difficult to reconcile with the behaviour of manganese observed in the field. For example, Tipping et al. (1984) found in a sample taken from Esthwaite Water that at pH 6.5 and 10^{o}C virtually all the manganese in solution was removed within 2 days. This is several orders of magnitude faster than would be expected on the basis of the model presented in this work. As is suggested by Tipping et al.(1984), it would seem that in this environment bacterial oxidation plays an important role in manganese geochemistry in this

lake. Based on Chapnick et al.'s (1982) work, sorptive removal of manganese by bacteria could also be an important removal mechanism for manganese in this system.

A possible removal mechanism not considered in this work is the autocatalytic oxidation of Mn(II). The typical level for dissolved manganese in stream waters is about 0.15 μM (Martin and Whitfield, 1983). But in most of the studies of reported in Table 6.5, the levels of dissolved manganese present are in excess of 2 μM.. Under these conditions the autocatalytic oxidation of manganese could be an important process. A rough estimate of the importance of autocatalytic oxidation of manganese can be made using Brewer's (1975) data. Brewer found that the rate of oxidation of manganese on MnO_2 could be described by the equation

$$-\frac{d[Mn(II)]}{dt} = k_{Mn}[OH^-]^2[Mn(II)][MnO_2][O_2(aq)] \qquad (6.4)$$

where $k_{Mn} = 5x10^{18}\ M^{-4}day^{-1}$. At pH 8.3, pO_2 0.21 atm. and an intial Mn(II) and MnO_2 concentration of 1 μM, the half-life for the oxidation of Mn(II) is 140 days. Though under these conditions this reaction is slow compared to the oxidation of Mn(II) on the lepidocrocite surface, the manganese oxide could enhance the oxidation of Mn(II) more effectively if it was present as a coating on other particles rather than as discrete particles.

6.5 Summary

In natural waters the oxidation of Mn(II) on iron oxides is a more significant pathway for Mn(II) oxidation than is the oxidation of Mn(II) on silicon or aluminium oxides.

The laboratory studies suggest that the factors that significantly influence the rate of Mn(II) oxidation on lepidocrocite in freshwater and estuarine environments are pH, iron oxide concentration, temperature, ionic strength and Mg^{2+} concentration. The model also predicts that in the estuarine environment Cl^- does slightly inhibit the rate of Mn(II) oxidation. The extent to which the presence of other ions effects the rate of Mn(II) oxidation is a function of pH. The model used predicts that in a freshwater environment at p_cH 8.0 the rate of oxidation of Mn(II) is not significantly affected by the other ions present. At this pH the model predicts that in an estuarine environment the rate of oxidation of Mn(II) is about 3 times slower that in 0.1 M $NaClO_4$.

It is difficult to generalize about the predicted time scales for Mn(II) oxidation in natural waters, for depending on the conditions prevailing in the natural water these predictions may vary over several orders of magnitude. The example outlined in Table 6.1 is perhaps as reasonable as any for a "typical" river water. In this example the $t_{\frac{1}{2}}$ for Mn(II) oxidation is 34 days at p_cH 8.0.

In some natural waters the observed rates of manganese removal agree favourably with the predictions made for the oxidative removal of manganese on lepidocrocite. But, in other environments the predicted rates for Mn(II) oxidation do not agree with those found in these natural waters, which suggests that other processes are important in manganese removal in these environments. Manganese removal in these environments may be due to bacterially mediated oxidation, autocatalytic oxidation, adsorption or biological uptake.

CHAPTER 7

CONCLUSIONS AND RECOMMENDATIONS

7.1 Conclusions

7.1.1 Mn(II) adsorption

The kinetics of Mn(II) adsorption on goethite, lepidocrocite, silica and alumina are comparatively fast. The half-life for removal is less than 5 minutes.

The adsorption of Mn(II) on the four metal oxides studied can be described by a constant capacitance model. On the goethite, lepidocrocite, and silica surface the model predicts that the predominant manganese species on the surface is either the the bidentate surface complex ($(\equiv SO)_2Mn$) or the hydrolysed complex ($\equiv SOMnOH$) (or some combination of these species). Since the pH dependence for adsorption for these two species is identical, it is impossible with the available information to determine the relative proportions of the bidentate and hydrolysed species present on the surface. On the alumina surface the bidentate or hydrolysed species are the most important Mn species on the surface at pH > 8.25. Below this pH the monodentate complex ($\equiv SOMn^+$) is the predominant Mn species found on the surface.

7.1.2 Mn(II) oxidation on metal oxide surfaces

The rate of oxidation of Mn(II) in the presence of goethite or lepidocrocite can be described by a rate

expression of the form:

$$-\frac{d[Mn(II)]}{dt} = k^* \frac{\langle \equiv SOH \rangle [Mn^{2+}]}{[H^+]^2} \cdot a \cdot pO_2 \qquad (7.1)$$

where $\langle \equiv SOH \rangle$ - concentration of surface hydroxyl groups in mole/g of solid

$[i]$ - concentration of species i in mole/L

a - solids concentration in grams

pO_2 - partial pressure of oxygen in atm.

The influence of oxygen concentration on the rate of Mn(II) oxidation in the presence of silica was not studied, but otherwise the data for the oxidation of Mn(II) on silica are consistent with the above rate expression. The rate of oxidation of Mn(II) on the alumina surface is considerably slower than that found for the other metal oxides studied. The rate of oxidation of Mn(II) in the presence of alumina was not studied in any detail, since it is so slow that it is not of interest in natural waters.

The influence of ionic strength on the kinetics of Mn(II) oxidation is significant. In the presence of lepidocrocite the rate of Mn(II) oxidation is about 4 times slower in 0.7 M $NaClO_4$ than in 0.1 M $NaClO_4$.

Normal laboratory lighting (fluorescent lights) has no effect upon the rate of Mn(II) oxidation in the presence of goethite or lepidocrocite.

The rate of Mn(II) oxidation on goethite and lepidocrocite is strongly temperature dependent. The

apparent activation energy for both reactions is approximately 100 kJ/mole. The extent of Mn(II) adsorption is strongly temperature dependent. About half the apparent activation energy measured is attributable to the temperature dependence of the adsorption process.

The rate of Mn(II) oxidation on goethite, lepidocrocite and silica can be described by a rate expression of the form:

$$-\frac{d[Mn(II)]}{dt} = k''<(\equiv SO)_2Mn>\cdot a\cdot pO_2 \qquad (7.2)$$

If the hydrolysed complex is more important on the metal oxide surface, then the appropriate form of the above rate expression is

$$-\frac{d[Mn(II)]}{dt} = k''<\equiv SOMnOH>\cdot a\cdot pO_2 \qquad (7.3)$$

A possible mechanism for the oxidation of Mn(II) on a metal oxide surface is suggested in section 4.4 (see Figure 4.18). Some possible explanations for the enhanced oxidation of Mn(II) on the metal oxide surface are discussed in section 4.4.

7.1.3 The influence of other ions on the rate of Mn(II) oxidation on lepidocrocite

The influence of other ions on the oxidation of Mn(II) on metal oxide surfaces can be explained at least in qualitative terms by the effect that they have on the binding of Mn(II) to the surface. At pH 8.3 the extent to

which other ions have an effect on the rate of Mn(II) oxidation on lepidocrocite is as follows:

10^{-2}M Mg^{2+} > 10^{-3}M silicate ~ $5x10^{-3}$M salicylate > 10^{-3}M phosphate ~ 10^{-3}M salicylate ~ 0.7M NaCl ~ 10^{-2}M Ca^{2+} > .0333M Na_2SO_4 > 10^{-4}M phosphate > 10^{-3} M phthlate

7.1.4 Mn(II) oxidation in natural waters: implications of experimental studies

Extrapolation of the experimental results to the conditions prevailing in natural waters shows that in natural waters the oxidation of Mn(II) on iron oxides is probably a more significant pathway for Mn(II) oxidation than is the oxidation of Mn(II) on silicon or aluminium oxides.

The results of the laboratory studies indicate that the important factors which influence Mn(II) oxidation on lepidocrocite are pH, iron oxide concentration, temperature, Mg^{2+} concentration, and ionic strength. Except for Cl^-, the other ions studied have little effect on the rate of Mn(II) oxidation. The experimental studies show that Cl^- does influence the rate of Mn(II) oxidation. The extent of the influence of Cl^- in natural waters is difficult to predict because the stability constants for the Mn(II)-chloro complexes are poorly known. In any case, even in sea-water the presence of Cl^- probably decreases the rate of Mn(II) oxidation by a factor of no more than 3, which is a rather

small effect compared to the influence of other factors (e.g. pH, Mg^{2+}).

The predicted rates of removal of Mn(II) in natural waters vary from a few days to thousands of years. At pH < 7.5 the rate of oxidation of Mn(II) is slow ($t_{1/2}$ > 100 days) under the conditions normally found in natural waters. The rates of oxidation of Mn(II) predicted using the results of this work sometimes agree favourably with the rates of manganese removal (from solution) found in natural waters. In other cases the rates of removal of manganese are much faster in natural waters than is expected on the basis of this work, which suggests that in these waters other processes of manganese removal are important. Manganese removal in these waters may be due to bacterially mediated oxidation, autocatalytic oxidation, adsorption and biological uptake.

7.2 Recommendations for further study

Certain aspects of the oxidation of Mn(II) on metal oxides seem to warrant further study; these include (i) the oxidation of Mn(II) in the presence of manganese oxides, (ii) the influence of ionic strength on the kinetics of Mn(II) oxidation, (iii) the influence of temperature on the kinetics of Mn(II) oxidation and (iv) oxidation of Mn(II) under conditions where the system is not oversaturated with respect to any Mn(II) solid. As shown in Chapter 6, the rate of oxidation of Mn(II) on manganese

oxides is, at higher manganese concentrations, of the same order as the rate of Mn(II) oxidation on iron oxides. For this reason the oxidation of Mn(II) on manganese oxides seems to warrant further investigation. The effects of ionic strength and temperature on Mn(II) oxidation are significant. The direction of further work in this area would be to try to extend the equilibrium model discussed in this work to consider the oxidation of Mn(II) at different ionic strengths and temperatures. In the work discussed in this thesis Mn(II) oxidation has been, for the most part, studied under conditions where the system is oversaturated with respect to rhodocrocite, $MnCO_3(s)$. The presence of rhodocrocite may influence the kinetics of Mn(II) oxidation (Diem and Stumm, 1984). The evidence suggests that rhodocrocite is not precipitated in these systems, but given that there is a possibility that it is precipitated, some work in systems not saturated with respect to any Mn(II) solid is warranted. Oversaturation could be avoided by using lower manganese concentrations or by using another buffer system.

The mechanism of Mn(II) oxidation on metal oxides warrants further investigation. Presently the mechanism for this reaction is poorly understood. In this work a possible mechanism for this reaction is suggested, but it is difficult to assess the validity of the mechanism, because the chemistry of the system is still poorly understood.

Recent studies have demonstrated the importance of bacterially mediated oxidation in natural waters (e.g. Emerson et al.,1982). Further investigations of the role of bacteria in Mn(II) oxidation are certainly warranted. From a chemical viewpoint the mechanism whereby the bacteria oxidize Mn(II) needs to be understood. Possibly the reaction has an autocatytic character, for these bacteria are often coated with manganese deposits (Marshall, 1979).

REFERENCES

Atkinson, R.J., A.M. Posner, and J.P. Quirk (1967) J. Phys. Chem. 71, 550-558.

Balistrieri, L.S. and J.W. Murray (1979) The surface of goethite (α-FeOOH) in seawater, in E.A.Jenne, ed., 'Chemical Modeling in Aqueous Systems- Speciation, Sorption, Solubility, and Kinetics'. Amer. Chem. Soc. Symposium Series 93. Amer. Chem. Soc., Washington, D.C. pp 275-298.

Balistrieri, L.S. and J.W. Murray (1981) Am. J. Sci. 281, 788-806.

Balistrieri, L.S. and J.W. Murray (1982) Geochim. Cosmochim. Acta. 46, 1253-1265.

Benjamin, M.M. and J.O. Leckie (1981) Environ. Sci. Technol. 15, 1050-1057.

Bewers, J.M. and P.A. Yeats (1978) Estuar. Coastal Mar. Sci. 7, 147-162.

Bourg, A.C.M. and P.W. Schindler (1978) Chimia. 32, 166-168.

Bourg, A.C.M., S. Joss, and P.W. Schindler (1979) Chimia. 33, 19-21.

Bowden, J.W., A.M. Posner, and J.P. Quirk (1977) Aust. J. Soil Res. 15, 121-136.

Bowen, H.J.M. (1966) 'Trace Metals in Biochemistry'. Academic Press, New York.

Brewer, P.G., (1975) Minor elements in seawater, in J.P. Riley and G. Skirrow, eds., 'Chemical Oceanography', Volume 1. Academic Press, London. pp 445-496.

Bricker, O. (1965) Amer. Mineral. 50, 1296-1354.

Burns, R.G. and V.M. Burns (1979) Manganese Oxides, in R.G. Burns, ed.,'Marine Minerals', Reviews in Mineralogy, Volume 6. Mineralogical Soc. of Amer. pp 1-46.

Carpenter, R. (1983) Geochim. Cosmochim. Acta. 47, 875-885.

Chapnick, S.D., W.S. Moore, and K.H. Nealson (1982) Limnol. Oceanogr. 27, 1004-1014.

Corey, R.B. (1981) Adsorption vs precipitation in M.A. Anderson and A.J. Rubin, ed., 'Adsorption of Inorganics at Solid-Liquid Interfaces. Ann Arbor Science Publ., Ann Arbor, Michigan.

Cornell, R.M., A.M. Posner, and J.P. Quirk (1974) J. Inorg. Nucl. Chem. 36, 1937-1946.

Cotton, F.A. and G. Wilkinson (1980) 'Advanced Inorganic Chemistry' 4th. Edition. John Wiley and Sons, New York.

Coughlin, R.W. and I. Matsui (1976) J. Catalysis. 41, 108-123.

Davis J.A. (1980) Adsorption of natural organic matter from freshwater environments by aluminum oxide, in R.A. Baker, ed., 'Contaminants and Sediments', Volume 2. Ann Arbor Science Publishers, Inc., Ann Arbor, Michigan. pp 279-304.

Davis, J.A. and R. Gloor (1981) Environ. Sci. Technol. 15, 1223-1229.

Davis, J.A. and J.O. Leckie (1978) Environ. Sci. Technol. 12, 1309-1315.

Davis J.A. and J.O. Leckie (1979) Speciation of adsorbed ions at the oxide/water interface, in E.A.Jenne, ed., 'Chemical Modeling in Aqueous Systems- Speciation, Sorption, Solubility, and Kinetics: Amer. Chem. Soc. Symposium Series 93. Amer. Chem. Soc., Washington, D.C. pp 299-317.

Davison, W. (1982) Hydrobiologia. 92, 463-471.

Delfino, J.J. and G.F. Lee (1971) Water Res. 5, 1207-1217.

Diem, D. and W. Stumm (1984) Geochim. Cosmochim. Acta. 48, 1571-1573.

Duinker, J.C., R. Wollast, and G. Billen, and J.C. Duinker (1979) Estuar. Coastal Mar. Sci. 9, 727-738.

Eaton, A. (1979) Geochim. Cosmochim. Acta. 43, 429-432.

Emerson, S., R.E. Cranston, and P.S. Liss (1979) Deep-sea Res. 26A, 859-878.

Emerson, S., S. Kalhorn, S. Jacobs, B.M. Tebo, K.H. Nealson, and R.A. Rosson (1982) Geochim. Cosmochim. Acta. 46, 1073-1079.

Fallab, S. (1967) Agnew. Chem. internat. Edit. 6, 496-507.

Faughnan, J. (1981) 'The SURFEQL/MINEQL Manual'. Environmental Engineering Science, California Institute of Technology, Pasadena, California.

Gibbs, R.J. (1977) Geol. Soc. Am. Bull. 88, 829-943.

Giovanoli, R. (1980), On natural and synthetic manganese nodules, in Varentsov, I.M. and Gy. Grasselly, ed., 'Geology and Geochemistry of Manganese', Volume 1 Mineralogy, Geochemistry, Methods'. Schweizerbart'sche Verlagbuchhandlung, Stuttgart.

Glasby, G.P. (1977) Editor, 'Marine Manganese Deposits'. Elsevier, Amsterdam.

Goulden, G.H. (1939) 'Methods of Statistical Analysis'. John Wiley and Son, New York.

Graham, W.F., and M. Bender, and G.P. Klinkhammer (1976) Limnol. Oceanogr. 21, 665-673.

Grimme, H. (1968) Z. Pflanzern Durg. Bodenk. 121 58-65.

Gupta, S.K. (1976) Ph.D. Thesis, University of Bern (cited in Schindler, 1981).

Handa, B.K. (1969/1970) Chem. Geol. 5, 161-165.

Hem, J.D. (1963) 'Chemical equilibria and the rates of manganese oxidation'. U.S. Geological Survey- Water Supply Paper 1667A. 64p.

Hem, J.D. (1981) Geochim. Cosmochim. Acta. 45, 1369-1374.

Hingston, F.J., A.M. Posner, and J.P. Quirk (1968) Adsorption of selenite by goethite, in R.F. Gould, ed., 'Adsorption from Aqueous Solution': Amer. Chem. Soc. Symposium Series 79. Amer. Chem. Soc., Washington, D.C. pp 82-90.

Hohl, H. and W. Stumm (1976) J. Colloid Interface Sci., 281-288.

Holdren, G.R., O.P. Bricker, and G. Matisoff (1975) A model for the control of dissolved manganese in the interstitial waters of Chesapeake Bay, in T.M. Church,ed., 'Marine Chemistry in the Coastal Environment'. Amer. Chem. Soc. Symposium Series 18. Amer. Chem. Soc., Washington, D.C. pp364-381.

Hunt, C.D. (1983) Limnol. Oceanogr. 28, 913-923.

Iler, R.K. (1979) 'The Chemistry of Silica'. John Wiley and Sons, New York.

Jenne, E.A. (1968) Controls on Mn, Fe, Co, Ni, Cu and Zn concentrations in soils and waters: the significant role of hydrous Mn and Fe oxides. R.F. Gould, ed.: Amer. Chem. Soc. Symposium Series 73. Amer. Chem. Soc. pp 337-387.

Kent, D.K. (1983) Ph.D. Thesis, University of California-San Diego, San Diego, California.

Kessick, M.A., J. Vuceta, and J.J. Morgan (1972) Environ. Sci. Technol. 6, 642-644.

Klinkhammer, G.P. (1980) Earth Planet. Sci. Lett. 49, 81-101.

Klinkhammer, G.P. and M.L. Bender (1980) Earth Planet Sci. Lett. 46, 361-384.

Kummert, R. and W. Stumm (1980) J. Colloid Interface Sci. 75, 373-385.

Landing, W.M. and K.W. Bruland (1980) Earth Planet Sci. Lett. 49, 45-56.

Marshall, K.C. (1979) Biogeochemistry of manganese minerals, in P.A. Trudinger and D.J. Swaine, ed., 'Biogeochemical Cycling of Mineral Forming Elements'. Elsevier, Amsterdam. pp 253-292.

Martin, J.H. and G.A. Knauer (1980) Earth Planet Sci. Lett. 51, 266-274.

Martin, J.H. and G.A. Knauer (1982) Deep-sea Res. 4A, 411-425.

Martin, J-M, and M. Whitfield (1983) The significance of the river input of chemical elements to the ocean, in C.S. Wong, E. Boyle, K.W. Bruland, J.D. Burton, and E.D. Goldberg, eds., 'Trace Metals in Sea Water', NATO Conference Series Volume 9. Plenum Press, New York.

Metcalf and Eddy, Inc., (1979) 'Wastewater Engineering: Treatment, Disposal and Reuse'. McGraw-Hill, New York.

Michard, G. (1969) Trans. Am. Geophys. Union. 50, 349.

Moore, R.M., J.D. Burton, P.J. leB. Williams, and M.L. Young (1979) Geochim. Cosmochim. Acta. 43, 919-926.

Morgan, J.J. (1964) Ph.D. Thesis, Harvard University, Cambridge, Massachusetts.

Morgan, J.J. (1967) Chemical equilibria and kinetic properties of manganese in natural waters, in S.D. Faust and J.V. Hunter, eds.,'Principles and applications of water chemistry'. Wiley and Sons, Inc., New York. pp 561-624.

Morgan, J.J. and W. Stumm (1965) J. Amer. Water Works Assoc. 57, 107-119.

Morris, A.W. and A.J. Bale (1979) Nature (London). 279, 318-319.

Morris, A.W., A.J. Bale, and R.J.M. Howland (1982) Estuar. Coastal Shelf Sci. 14, 175-192.

Murray, J.W. and P.G. Brewer (1977) Mechanisms of removal of manganese, iron and other trace metals from seawater, in G.P. Glasby, ed., 'Marine Manganese Deposits'. Elsevier, Amsterdam.

Nichols, A.R. and J.H. Walton (1942) J. Amer. Chem. Soc. 64, 1866-1870.

Parfitt, R.L., V.C. Farmer and J.D. Russell (1977b) J. Soil Sci. 28, 29-39.

Parfitt, R.L., A.R. Fraser, and V.C. Farmer (1977a) J. Soil Sci. 28, 289-296.

Parfitt, R.L., J.D. Russell, and V.C. Farmer (1976) J.C.S. Faraday I72, 1082-1087.

Pedersen, T.F. and N. B. Price (1982) Geochim. Cosmochim. Acta. 46, 59-68.

Robertson, D.E. (1968) Anal. Chem. 40, 1067-1072.

Roy, S. (1981) 'Manganese Deposits'. Academic Press, London.

Santschi, P. and P.W. Schindler (1976) J. Chem. Soc. Dalton. 2, 181-184.

Schindler, P.W. (1981) Surface complexes at oxide-water interfaces, in M.A. Anderson and A.J. Rubin, ed., 'Adsorption of Inorganics at Solid-Liquid Interfaces. Ann Arbor Science Publ., Ann Arbor, Michigan.

Schwertmann, U. and R.M. Taylor (1977) Iron Oxides, in J.B. Dixon, ed., 'Minerals in soil environments'. Amer. Soc. Agron. Publ., Madison, Wisconsin.

Schwertmann, U. and R.M. Taylor (1979) Clay Miner. 14, 285-293.

Sholkovitz, E.R. (1976) Geochim. Cosmochim. Acta. 40, 831-845.

Sigg, L. and W. Stumm (1981) Colloids and Surfaces. 2, 101-117.

Sillen, L.G. and A.E. Martell (1971) 'Stability Constants of Metal Ion Complexes', Supplement No. 1, Chemical Society Special Publication No. 25. The Chemical Society, London.

Singh, S.K. and V. Subramanian (1984) Crit. Rev. in Environ. Control. 14, 33-90.

Spencer, D.W. and P.G. Brewer (1971) J. Geophys. Res. 76, 5877-5892.

Standard Methods for the Examination of Water and Wastewater (1980) 15th edition. APHA, AWWA and WPCF, New York.

Stone, A.T. and J.J. Morgan (1984) Environ. Sci. Technol. 18, 617-624.

Stumm, W. and R. Giovanoli (1976) Chimia. 30, 423-425.

Stumm, W. and J.J. Morgan (1981) 'Aquatic Chemistry', 2nd ed.. Wiley-Interscience, New York.

Stumm, W., R. Kummert, and L. Sigg (1980) Croat. Chem. Acta. 53, 291-312.

Suess, E. (1979) Geochim. Cosmochim. Acta. 43, 339-352.

Sunda, W.G., S.A Huntsman, and G.R. Harvey (1983) Nature (London). 301, 234-236.

Sung, W. (1981) Ph.D. Thesis, California Institute of Technology, Pasadena, California.

Sung, W. and J.J. Morgan (1980) Environ. Sci. Technol. 14, 561-568.

Sung, W. and J.J. Morgan (1981) Geochim. Cosmochim. Acta. 45, 2377-2383.

Tipping, E. (1981a) Geochim. Cosmochim. Acta. 45, 191-199.

Tipping, E. (1981b) Chem. Geol. 33, 81-89.

Tipping, E., D.W. Thompson, and W. Davison (1984) Chem. Geol. 44, 359-383.

Trefry, J.H. and B.J. Presley (1982) Geochim. Cosmochim. Acta. 46, 1715-1726.

Varentsov, I.M. and Gy. Grasselly (1980) Editors 'Geology and Geochemistry of Manganese', Volume 1 Mineralogy, Geochemistry, Methods. Schweizerbart'sche Verlagbuchhandlung, Stuttgart.

Vuceta, J. and J.J. Morgan (1978) Environ. Sci. Technol. 12, 1302-1309.

Vydra, F. and J. Galba (1969) Coll. Czech. Chem. Comm. 34, 3471-3478.

Waite, T.D. (1983), Ph.D. Thesis, Massachusetts Institute of Technology, Cambridge, Massachusetts.

Warner, T.B. (1975) Ion selective electrodes in thermodynamic studies, in E.D. Goldberg, ed. 'The Nature of Seawater'. Dahlem Konferenzen, Berlin.

Weiss, R.F. (1977) Earth Planet Sci. Lett. 37, 257-262.

Westall, J. and Hohl, H. (1980) Adv. Colloid Interfac. Sci. 12, 265-294.

Westall, J., J.L. Zachary, and F.M.M. Morel (1976) 'MINEQL: A Computer Program for the Calculation of Chemical Equilibrium Composition of Aqueous Systems'. Technical Note No. 18, Department of Civil Engineering, Massachusetts Institute of Technology, Cambridge, Massachusetts.

Wetzel, R.G. (1975) 'Limnology'. W.B. Saunders Co., Philadelphia, Pennsylvania.

Wilson, D.E. (1978) Limnol. Oceanogr. 23, 499-507.

Wilson, D.E. (1980) Geochim. Cosmochim. Acta. 44, 1311-1317

Wollast, R., G. Billen, and J.C. Duinker (1979) Estuar. Coastal Mar. Sci. 9, 161-169.

Yates, D.E. and T.W. Healy (1975) J. Colloid Interface Sci. 52, 222-228.

Yeats, P.A., B. Sundby, and J.M. Bewers (1979) Mar. Chem. 8, 43-55.

Young, J.R. (1981) Ph.D. Thesis, California Institute of Technology, Pasadena, California.

APPENDIX A

STABILITY CONSTANTS FOR THE FORMATION OF COMPLEXES AND SOLID

Complexes			log K
$H^+ + CO_3^{2-}$	$\rightleftharpoons$	HCO_3^-	10.2
$2H^+ + CO_3^{2-}$	$\rightleftharpoons$	$H_2CO_3^o$	16.5
$H^+ + SO_4^{2-}$	$\rightleftharpoons$	HSO_4^-	2.2
$H^+ + PO_4^{3-}$	$\rightleftharpoons$	HPO_4^{2-}	12.5
$2H^+ + PO_4^{3-}$	$\rightleftharpoons$	$H_2PO_4^-$	19.9
$3H^+ + PO_4^{3-}$	$\rightleftharpoons$	$H_3PO_4^o$	21.9
$H^+ + H_2SiO_4^{2-}$	$\rightleftharpoons$	$H_3SiO_4^-$	13.1
$2H^+ + H_2SiO_4^{2-}$	$\rightleftharpoons$	$H_4SiO_4^o$	22.96
$2H^+ + 2H_2SiO_4^{2-}$	$\rightleftharpoons$	$H_6Si_2O_8^{2-}$	26.16
$4H^+ + 4H_2SiO_4^{2-}$	$\rightleftharpoons$	$H_{12}Si_4O_{16}^{4-}$	55.9
$6H^+ + 4H_2SiO_4^{2-}$	$\rightleftharpoons$	$H_{14}Si_4O_{16}^{2-}$	78.2
$H^+ + sal^{2-}$	$\rightleftharpoons$	$Hsal^-$	14.0
$2H^+ + sal^{2-}$	$\rightleftharpoons$	H_2sal^o	17.0
$H^+ + phth^{2-}$	$\rightleftharpoons$	$Hphth^-$	5.5
$2H^+ + phth$	$\rightleftharpoons$	H_2phth^o	8.5
H_2O	$\rightleftharpoons$	$H^+ + OH^-$	-14.0
$Ca^{2+} + H_2O$	$\rightleftharpoons$	$CaOH^+ + H^+$	-12.2
$Mg^{2+} + H_2O$	$\rightleftharpoons$	$MgOH^+ + H^+$	-11.2
$Mn^{2+} + H_2O$	$\rightleftharpoons$	$MnOH^+ + H^+$	-10.0
$Mn^{2+} + 3H_2O$	$\rightleftharpoons$	$Mn(OH)_3^- + 3H^+$	-34.2
$Ca^{2+} + CO_3^{2-}$	$\rightleftharpoons$	$CaCO_3^o$	3.0
$Ca^{2+} + H^+ + CO_3^{2-}$	$\rightleftharpoons$	$CaHCO_3^+$	11.6
$Ca^{2+} + SO_4^{2-}$	$\rightleftharpoons$	$CaSO_4^o$	2.3

		log K
$Ca^{2+} + H^+ + PO_4^{3-}$	$\rightleftharpoons CaHPO_4^o$	14.6
$Mg^{2+} + CO_3^{2-}$	$\rightleftharpoons MgCO_3^o$	3.2
$Mg^{2+} + H^+ + CO_3^{2-}$	$\rightleftharpoons MgHCO_3^+$	11.6
$Mg^{2+} + SO_4^{2-}$	$\rightleftharpoons MgSO_4^o$	2.4
$Mg^{2+} + H^+ + PO_4^{3-}$	$\rightleftharpoons MgHPO_4^o$	15.1
$Na^2 + CO_3^{2-}$	$\rightleftharpoons NaCO_3^-$	1.2
$Na^+ + SO_4^{2-}$	$\rightleftharpoons NaSO_4^-$	0.7
$Mn^{2+} + H^+ + CO_3^{2-}$	$\rightleftharpoons MnHCO_3^+$	12.1
$Mn^{2+} + SO_4^{2-}$	$\rightleftharpoons MnSO_4^o$	2.3
$Mn^{2+} + Cl^-$	$\rightleftharpoons MnCl^+$	1.1
$Mn^{2+} + 2Cl^-$	$\rightleftharpoons MnCl_2^o$	1.1
$Mn^{2+} + 3Cl^-$	$\rightleftharpoons MnCl_3^-$	0.6
$Mn^{2+} + H^+ + PO_4^{3-}$	$\rightleftharpoons MnHPO_4^o$	16.2
$Mn^{2+} + sal^{2-}$	$\rightleftharpoons Mnsal$	7.0
$Mn^{2+} + 2sal^{2-}$	$\rightleftharpoons Mnsal_2^{2-}$	10.9

Solids

$Ca^{2+} + 2H_2O$	$\rightleftharpoons Ca(OH)_2(s)+2H^+$	-21.9
$Ca^{2+} + CO_3^{2-}$	$\rightleftharpoons CaCO_3(s)$	8.3
$Ca^{2+} + SO_4^{2-}$	$\rightleftharpoons CaSO_4(s)$	4.7
$4Ca^{2+} + H^+ + 3PO_4^{3-}$	$\rightleftharpoons Ca_4H(PO_4)_3(s)$	48.2
$Ca^{2+} + H^+ + PO_4^{3-}$	$\rightleftharpoons CaHPO_4(s)$	19.3
$5Ca^{2+} + 3PO_4^{3-}$	$\rightleftharpoons Ca_5(OH)(PO_4)_3(s)+H^+$	45.1
$Ca^{2+} + H_2SiO_4^{2-}$	$\rightleftharpoons CaH_2SiO_4(s)$	8.7
$Mg^{2+} + 2H_2O$	$\rightleftharpoons Mg(OH)_2(s)+2H^+$	-16.4
$Mg^{2+} + CO_3^{2-}$	$\rightleftharpoons MgCO_3(s)$	5.4

			log K
$3Mg^{2+} + 2PO_4^{3-}$	$\rightleftharpoons$	$Mg_3(PO_4)_2(s)$	28.4
$Mn^{2+} + 2H_2O$	$\rightleftharpoons$	$Mn(OH)_2(s) + 2H^+$	-14.5
$Mn^{2+} + CO_3^{2-}$	$\rightleftharpoons$	$MnCO_3(s)$	10.4
$Mn^{2+} + H_2SiO_4^{2-}$	$\rightleftharpoons$	$MnH_2SiO_4(s)$	10.7
$2H^+ + H_2SiO_4^{2-}$	$\rightleftharpoons$	$SiO_2(s) + 2H_2O$	25.7

Redox

Mn^{2+}	$\rightleftharpoons$	$Mn^{3+} + e^-$	-25
$MnOH^+$	$\rightleftharpoons$	$MnOH^{2+} + e^-$	-15
$Mn^{2+} + 2H_2O$	$\rightleftharpoons$	$MnOOH(s) + 3H^+ + e^-$	-25.3
$2Mn^{3+} + 2H_2O$	$\rightleftharpoons$	$Mn^{2+} + MnO_2 + 4H^+$	9

Other

$CO_2(g)$	$\rightleftharpoons$	$H_2CO_3^*(aq)$	-1.5

APPENDIX B REACTION VESSEL USED FOR ADSORPTION AND OXIDATION EXPERIMENTS.